# Distribution and Partitioning of Mercury in the Arctic Cryosphere: Transport Across Snow-Sea Ice-Water Interfaces in the Western Arctic Ocean

By

Amanda Holly Chaulk

A Thesis submitted to the Faculty of Graduate Studies of

The University of Manitoba

in partial fulfilment of the requirements of the degree of

**MASTER OF SCIENCE**

Department of Environment and Geography

University of Manitoba

# Abstract

The high toxicity and ability to be transported over long distances and biomagnify up food chains have earned Mercury (Hg) recognition as a contaminant of global concern. The Arctic region is particularly vulnerable to Hg with high levels of Hg being detected in marine mammals. The importance of the cryosphere, especially sea ice, has often been neglected in considerations of the extent to which atmospherically derived Hg impinges on the underlying marine system. This thesis reports the first systematic study of Hg transport in the Arctic cryosphere (sea ice, brine, snow, and melt ponds) conducted in the Amundsen Gulf from February to June 2008. Hg concentrations in bulk first-year sea ice were generally low (0.5 – 4 ng $L^{-1}$), with the highest concentration in the surface granular ice layer. The highest concentrations of Hg were found in sea ice brine (up to 70 ng $L^{-1}$). Atmospheric mercury depletion events (AMDEs) appear not to be an important factor in determining Hg in sea ice, with the exception of in frost flowers. Evidence of Hg accumulation during melt – refreezing cycles is seen in multi-year ice. Significant impact of AMDEs is observed on Hg concentrations in snow. Rates of deposition of atmospheric Hg ranged from 200 – 784 ng $m^{-2}$ into the top 1 cm of snow. Although photo reduction and reemission to the atmosphere does occur, a considerable fraction of deposited Hg is retained in the snowpack due to subsequent burial. At one station it is estimated that less than 50% of the deposited Hg is re-emitted to the atmosphere. It is suggested that in the Beaufort Sea, where AMDEs occur frequently due to dynamic nature of the sea ice environment, a larger than suspected portion of atmospherically deposited Hg can be retained in the snowpack and enter the underlying marine system upon melt later in the season.

# Acknowledgements

Foremost, I express my sincere gratitude to my supervisors Dr. Feiyue Wang and Dr. Gary Stern for the opportunity to do this research. Their support, guidance, patience, and expertise throughout this process have been invaluable. A big thank you is necessary for Debbie Armstrong for her time spent teaching me, support in the field, advice and encouragement throughout this project. I would also like to express my gratitude to Monika Pucko for all the assistance she has given me since this project began.

I am indebted to many of my colleagues at the University of Manitoba for their support, advice, and friendship throughout this project. Thank you to the members of the IPY-CFL sea ice team and IPY-CFL contaminants team for all of their assistance in the field, advice and support: Alexis Burt, Jeffrey Latonas, Alex Hare, Marcos Lemes, Joanne DeLaronde, Allison MacHutchon, Hayley Hung, Alexandra Steffen, Lauren Candlish, Pascal Collin, Matthew Asplin, Dan Leitch, John Iacozza, Rodd Laing, and Garry Codling. Special thanks to the captains and crew of the CCGS Amundsen for all of their hard work in this scientific endeavour. I would like to thank the members of my advisory committee Drs. David Barber and Annemieke Farenhorst for their advice and support. I would also like to thank Dr. Barber for his expertise and advice in the preparation of conference posters and a manuscript.

Finally, this study was made possible thanks to financial support from the University of Manitoba, the Circumpolar Flaw Lead System Study, Arctic Net, the Canada Foundation for Innovation, and the Northern Scientific Training Program of Indian and Northern Affairs Canada.

# Dedications

This thesis is dedicated to my parents, Barbara and the late Larry Chaulk, whose never-ending love and support were the catalyst in making this - and all of my accomplishments - possible.

# Table of Contents

# List of Tables

# List of Figures

# List of Acronyms

AMDE – Atmospheric Mercury Depletion Event
Br – Bromine
BrCl – Bromine chloride
CCGS – Canadian Coast Guard Ship
CFL – Circumpolar Flaw Lead
CVAFS – Cold Vapor Atomic Fluorescence Spectroscopy
FYI – First Year Ice
GC – CVAFS – Gas Chromatography Cold Vapor Atomic Fluorescence Spectroscopy
GEM – Gaseous Elemental Mercury
HCl – Hydrochloric Acid
Hg – Mercury
$Hg^0$ – Elemental Mercury
$Hg^{2+}$ - Mercuric Ion
Hg (II) – Divalent Mercury (Complexed)
HH - Hydroxylamine Hydrochloride
IPY – International Polar Year
MeHg – Methyl Mercury
MMHg – Monomethyl Mercury
MYI – Multi Year Ice
PHg – Particulate Bound Mercury
PILMS – Portable In-situ Laboratory for Mercury Speciation
RGM – Reactive Gaseous Mercury
THg – Total Mercury
$[Hg]_T$ – Concentration of Total Mercury
UCTEL – Ultra Clean Trace Elements Laboratory
WHAM - Windermere Humic-Aqueous Model

# Chapter 1: Introduction to Mercury in the Arctic Environment

## 1.1 Mercury in the Environment

*Mercury*

Mercury (Hg), the eightieth element on the Periodic Table, is unique in that it is one of two naturally occurring elements that are liquid at standard temperature and pressure. Mercury's high vapor pressure (0.2460 kPa at 298 K) allows it to partition readily into the gaseous phase. Seven stable isotopes exist for Hg, with $^{202}$Hg being the most abundant accounting for 29.86% of all Hg. Mercury, also known as quick silver, is a rare element in the earth's crust and occurs naturally throughout the world, most commonly in deposits of cinnabar (mercuric sulphide, HgS). Mercury has been used for millennia in many applications including thermometers, barometers, fluorescent light bulbs, and dental amalgam. It is also used industrially in mining, smelting and the production of precious metals, chlorine and caustic soda. Mercury can be emitted naturally into the atmosphere via volcanoes and forest fires, although currently the majority of atmospheric Hg is anthropogenic in origin, being emitted from coal fired power plants, mining and smelting industries, and paper and chloro-alkali plants (Hylander and Goodsite 2006). Global Hg cycling has been enhanced by human activities such that levels are two to three times higher than pre-industrial times (Mason *et al.* 1994; Mason and Fitzgerald 1996; Lamborg *et al.* 2002). The most familiar example of Hg toxicity is the "mad hatter"; hat makers in the mid-18$^{th}$ – 19$^{th}$ century using fur treated with mercuric nitrate often experienced psychological ill-effects. Minamata disease, another well-known example of Hg toxicity, is a neurological

condition caused by severe Hg poisoning. It is named after the city Minamata in Japan, where, in the 1950s, the release of industrial Hg into wastewater caused a bioaccumulation of Hg in shellfish and fish in the region. These contaminated fish were then consumed by humans and animals in the area who suffered neurological effects.

Mercury can exist in several different forms, each with unique chemical and physical properties. The forms of Hg discussed in this thesis are summarized in Table 1-1.

**Table 1-1: A summary of key mercury species**

| Species | Abbreviation | Oxidation State of Hg | Properties |
|---|---|---|---|
| Gaseous Elemental Mercury | GEM | 0 | Low aqueous solubility & reactivity; High stability |
| Reactive Gaseous Mercury | RGM | 1+, 2+ | Highly reactive, water soluble<br>Operationally defined*; most often bound to halogen anions ($HgCl_2$, $HgBr_2$) or as an oxide (HgO)<br>Subject to rapid deposition |
| Particulate Mercury | PHg | 2+ | Operationally defined* as Hg bound to particles<br>Subject to rapid deposition |
| Methyl Mercury (most common form of organic mercury) | MeHg | 2+ | Hg bound to a methyl group ($-CH_3$) and another anion or particle.<br>Subject to bioaccumulation and biomagnification<br>Capable of transporting across blood-brain barrier and thus causing neurotoxic effects |
| Total Mercury | THg | | A measure of the sum of all mercury species (organic and inorganic) in media. |

* Both RGM and PHg are operationally defined as their exact chemical structures are unknown (Steffen 2008).

When compared to other metals, that are primarily associated with aerosols in the atmosphere, Hg is unique in that globally 95% of atmospheric Hg is present in the gaseous elemental form (Slemr *et al.* 1985). This form of Hg has a low aqueous solubility and reactivity. These properties make it stable and allow a long atmospheric residence time enabling global transport to areas where there is little anthropogenic input of Hg (e.g., the

Arctic) (Slemr *et al.* 1985; Hylander and Goodsite 2006). Atmospheric transport is a major pathway for Hg to be delivered to the Arctic (Cheng and Schroeder 2000). Since the 1990s Hg emissions from North America and Europe have decreased; however emissions from Asia and Africa have increased (Pacyna *et al.* 2006). In the atmosphere, Hg is able to undergo chemical reactions and be subsequently deposited into the surface environment. Once deposited Hg can be converted to its neurotoxic organic form methyl mercury (MeHg).

*Mercury in the Arctic*

The Arctic is often thought as one of the last pristine environments on Earth, untouched by human industrial activities. In fact the opposite is true: polar regions are particularly sensitive to chemical contamination (Macdonald *et al.* 2005). Global Hg models have suggested that the Arctic is a sink for Hg (Ariya *et al.* 2004). Presently, the Arctic is faced with a large-scale problem where both ecosystems and human communities are at risk due to high exposure to Hg. In the Beaufort Sea of the Arctic Ocean, where there are no anthropogenic outputs of Hg, high levels of Hg in the marine ecosystem, particularly marine mammals, have been documented in recent years (Lockhart *et al.* 2005; Loseto *et al.* 2008; Gaden *et al.* 2009). Mercury contamination is particularly troublesome in this region as concentrations in certain biota remain very high despite relatively constant or decreasing Hg concentrations in the Arctic troposphere (Lockhart *et al.* 2005). Mercury, more specifically the neuro-toxic species MeHg, has been shown to biomagnify in the Arctic food web (Atwell *et al.* 1998; Muir *et al.* 1999; Campbell *et al.* 2005; Dehn *et al.* 2006).

This biomagnification of Hg in the food web raises concerns over the health of marine mammals and Northern inhabitants who consume animal tissue as part of their

traditional diet (Van Oostdam *et al.* 2005). Inuit consuming regional food often have a mean MeHg intake that approaches or exceeds the tolerable daily intake set by the World Health Organization (1.6µg / kg) (Van Oostdam *et al.* 2005; Hylander and Goodsite 2006). Along with consuming dangerous amounts of Hg post-natally, Northern inhabitants are exposed to alarming levels of MeHg pre-natally (Hylander and Goodsite 2006). Methyl mercury is among the few toxic chemicals known to cross the placental barrier. High levels of pre-natal Hg exposure have been associated with diminished mental capacity and neuro-behavioral damage to children (Van Oostdam *et al.* 2005; Hylander and Goodsite 2006). Human exposure to Hg is almost exclusively diet dependant. In animals, Hg is known to accumulate in muscle, epidermis, hair and other keratinized structures (Dehn *et al.* 2006).

*Atmospheric Mercury Chemistry*

In spring 1995 at the Alert Research Station in the Canadian high Arctic, a unique phenomenon was observed: very low concentrations of Hg were measured episodically in the lower troposphere (Schroeder *et al.* 1998). The discovery and characterization of the so-called atmospheric mercury depletion events (AMDEs, wherein elemental mercury in the troposphere is depleted) provides a possible pathway of increased Hg deposition from the atmosphere (Schroeder *et al.* 1998; Lu *et al.* 2001; Skov *et al.* 2004). During polar sunrise, occurring anywhere from late January to early June depending on location, gaseous elemental mercury (GEM) is rapidly oxidized to reactive gaseous mercury (RGM) (Schroeder *et al.* 1998; Skov *et al.* 2004). The occurrence of AMDEs is linked with reactive halogens, predominantly bromine (Br) derived from photochemical reactions of sea salt aerosols (Barrie and Platt 1997; Ariya *et al.* 2002; Lindberg *et al.* 2002; Skov *et al.* 2004). High

amounts of Br species are released episodically during spring at high latitudes, resulting in the so-called "bromine explosions" (Wennberg 1999).

During polar sunrise a strong correlation between depletion of $Hg^0$ and ozone ($O_3$) exists; the difference being ozone is converted to oxygen gas and halide oxides whereas Hg is merely changing oxidation states (Lindberg *et al.* 2002). The proposed mechanism of GEM to RGM conversion begins with halogen (Br or Cl) radicals being produced auto-catalytically from a heterogeneous photochemical reaction (Lindberg *et al.* 2002):

$$Br_2 / Cl_2 + h\nu \rightarrow 2Br^{\cdot}/Cl^{\cdot}$$

$$Hg^0 + 2\ Br^{\cdot}/Cl^{\cdot} \rightarrow HgBr_2 / HgCl_2$$

And / or

$$Br/Cl + O_3 \rightarrow ClO/BrO + O_2$$

$$BrO/ClO + Hg^0 \rightarrow HgO + Br^{\cdot}/Cl^{\cdot}$$

AMDEs are unique to polar regions because they possess the necessary conditions: available of halogens (via sea salt or frost flowers), calm weather, a temperature inversion, the presence of sunlight, and sub-zero temperature (Macdonald *et al.* 2005). The Hg oxidation itself does not require the input of solar energy. However, in order to generate the oxidants needed to oxidize Hg solar radiation is required; thus AMDEs occur in conjunction with a time when the Arctic is receiving an increased flux of solar radiation (polar sunrise). Since their characterization in Schroeder's 1995 work, the chemistry and mechanisms of AMDEs remains a hot topic for scientific study. AMDEs have been recorded throughout the Arctic region (Figure 1-1) (Steffen *et al.* 2007; Steffen 2008); these events are highly local and can vary greatly in a small spatial scale (Lindberg *et al.* 2002; Steffen 2008).

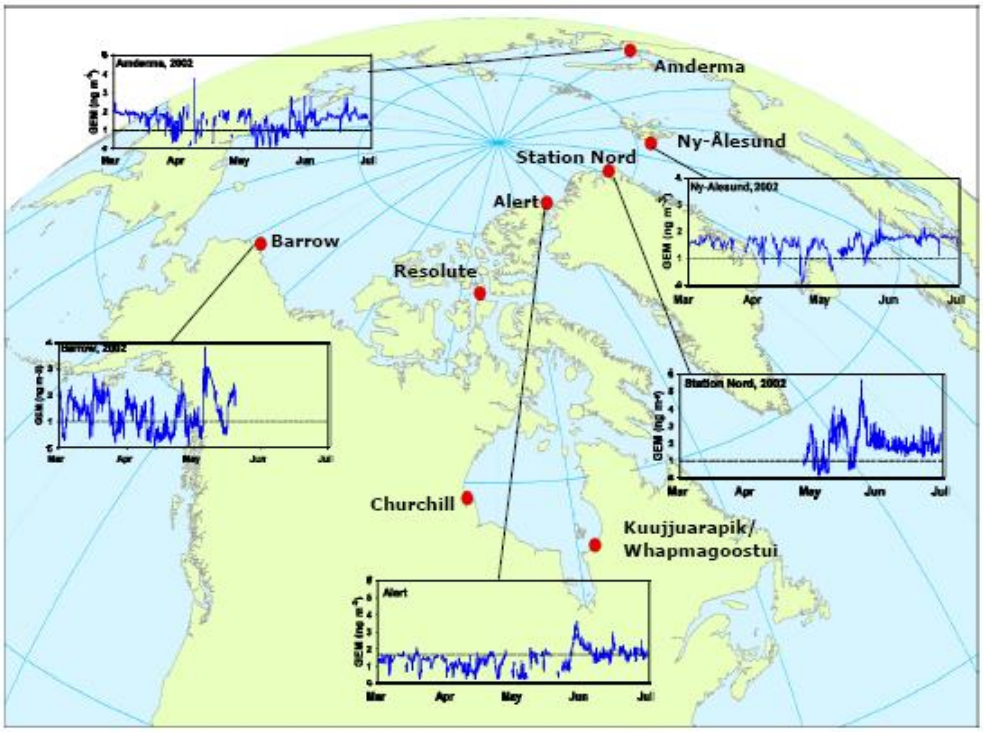


**Figure 1-1: Atmospheric elemental mercury (GEM) measurements at various Northern locations. (Steffen *et al*, 2007)**

During AMDEs the generated RGM is rapidly deposited onto snow and ice surfaces. It is well know that a fraction of the deposited Hg is quickly re-volatilized to the atmosphere (Lalonde *et al.* 2002) following photoreduction to Hg(0). However, the fraction of Hg that is re-volatilized and the fate of the remaining Hg remain a topic of debate. Some studies have suggested that the net deposition of AMDE Hg is low (St. Louis *et al.* 2005; Kirk *et al.* 2006; St. Louis *et al.* 2007) whereas others have concluded otherwise, that is, the fraction of atmospherically deposited Hg that remains in the cryosphere is more significant than otherwise reported (Steffen *et al.* 2005; Johnson *et al.* 2008; Hirdman *et al.* 2009). The impact of atmospherically deposited Hg remaining in the snow pack is highlighted by studies implicating the snow pack and melt water as a major source of Hg. Losetto, *et al.* (2004) suggested snowmelt as a primary source of Hg to lakes in the Canadian High Arctic and a significant source to water bodies downstream, including the Arctic Ocean. Dommergue *et*

*al.* (2010) estimated that cryospheric melt water contributes 8 – 21% of the Hg content of the fjord near Ny-Alesund Sweden.

It is important to note that despite the occurrence of AMDEs, atmospheric Hg concentrations have remained fairly constant for at least the past ~10 years (Steffen *et al.* 2005). During the time of year when AMDEs occur, the water column is largely covered by an ice and snow barrier. This raises the critical question: are AMDEs a major contributor to Hg in the water column AND Hg bioaccumulation in biota?

*Arctic Mercury Cycling*

Due to its unique scavenging process (AMDEs), biomagnifications in food webs, and chemical transformations (methylation), Hg has a complex cycle in the Arctic when compared to other trace elements (Macdonald *et al.* 2005). Hg cycling in coastal and marine environments is highly dynamic, potentially leading to Hg accumulation in these areas (Douglas and Sturm 2004). Figure 1-2, adapted from Macdonald *et al*. (2005), shows the intricate cycling Hg is subject to in the Arctic.

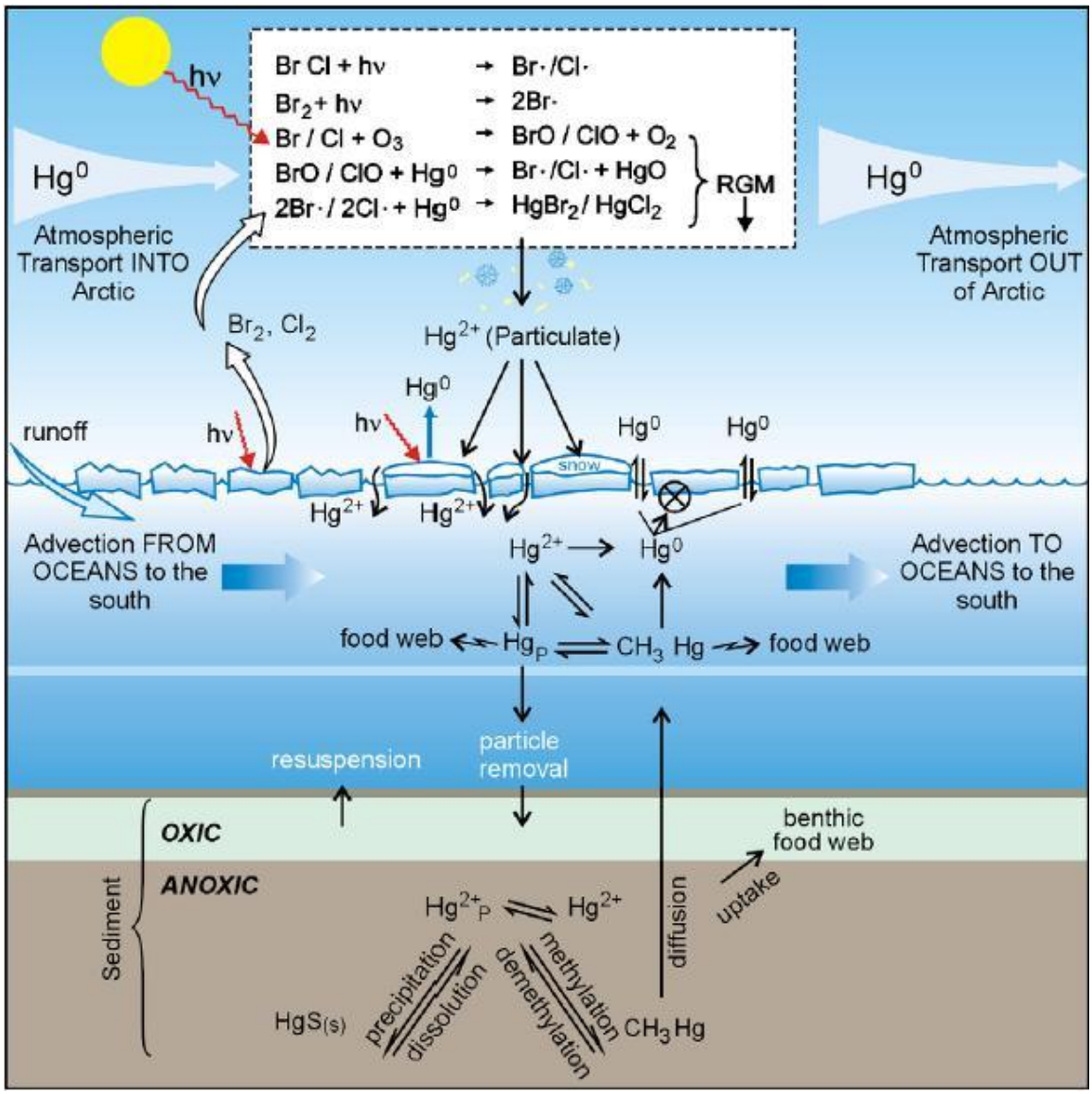


**Figure 1-2: schematic diagram illustrating the mercury cycle in the Arctic. The chemical processes initiated by light radiation after polar sunrise are listed in the inset box at top (Macdonald et.al. 2005).**

Hg concentration in biota is increasing whereas atmospheric Hg concentrations have remained fairly constant over time. This suggests that changes in the physical (ice cover, permafrost, etc.) and biological system (habitat, feeding, food web structure, etc.) may be more important in Hg bioaccumulation than human activities (Macdonald *et al.* 2005; Outridge *et al.* 2008; Wang *et al.* 2010).

*Role of the Cryosphere in Mercury Chemistry*

The exact role of the snow and ice cover plays in AMDE chemistry remains to be understood. It is believed that sea ice, particularly first year ice and the flaw leads formed within, play a role in AMDEs by providing a source of reactive halogens required for the GEM to RGM conversion (Douglas *et al.* 2005). In areas where flaw leads form bromine explosions can occur (Bottenheim and Chan 2006; Simpson *et al.* 2007). In coastal regions, these events are abundant (Simpson *et al.* 2005). The primary source of Br is thought to be the highly saline brine layer that forms on the surface of newly frozen sea ice (Simpson *et al.* 2007; Zhao *et al.* 2008). Dynamic regions of the Arctic Ocean, such as the Beaufort Sea, known to experience frequent flaw lead systems, would have increased availability of halides as leads open and re-freeze.

Frost flowers, a unique feature on newly formed ice (discussed further below) have a large surface area that may provide a surface for chemical reactions involving atmospheric exchange. Frost flowers have been proposed as a potential source of reactive Br to the troposphere, driving AMDEs (Rankin and Wolff 2002; Kaleschke *et al.* 2004; Jones *et al.* 2006). Frost flowers yield the highest concentrations of Hg in the cryosphere reported in literature in the range of 45 – 820 ng $L^{-1}$ (Douglas *et al.* 2005; Douglas *et al.* 2008). This can be attributed to several factors. It has been postulated that, because of their high concentration of halide salts and large surface area, frost flowers are able to act as a surface for GEM to RGM conversion (Rankin and Wolff 2002). Frost flowers may also be effective scavengers of atmospherically derived RGM (Legagneux *et al.* 2002).

Studies of Hg concentrations in surface snow support the claim that AMDE activity and Hg deposition is enhanced over sea ice. A comparison of coastal versus inland Arctic

snow shows higher concentrations of total Hg in snow over ice than in snow over land (Poulain *et al.* 2007). Snow deposited onto the ice cover or directly blown into an open lead may be a possible vector of Hg transport into the water column and subsequently into marine biota (Steffen *et al.* 2002). Scavenging of Hg from the air may be enhanced near open leads as the frost flowers and surface hoar crystals present provide a larger surface area for scavenging (Douglas *et al.* 2005). Falling snow also has a large surface area that makes it an effective scavenger of contaminants (Domine *et al.* 2007).

*Mercury in the Cryosphere*

The snow pack has a strong impact on tropospheric chemistry due to both the wide range of chemical processes that occur within and the host of important chemicals that temporarily or permanently reside in snow (Domine *et al.* 2002). Atmospheric gas exchange, photolysis reactions, along with heterogeneous reaction on snow surface (such as ozone depletion) and solid state diffusion of contaminants occur within the snow (Domine *et al.* 2002). The metamorphism (sublimation and condensation) that snow undergoes leads to the release of important gases such as $CO_2$, halides, and $NO_x$ species (Domine *et al.* 2002).

*The Fate of Atmospherically Deposited Mercury*

During an AMDE when atmospheric GEM decreases, a corresponding increase in THg in surface snow is observed. RGM species generated during AMDEs are water soluble and exhibit a much shorter atmospheric lifetime than GEM (Lindberg *et al.* 2002). RGM, and in smaller amounts GEM and PHg, are often rapidly (within minutes) deposited onto snow or ice surfaces (Lu *et al.* 2001; Steffen *et al.* 2002). In general, wet and dry deposition

account for comparable amounts of Hg deposited (Lin *et al.* 2006). Total Hg concentrations in surface snow range from <10 ng/L prior to AMDEs (Lahoutifard *et al.* 2005), to concentrations >100 ng/L during or immediately following and AMDE (Ferrari *et al.* 2004; Douglas *et al.* 2005; Lahoutifard *et al.* 2005; Kirk *et al.* 2006; Poulain *et al.* 2007; Fain *et al.* 2008; Ferrari *et al.* 2008; Johnson *et al.* 2008; Dommergue *et al.* 2010). RGM does not remain deposited onto surfaces, a fraction, the magnitude of which is under debate, is photoreduced, within hours of deposition, back to GEM and re-volatilized to the atmosphere (Steffen *et al.* 2002; Lalonde *et al.* 2003; Lahoutifard *et al.* 2005). The deposited Hg remaining in snow can enter the aquatic system during spring melt, with snow effectively acting as a reservoir for this toxin (Ferrari *et al.* 2005).

Figure 1-3 summarizes the transformations and cycling of Hg from the atmosphere to the snow as discussed below.

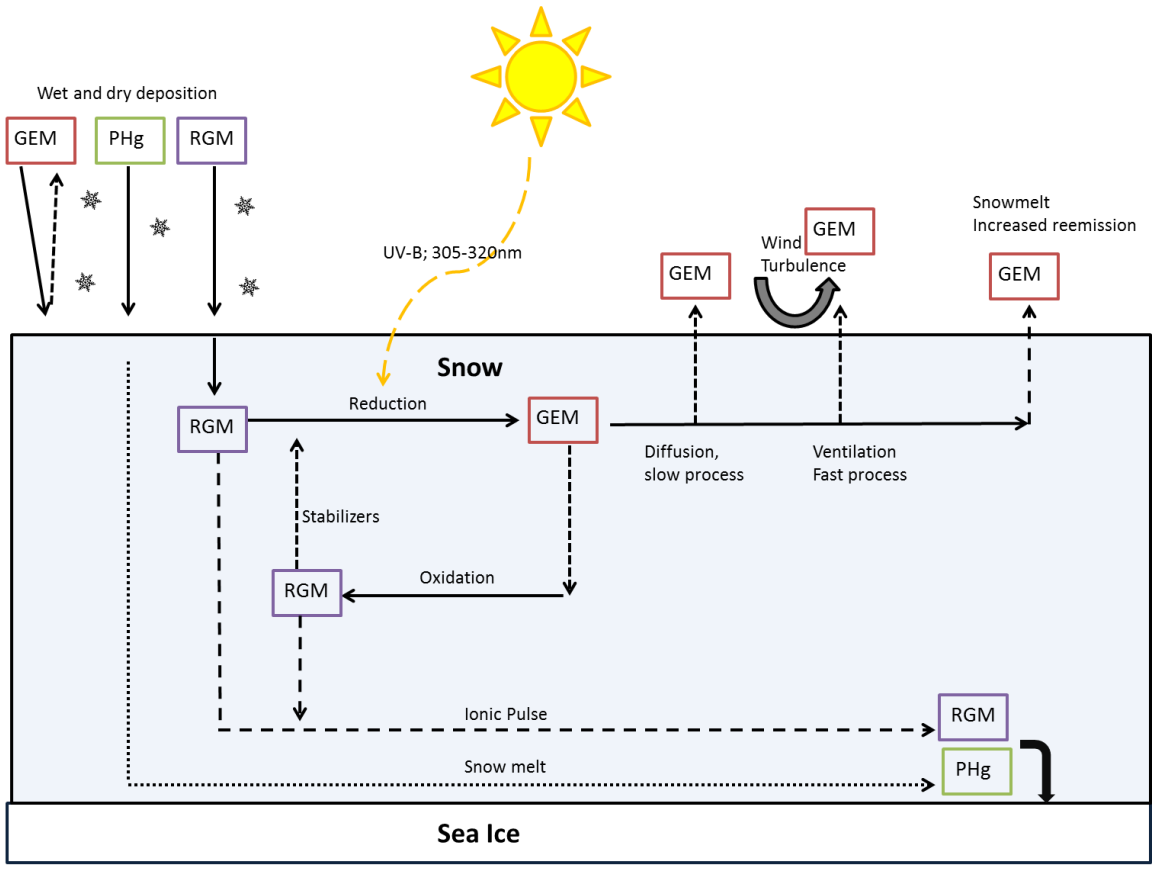


**Figure 1-3: Schematic of the fundamental physical and chemical processes that govern the behaviour of mercury in the snow pack. Adapted from Durnford, (2011).**

*Chemical Reactions in the Snow pack: Oxidation and Reduction*

The concentration of Hg in the snow pack is governed by the balance between deposition and emission processes, and the chemical reactions that accompany each. For deposited RGM to be re-emitted to the atmosphere, it must first be reduced to a more volatile form, GEM. Reduction of $Hg^{2+}$ to $Hg^{0}$ is one of the primary reactions Hg can undergo in the snow pack. Although evidence has shown this process can occur in the dark (Lalonde *et al.* 2003; Ferrari *et al.* 2004; Fain *et al.* 2007; Ferrari *et al.* 2008), laboratory and field studies suggest that the majority of Hg reduction that occurs is sunlight driven (Lalonde *et al.* 2003; Johnson *et al.* 2008). Hg reduction is primarily forced by UV-B radiation (Lalonde *et al.* 2003; Poulain *et al.* 2004; Fain *et al.* 2007). A wide range of reductants are possible for the

reaction, these include hydrogen peroxide ($H_2O_2$) in pH neutral snow (Lahoutifard *et al.* 2005), the hydroperoxyl radical ($HO_2$*) (Dommergue *et al.* 2007; Fain *et al.* 2007), molecules related to humic acids (Dommergue *et al.* 2007), sulphite-based compounds (Van Loon *et al.* 2000), and oxalic acid ($C_2H_4O_2$) (Garfeldt and Jonsson 2003).

Despite sufficient UV-B radiation and an ample supply of reductants, not all oxidized Hg is reduced and re-emitted (Dommergue *et al.* 2010). This is because not all forms of oxidized Hg are easily reducible via photo reduction (Dommergue *et al.* 2007). As discussed above, both RGM and PHg are deposited on the snow pack during an AMDE. Once deposited to the snow pack it possible for RGM to become associated with particles in the snow. It has been suggested that particulate-bound Hg is less available for reduction processes, and therefore minimally emitted back to the atmosphere (Larose *et al.* 2010). Areas with higher deposition of PHg would therefore retain a higher percentage of the deposited Hg (Durnford and Dastoor 2011).

In aqueous environments, photochemical reduction of Hg leads to both mass dependant fractionation and mass independent fractionation (Bergquist and Blum 2007). During emission of atmospherically deposited Hg, light isotopes and odd mass number isotopes of mercury are lost preferentially (Sherman *et al.* 2010). Mass-independent fractionation, where odd-number isotopes are lost preferentially, of Hg in surface snow collected at Barrow Alaska has recently been reported (Sherman *et al.* 2010). In the same study, mass-dependent fractionation, wherein light isotopes of Hg are preferentially lost, was also reported (Sherman *et al.* 2010). An understanding of isotopic fractionation of Hg during biogeochemical process in the Arctic is important, as isotopic signatures of Hg may be useful in tracing its pathway through the environment.

Oxidation of Hg in the snow pack can also occur. While some studies find no evidence for Hg oxidation in the snow pack (Dommergue *et al.* 2007; Fain *et al.* 2007), many suggest that oxidation of $Hg^0$ does indeed occur, with Br radicals acting as oxidants, and chloride ions as stabilizing agents (Lalonde *et al.* 2003; Ferrari *et al.* 2004; Fain *et al.* 2008). Newly reduced $Hg^0$, atmospheric GEM deposited to snow surfaces, and GEM trapped in the snow pack are subject to oxidation to $Hg^{2+}$. Much like the accompanying reduction process, a wide range of oxidants are possible to oxidize Hg. Hydrogen peroxide ($H_2O_2$) in an acidic snow pack (Lahoutifard *et al.* 2006), Br radicals (Br*) in the light and bromine ($Br_2$) in the dark (Fain *et al.* 2008), ozone ($O_3$), the hydroxyl radical (OH*) (Lin *et al.* 2006), and alkenes and alkyl nitrates (Mann *et al.* 2005) are all potential oxidants of Hg in the snow pack. A growing body of evidence highlights the importance of halides for stabilizing oxidized Hg within in the snow pack (Lalonde *et al.* 2003; Poulain *et al.* 2007; St. Louis *et al.* 2007; Larose *et al.* 2010).

*Physical Processes Affecting Mercury in the Snow Pack*

Once in the snow pack, aside from the chemical processes discussed above, physical process can affect the distribution of Hg within. Subsurface peaks of Hg have been previously reported in literature throughout the Arctic region (Poulain *et al.* 2004; Dommergue *et al.* 2010; Larose *et al.* 2010). These subsurface peaks have been postulated to be a result of several processes. Heavy winds and blowing snow can both bury a surface layer enriched with Hg, creating a sub-surface Hg peak no longer available for photochemical reactions (Brooks, 2008) or it can expose a formerly buried layer, making the Hg once again available for emission (Durnford and Dastoor 2011). Snowfall can also bury a surface layer

enriched in Hg. The creation of a subsurface Hg peak via burial by falling snow is described by Witherow and Lyons (2008).

Lalonde *et al*. (2002) identified three major loss mechanisms for cryospheric Hg, the first two of which are physical processes: (1) percolation, (2) the settling of particulate Hg (PHg), and (3) the reduction of deposited oxidized Hg, which may then be re-emitted to the atmosphere as GEM. Outside of the melting period, where percolation and settling predominantly occur, the primary mechanism by which Hg is lost from the snow pack is likely emission of GEM (Lalonde *et al.* 2002).

As ambient temperatures rise and solar radiation increases, the snow pack will begin to melt. As melt beings, percolation columns form and channel melt water downward (Kuhn 2001). Ions are eluted from the snow pack in a high-concentration short lived pulse at the onset of snowmelt, known as the 'ionic pulse' (Kuhn 2001). During this 'pulse' a massive influx of contaminants to the aquatic system occurs (Barrie *et al.* 1992). The first 10% and 30% of the melt water depletes 25-35 and 50-80% respectively of the ions contained in the snow pack (Kuhn 2001). Mercury is included in this ionic pulse.

At the onset of snowmelt, 50-70% of total Hg is removed from the snow pack and released either into melt water or back into the atmosphere (Domine *et al.* 2002). Whether this snow pack Hg is emitted to the atmosphere or released into melt water depends on the location of the Hg within the snow pack, the speciation of Hg (PHg vs. RGM), and the rate of melting. The timing of this ionic flux is important, as it coincides with a time period when biological activity is increasingly active (Loseto *et al.* 2004). The Hg that makes its way into the water column is then available for methylation in the water column, or by sulphate reducing bacteria in the sediment.

*Methyl Mercury in Snow*

It is important to remember that MeHg is the species of Hg that biomagnifies in the food web and is primarily responsible for its neurotoxicity. Several studies indicate that the snow pack itself may constitute a major input of MeHg to the water column during spring melt (Loseto *et al.* 2004; Lahoutifard *et al.* 2005), despite the fact that MeHg only accounts for a small percentage (0.5 - 5.0%) of total Hg in snow (Dommergue *et al.* 2003; Ferrari *et al.* 2004; Lahoutifard *et al.* 2005). Values as high as 140 pg $L^{-1}$ of MeHg in melt water have been reported (Lahoutifard *et al.* 2005). Unlike RGM deposited on the snow pack that is photo reduced to GEM and re-enters the atmosphere, MeHg remains largely unaltered in the snow pack (St. Louis *et al.* 2005).

Several potential sources of MeHg in the snow pack have been identified: 1) atmospheric transport of anthropogenic emitted MMHg (monomethyl mercury) (St. Louis *et al.* 2005), 2) in-situ microbial methylation of Hg in the snow pack, 3) biotic or abiotic methylation in the atmosphere, 4) in-situ phytoplankton MMHg production (Larose *et al.* 2010), and 5) transport of marine MeHg (St. Louis *et al.* 2005).

*Mercury in the Water Column*

In the Arctic Ocean, total Hg concentrations are low (<0.5 ng $L^{-1}$) (Aspmo *et al.* 2006; Outridge *et al.* 2008); in the Beaufort Sea specifically the concentration of total Hg is ~ 0.2 ng $L^{-1}$ (This study). The concentration of Hg in a body of water is partly controlled by direct deposition from the atmosphere of the oxidized form, Hg (II) and by volatilization of the reduced form $Hg^0$.

Sources of MeHg to marine organisms remain unknown. Various potential sources include export from coastal (Hallwag *et al.* 2009), and deep-sea (Ogrinc *et al.* 2007) sediments and major river systems (Leitch *et al.* 2007; Graydon *et al.* 2009; Kirk and St. Louis 2009), atmospheric deposition (St. Louis *et al.* 2007), and water column production (Mason and Fitzgerald 1990).

Water column methylation of Hg has been investigated recently as a potential source of MeHg in the water column (Kirk *et al.* 2008). Lehnherr *et al* (2011) have estimated that water column methylation of Hg to MeHg accounts for 47% of the MMHg in polar marine waters, making the water column a significant source of MMHg to the pelagic marine food web in the Arctic (Lehnherr *et al.* 2011).

*Biological Transformation of Mercury in the Arctic*

In order for Hg to undergo biological transformation, it must be present a bioavailable form to microorganisms. The bioavailability of a metal depends on several factors including environmental pH and the concentration of complexing ligands. In terms of Hg, the fraction of Hg that is biologically available is highly dependent on atmosphere deposition processes (Larose *et al.* 2011).

Reduction of Hg(II) to Hg(0) can be both photochemically mediated (Amyot *et al.* 1994; Zhang and Lindberg 2001) as discussed above and microbially mediated (Mason *et al.* 1995; Sicilano *et al.* 2002). In order for microbial reduction of Hg to occur, the bacterium must possess the *merA* gene. This gene is specific for the mercuric reductase enzyme, which is responsible for the conversion of $Hg^{2+}$ to $Hg^{0}$. Bacteria in Arctic biofilms are reported to contain this gene (Poulain *et al.* 2007),(Møller *et al.* 2010).

Oxidation of Hg(0) is also reported to be mediated photochemically (Lalonde *et al.* 2001; Lalonde *et al.* 2004) and biotically (Sicilano *et al.* 2002). Microbial oxidation of Hg is mediated by the enzyme mercury oxidase. In freshwater aqueous systems, the activity of mercury oxidase is linked to the concentration of hydrogen peroxide ($H_2O_2$) (Sicilano *et al.* 2002).

MeHg, the neurotoxic bioaccumulative form of Hg, can occur via biotic methylation of inorganic Hg. For over two decades it has been known that microbial Hg methylation is dominated by sulphate reducing bacteria (SRB) in the sediment (Anderson 1961; Blum and Bartha 1980; Compeau and Bartha 1985; Andersson *et al.* 1990). The methylation of Hg is a side reaction performed by the bacteria as they reduce sulphate in the sediment. Methylation of Hg by bacteria is dependent on both the concentration of bioavailable Hg and the extent of microbial activity (Barkay and Poulain 2007).

Whether or not MeHg is produced in the snow pack remains unclear. Constant *et al* (2007) hypothesized that the positively correlated increases in MMHg: THg ratios with bacterial colony counts suggests that methylation may be occurring in the snow pack, despite the absence of SRB (Constant *et al.* 2007).

## 1.2 Sea Ice

*Sea Ice and Brine*

Arctic snow and ice cover plays an important role both on a local and global scale. First, it constitutes a crucial part of Arctic ecosystem by providing a habitat for wildlife ranging from primary producers up to marine mammals. Second, sea ice and snow are of enormous importance climatically as they have a major influence on the atmospheric and

oceanic circulation through a number of complex interactions and feedbacks (Barry 2002). Arctic sea ice cover exerts a major influence on the radiation balance, surface fluxes of heat, mass and momentum as well as on the thermohaline circulation (Maykut 1978; Aagaard 1989; Curry 1995).

*Sea Ice Thermodynamics*

The formation of sea ice begins with the freezing of sea water. The freezing point of sea water with a salinity of 34 psu is $-1.86^0$C; a freezing point depression is caused by the presence of inorganic salts. The ice crystal lattice begins to form as liquid $H_2O$ molecules become solid. The most common crystal structure of ice is the Ih form, in which water molecules are arranged tetrahedrally around one another in a sixfold rotational symmetry (Petrich and Eicken 2010). The plane of this rotational symmetry is called the basal plane (a-axis). Ice crystals are formed in the surface layers of the ocean, and float to the surface as the density of solid water is less than that of liquid water. Under calm conditions, a skim of 2-3mm consisting of a collection of ice crystals forms. With time, frazil ice crystals coagulate into a surface layer, called grease ice. Once the surface layer grease layer has formed the mixing of the surface waters via wind is greatly reduced. Further coagulation leads to a thickening of the ice cover, this is known as dark nilas. Granular sea ice refers to sea ice formed by the agglomeration of individual ice crystals, in random orientation. At this stage, direct heat transfer from the atmosphere to the underlying ocean is cut off; any future growth in the ice is restricted to the conduction of latent heat upward through the sea ice- sea water interface (Petrich and Eicken 2010). This thermodynamically grown ice is known as congelation ice. The growth rate of congelation ice is determined by the temperature

gradient and its effect conductivity (Weeks and Ackley 1982). In the zone directly under the newly formed layer of thin ice, ice crystals with their basal plane parallel to the direction of heat conduction are geometrically selected. These crystals grow slightly faster than those not in the preferred axis (Weeks and Ackley 1982). This geometrically selective growth is rationalized by Weeks and Ackley (1986) using the crystal growth theory which predicts that growth perpendicular to the basal plane would require more energy than adding atoms to the existing basal plane. The shift from randomly oriented ice crystals to preferential growth of elongated crystals marks the "transitional" classification of sea ice texture. During the growth of congelation ice, a skeletal layer is formed at the sea ice- sea water interface that promotes the further growth of sea ice. The skeletal layer is formed by the competing gradient in salt concentration and heat transfer from the ocean. As brine is rejected from the growing sea ice- sea water interface, this gives rise to a salt gradient which causes salt diffusion away from the interface and a diffusion of heat towards the interface (Petrich and Eicken 2010). The heat transfer from the ocean into the sea ice is about 10x faster than the diffusion of salt away from the interface (Eicken 2003). This results in the formation of a thin layer directly below the interface which has been supercooled, but not yet salinated. The growth of elongated ice crystals, parallel to the direction of heat flow, is termed "columnar" sea ice texture.

A typical young ice cover, as shown in Figure 1-4, can be grouped into three layers. The granular ice layer, accounting for 5 – 25% of ice volume, is at the ice-air interface. This is followed by a transitional layer composed of both columnar and granular ice. Finally a columnar layer that accounts for 75 – 95% of ice volume extended from the transitional layer to the ice sea-water interface.

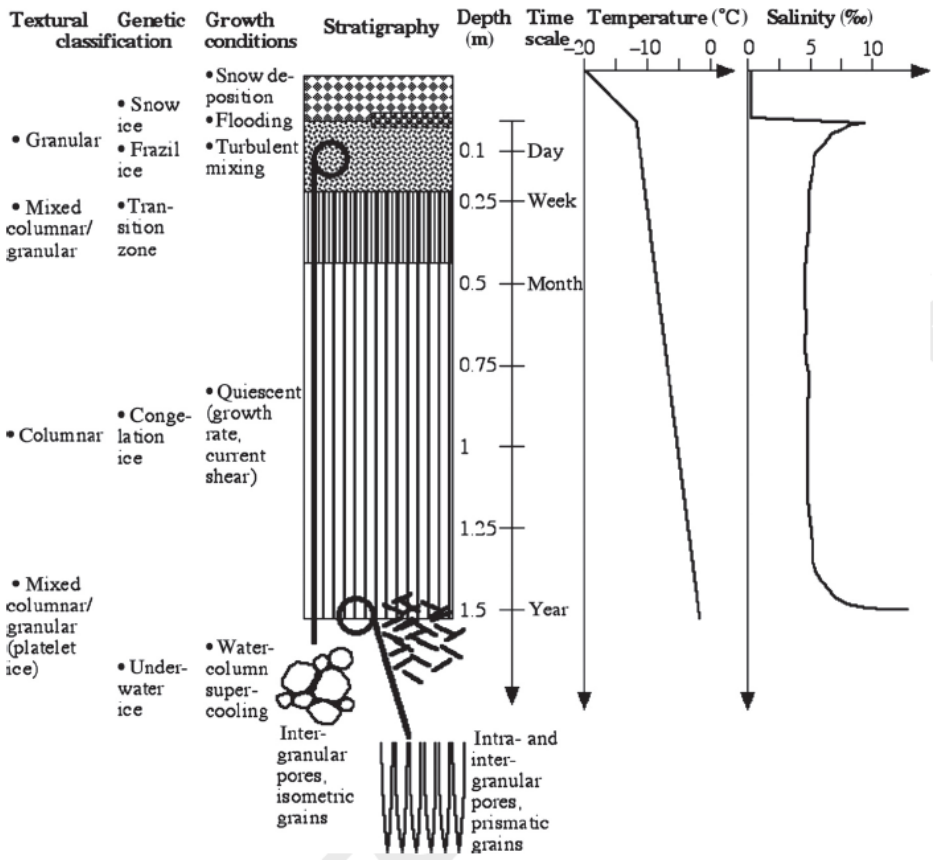


**Figure 1-4: Summary of ice textures, growth conditions, timescales, and temperatures of typical first year winter sea-ice (Petrich and Eicken 2010)**

Young sea ice is a complex mixture of ice, liquid brine, air and salt crystals. The proportions of these constituents are determined by thermodynamic controls within the ice (Weeks 1982). The idealized phase diagram shown below (Figure 1-5), developed by Assur (1958), illustrates the thermodynamic control on these phase relationships.

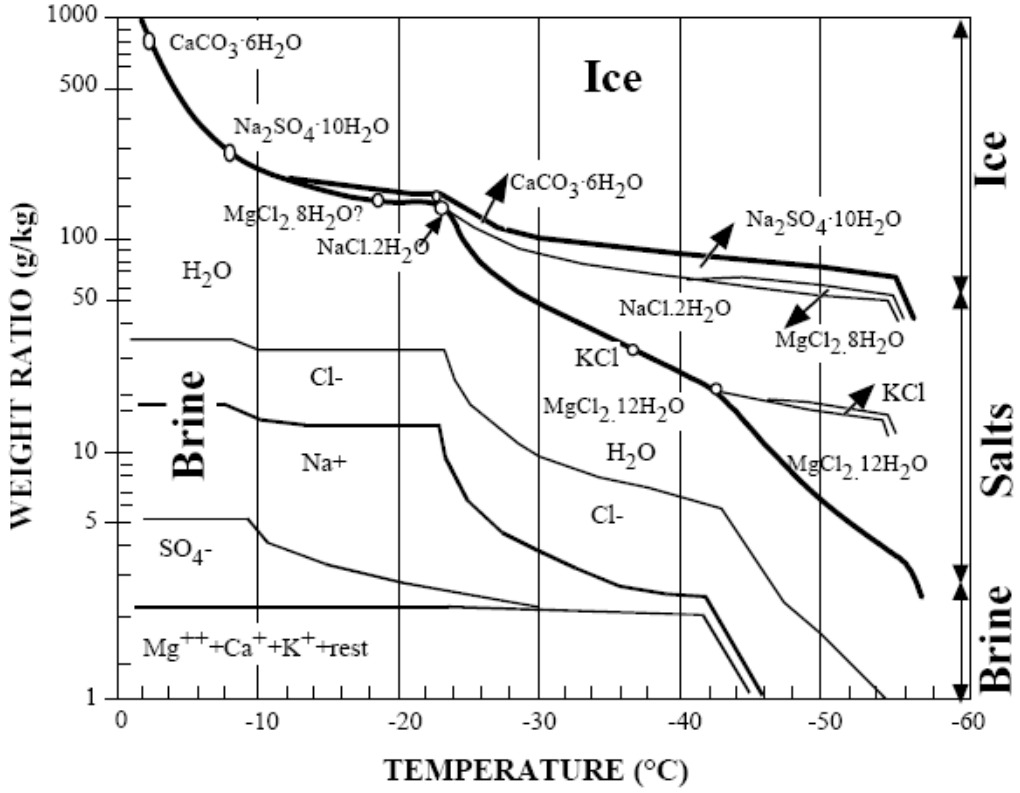


**Figure 1-5: Phase diagram of sea ice illustration the relationships between solid ice, brine and salts (Assur 1960)**

The composition of sea ice depends on salinity and temperature (Figure 1-5). In addition to thermodynamic properties, sea ice salinity and brine volume fraction influences the nutrient supply for microorganisms living in the ice.

Melting of sea ice occurs when the heat flux into the sea ice exceeds the conductive heat flux out of the sea ice. On the microscopic scale, melt begins as soon as the sea ice is warmed. Despite no superficial melting of the sea ice, as the temperature profile of the ice core becomes isothermal and reaches its melting point, brine channels interconnect and much of the bulk salinity of the ice core is lost. Once the bulk ice core has been warmed to its melting point, the input of any further solar energy will then begin to reduce the thickness of the ice at its surface (Petrich and Eicken 2010). Surface melt is the dominant ablation

process in the Arctic accounting for seasonal losses between 0.3 and 1 m of the ice surface (2003; Notz 2003). Melt ponds formed on the surface of the ice will lower the albedo significantly, causing more solar radiation to be absorbed by the ice, promoting further melt. A fraction of the melt water within melt ponds will not remain in the pond and will either percolate down into the ice or run off into the upper ocean (Eicken 2003). Surface snow present on sea ice preconditions the ice, melt ponds will form in the hollows between snow drifts (Eicken 2003).

Multi-year sea ice is ice that survives the Arctic summer melt season. Surface melting and winter accretion results in a gradual thickening of the ice cover. Perennial sea ice reaches a maximum equilibrium thickness, at the onset of summer melt, between 2.5 and 3m thick as calculated by Maykut and Untersteiner (1986). The low salinity in multi-year sea ice is a result of melt water flushing (Untersteiner 1968). This desalination is caused by melt water produced on the surface of ice percolating down in the ice causing the brine to be displaced as is descends.

*Brine and Frost Flowers*

Sea ice brine is a hyper-saline solution found in between individual ice crystals; it remains in the liquid state as the increased concentration of salts raise the freezing point of brine considerably. Brine channels and pockets in ice are formed as ocean water freezes; as water crystalizes to its solid form, the enclosed salts in ocean water are expelled and remain trapped in between ice crystals (2003; Eicken 2003). Brine drainage tubes are a complex capillary system of interconnected brine pockets. The number of brine channels is related to the growth rate of the sea ice (2003; Eicken 2003).

As frazil ice continues to freeze and consolidate pressure builds up in the brine pockets, resulting in brine expulsion. Most of the brine is expelled downwards; however, brine is also expelled upwards into the ice-air interface resulting in formations known as frost flowers. Frost flowers, a common feature on young ice in the Arctic, are formed rapidly as salt is wicked up by surface tension. The flowers consist of fragile saline (up to a salinity of 100 psu; 2-3x oceanic values) ice crystals of varying shapes (clumps, stellar dendrite, and needles) (2003; Eicken 2003).

The process of brine drainage begins immediately after entrapment by ice crystals by two principal mechanisms: gravity drainage and brine expulsion. Gravity drainage is the dominant desalination mechanism in both young and multi-year ice; it is related to the temperature profile of the ice sheet. Colder temperatures are found at the ice-atmosphere interface thus the brine in the upper layers of the ice will be cold and dense and tend to drain downwards. Brine drainage occurs through brine channels created by the interconnection of brine pockets (Weeks 1988). As a result of the desalination processes, bulk salinity of an ice sheet decreases as it thickens and ages.

*The Cape Bathurst Flaw Lead*

Flaw leads and polynyas, an important physical feature of the Arctic, occur annually when the mobile pack ice pulls away from land fast ice. The Cape Bathurst (CB) flaw lead ($70^{o}$N, $124.5^{o}$W), formed annually in the Western Arctic Ocean, is where this study took place (discussed further below). The CB flaw lead region is generally comprised of the following: a) offshore pack ice (mobile annual and multiyear ice pans with a network of leads) b) land fast sea ice formed annually in the coastal margins over the continental shelf,

c) a flaw lead polynya (series of non-linearly shaped areas of open water with snow and new and young ice) (Barber and Hanesiak 2004).

*Sea Ice in a Changing Climate*

Arctic sea ice is undergoing rapid change; both the extent of sea ice cover and average ice thickness have been decreasing (Parkinson *et al.* 1999; Comiso 2002; Rigor 2005; Comiso *et al.* 2008). Satellite data show that between 1981 and 2000 the Arctic sea ice extent was declining at a rate of 2% per decade; however, the extent of perennial ice cover (measured in September) was shrinking at a much faster rate of 7% per decade (Comiso 2002). In late summer 2009, a large section of what was thought to be thick multi-year ice, in the Beaufort Sea, turned out to be predominantly heavily decayed ice (Barber *et al.* 2009). On average winter Arctic sea ice decreases of 39,500 $km^2$/year ($\pm$5600 $km^2$) between 1979 and 2006 was observed using passive microwave remote sensing (Parkinson and Cavalieri 2008). A seasonally ice-free Arctic is predicted by the end of this century or earlier (Flato and Boer 2001; Comiso 2002; Holland *et al.* 2006).

## 1.3 Impacts of Global Climate Change to Mercury Cycling and Bioaccumulation

Both global climate change and the changing sea ice regime will affect the Hg cycling in the Arctic. Global climate change will affect the Hg problem in the Arctic in several ways. Initially, climate change will lead to an Arctic predominantly occupied by first year ice, which is highly saline compared to multi-year ice previously dominant in the Arctic. This increase in first year ice will lead to saltier ice and snow, potentially providing more halogens thus enhancing halide oxide production and the GEM to RGM conversion (Macdonald *et al.*

2005). With climate change, the time interval between atmospheric mercury deposition (AMDE) and mobilization (spring melt) is diminishing; this shrinking window of time could affect the amount of Hg re-emission from the snow pack to the atmosphere (Steffen, *et al* 2008). Warmer temperatures will also see more organic matter being released into oceans as permafrost melts, which will lead to higher methylation rates of Hg, along with increasing its residence time in the water column (Hylander and Goodsite 2006).

The likely impacts of climate warming on Arctic marine biota, summarized in Table 1-2, have been postulated by Outridge *et al* (2008).

**Table 1-2: Likely changes in processes for methylation and demethylation; + indicates increase, - indicates decrease and + indicates no significant changes (Outridge *et al,* 2008).**

| Process | Likely change | Likely impact on biotic Hg |
|---|---|---|
| Evasion | + | − |
| Mercury depletion events | + | + (near-term only) |
| Precipitation | + | + |
| Riverine inputs | + | + |
| Coastal erosion | + | + |
| Methylation | + | + |
| Demethylation | ± | ± |
| Marine primary productivity | + | − |
| Scavenging and sedimentation | + | − |

In an environment of reduced sea ice cover, more solar radiation will penetrate into the water column causing an increase in microbial metabolism and Hg(II) to Hg(0) photoreduction. This increase in evasion will coincide with a decrease in biotic Hg concentrations. Climate warming is likely to increase precipitation, river inputs, coastal erosion, and Hg methylation rates all of which will increase the levels of Hg in marine biota (Outridge *et al.* 2008).

## 1.4 Objective of This Thesis Research

To date, our knowledge of Hg cycling, transformations, and distribution is fairly extensive. Major research initiatives are on-going to understand Hg chemistry in the atmosphere, water column, snow, and biota. Recently the role of frost flowers in Hg chemistry has been investigated (Douglas *et al.* 2005; Douglas *et al.* 2008). However, the current dataset on Arctic Hg chemistry is lacking information about the distribution and behavior of Hg in several key components of the cryosphere: snow, sea ice and brine.

The role of snow, ice, and particularly brine, in the transport and ultimate fate of Hg and other contaminants is poorly characterized. Complete understanding of the Hg cycle in the Arctic environment, including bioaccumulation, requires investigation to understand and clarify the role of snow, ice and brine in AMDEs during and after polar sunrise, the net contribution of atmospheric Hg in the aquatic system, as well as to predict relations between these processes and global climate change.

This thesis research was part of the Hg project of the International Polar Year (IPY) Circumpolar Flaw Lead System Study (CFL). Taking the advantage of an 18-month expedition of the Canadian Research Icebreaker CCGS Amundsen, the overall goal of the CFL-Hg project is to determine the net contribution of AMDE-deposited Hg to Arctic marine ecosystems, and identify whether AMDEs are a significant contributing factor to increased Hg levels observed in the Arctic. This goal requires the collaboration of several research projects including atmospheric, hydrospheric, biospheric, and cryospheric components. The specific objective of this thesis research is to advance our understanding of Hg cycling in the Arctic Ocean by filling a major gap in Hg transport across the Arctic cryosphere. This will be achieved by answering the following three key questions:

1. How do AMDEs affect Hg concentrations in snow and sea ice?
2. How is Hg distributed in snow and sea ice?
3. What is the role of brine drainage and melt pond in Hg transport between the atmosphere and the ocean?

## 1.5 Experimental Design

Research was carried out aboard the CCGS Amundsen as part of the IPY-CFL study. Details about the IPY-CFL research are provided elsewhere (Barber *et al.* 2010). The ice breaker remained mobile in the Beaufort Sea of the Arctic Ocean (Figure 1-6).


**Figure 1-6: Map showing the approximate location of the CCGS Amundsen during the 2007 – 2008 field seasons**

Sampling took place between December 2007 and August 2008. All analysis was performed onboard the icebreaker in the CFI funded Portable In-situ Laboratory for Mercury Speciation (PILMS), a portable class 100 clean room lab facility. The clean hands / dirty hands sampling method were used for all in-field sampling (Fitzgerald 1999). On board the CCGS Amundsen continuous atmospheric Hg measurements (GEM, RGM, & PHg) were

taken. Cryospheric samples of snow, sea ice, brine, frost flowers, water and melt-ponds were collected (discussed further in chapters 2 and 3). This research project is unique in that it has provided a continuous time series of THg in surface snow, coinciding with atmospheric measurements, in the open ocean. Previous work has been at inland and coastal sites. All cryospheric samples were analyzed for total Hg using a Tekran 2600 cold-vapor atomic fluorescence spectroscopy instrument (discussed below).

As noted above, MeHg is the neurotoxic species shown to bioaccumulate and raises concerns over the health of Arctic marine mammals and Inuit consuming them. However, all cryospheric samples collected in this study were analyzed for total Hg, not MeHg. In many marine animals, the majority of Hg in tissues consumed by humans (liver, muscle, skin) is MeHg (Lockhart *et al.* 2005). Conversely, in abiotic samples (specifically snow & water) MeHg accounts for a smaller percentage of the total Hg. One study that sampled the water column during the spring melt found MeHg accounting for 30 – 45% of the total Hg in surface waters (St. Louis *et al.* 2007). Water profiles collected during the IPY-CFL project show much lower percentages of MeHg in the water column (<30%), with under ice water having the lowest MeHg concentrations. In snow MeHg accounts for 0.5% - 5.0% of total Hg (Dommergue *et al.* 2003; Ferrari *et al.* 2004; Lahoutifard *et al.* 2005). It stands to reason that since sea ice is formed from ocean water, it will have similar ratios between total and MeHg. Methyl mercury analysis is done via a purge and trap GC – CVAFS method, because MeHg concentrations are much lower than total Hg, a larger sample volume would be required. Since this investigation would be the first of its kind, analyzing sea ice and brine samples, total Hg measurements are a good first step as compared to MeHg; the analysis is easier, less time consuming to complete, and requires less sample volume.

*Total Mercury Analysis*

Following collection, samples are immediately acidified in PILMS using ultrapure concentrated hydrochloric acid to prevent Hg from sorbing onto the container walls. Bromine chloride (BrCl) is added to further preserve the sample, and oxidize all Hg species present to Hg (II). Prior to analysis, hydroxylamine hydrochloride (HH) is added to the sample to neutralize the low pH and destroy any free halogens. Total Hg analysis is done following EPA method 1631 (USEPA 2002) on a Tekran 2600 cold vapor atomic fluorescent spectroscopy instrument. Reaction with stannous chloride ($SnCl_2$) reduces all Hg (II) in the sample to volatile $Hg^0$. The reduced sample is passed through a vapor/liquid phase separator releasing $Hg^0$ from the aqueous sample. The $Hg^0(g)$ is amalgamated onto a gold substrate; the substrate is then heated and the Hg subsequently thermally desorbed from the gold. An inert gas carries the $Hg^0$ to a second gold trap where it is collected. Following a second heating and desorption an Argon gas stream carries the $Hg^0$ to an atomic fluorescent cell where the Hg atoms are excited. The light released as the electrons relax is detected and used to quantify Hg concentrations.

## 1.6 Organization of This Thesis

This thesis is organized into 4 chapters. Chapter 1 (this chapter) provides an introduction to Hg in the Arctic environment and a thorough literature review on topics relevant to this study. Chapter 2 is a published paper in the Journal of Environmental Science and Technology (Chaulk A., Stern G.A., Armstrong D., Barber D., and Wang F. 2011. Mercury distribution and transport across the ocean-sea ice-atmosphere interface in the

Arctic Ocean. Environ. Sci. Technol. 45, 1866-1872). It provides an overview of Hg distribution in sea ice and brine and discusses these results in terms of Hg transport within sea ice. Chapter 3 reports findings on THg concentrations within the snow pack and melt ponds during the study period. The transport and fate of atmospherically derived Hg is discussed within. A manuscript is being prepared based on Chapter 3 of this thesis. Chapter 4 summarizes the major findings from this study. A critical analysis of the advantages and pitfalls of this study is discussed and the need for future investigations is highlighted.

## 1.6 References


Aagaard, K., Carmack, E.C. (1989). The role of sea ice and other fresh water in the Arctic circulation. *Journal of Geophysical Research* **94**: 14485 - 14498.

Amyot, M., Mierle, G., Lean, D. and McQueen, D. (1994). Sunlight induced formation of dissolved gaseous mercury in lake waters. *Environmental Science and Technology* **28**: 2366-2371.

Anderson, D. L. (1961). Growth rate of sea ice. *Journal of Glaciology* **3**: 1170 - 1172.

Andersson, I., Parkman, H. and Jernelov, A. (1990). The role of sediments as sink or source for environmental contaminants: a case study of Hg and chlorinated organic compounds. *Limnologica* **20**: 347-359.

Ariya, P., Dastoor, A., Amyot, M., Schroeder, W., Barrie, L., Anlauf, K., Raofie, F., Ryzhkov, A., Davignon, D., Lalonde, J. and Steffen, A. (2004). The Arctic: a sink for mercury. *Tellus* **56B**(5): 397 - 403.

Ariya, P., Khalizov, A. and Gidas, A. (2002). Reactions of gaseous mercury with atomic and molecular halogens. *Journal of Physical Chemistry* **106**: 7310-7320.

Aspmo, K., Temme, C., Berg, T., Ferrari, C., Gauchard, P., Fain, X. and Wibetoe, G. (2006). Mercury in the atmosphere, snow and melt water ponds in the North Atlantic Ocean during Arctic summer. *Environmental Science and Technology* **40**: 4083 - 2089.

Atwell, L., Hobson, K. and Welch, H. (1998). Biomagnification and bioaccumulation of mercury in an arctic marine food web: insights from stable nitrogen analysis. *Canadian Journal of Fish and Aquatic Science* **55**: 1114-1121.

Barber, D., Asplin, M., Gratton, Y., Lukovich, J., RJ, G., Raddatz, R. and Leitch, D. (2010). The International Polar Year (IPY) Circumpolar Flaw Lead (CFL) System Study: Overview and the Physical System. *Atmosphere-Ocean*.

Barber, D., Galley, R., Asplin, M., De Abreu, R., Warner, K., Pucko, M., Gupta, M., Prinsenberg, S. and Julien, S. (2009). Perennial pack ice in the sourther Beaufort Sea was not as it appeared in the summer of 2009. *Geophysical Research Letters* **36**(L24501).

Barber, D. and Hanesiak, J. (2004). Meteorological forcing of sea ice concentrations in the southern Beaufort Sea over the period 1979 to 2000. *Journal of Geophysical Research* **109**.

Barkay, T. and Poulain, A. (2007). Mercury (micro)biogeochemistry in polar environments. *FEMS Microbiology Ecology* **59**: 232-241.

Barrie, L., Gregor, D., Hargrave, B., Lake, R., Muir, D. and Shearer, R. (1992). Arctic contaminants: sources, occurance and path-ways. *Science of the Total Environment*: 1-92.

Barrie, L. and Platt, U. (1997). Arctic troposhperic chemistry: an overview. *Tellus* **49B**: 450-454.

Barry, R. G. (2002). The role of snow and ice in the global climate system: a review. *Polar Geography* **26**: 235-246.

Bergquist, B. and Blum, J. (2007). Mass-dependent and -independent fractionation of Hg isotopes by photoreduction in aquatic systems. *Science* **318**(5849): 417-420.

Blum, J. and Bartha, R. (1980). Effects of salinity on methylation of Hg. *Bulletin of Environment, Contamination and Ecology* **25**: 404-408.

Bottenheim, J. and Chan, E. (2006). A trajectory study into the origin of spring time Arctic boundary layer ozone depletion. *Journal of Geophysical Research* **111**.

Campbell, L., Norstrom, R., Hobson, K., Muir, D., Backus, S. and Fisk, A. (2005). Mercury and other trace elements in a pelagic Arctic marine food web (Northwater Polynya, Baffin Bay). *Science of the Total Environment* **351-352**: 247-263.

Cheng, M. and Schroeder, W. (2000). Potential atmospheric transport pathways for mercury measured in the Canadian high Arctic. *Journal of Atmospheric Chemistry* **35**: 101-107.

Comiso, J. (2002). Correlation and trend studies of the sea ice cover and surface temperatures in the Arctic. *Annals of Glaciology* **34**: 420-428.

Comiso, J. (2002). A rapidly declining perennial sea ice cover in the Arctic. *Geophysical Research Letters* **29**(20).

Comiso, J., Parkinson, C., Gersten, R. and Stock, L. (2008). Accelerated decline in the Arctic sea ice cover. *Geophysical Research Letters* **35**.

Comiso, J. C. (2002). Correlation and trend studies of the sea ice cover and surface temperatures in the Arctic. *Annals of Glaciology* **34**: 420 - 428.

Compeau, G. and Bartha, R. (1985). Sulfate reducing bacteria: principal methylators of Hg in anoxic estuarine sediments. *Applied Environmental Microbiology* **50**: 498-502.

Constant, P., Poissant, L., Villemur, R., Yumvihoze, E. and Lean, D. (2007). Fate of inorganic mercury and methyl mercury within the snow cover in the low Arctic tundra on the shore of Hudson Bay (Quebec, Canada). *Journal of Geophysical Research* **112**.

Dehn, L., Follmann, E., Thomas, D., Sheffield, G., Rosa, C., Duffy, L. and O'Hara, T. (2006). Trophic relationships in an arctic food web and implications for trace metal transfer. *Science of the Total Environment* **362**: 103 - 123.

Domine, F., Cabanes, A. and Legagneux, L. (2002). Structure, microphysics, and surface area of the Arctic snowpack near Alert during the ALERT 2000 campaign. *Atmospheric Environment* **36**: 2753 - 2765.

Domine, F., Cincinelli, A., Bonnaud, E., Martellini, T. and Picaud, S. (2007). Adsorption of phenanthrene of natural snow. *Environmental Science and Technology* **41**: 6033 - 6038.

Dommergue, A., Bahlmann, E., Ebinghaus, R., Ferrari, C. and Boutron, C. (2007). Laboratory simulation of Hg0 emissions from a snowpack. *Anals of Bioanalytical Chemistry* **388**: 319-327.

Dommergue, A., Ferrari, C., Gauchard, P. and Bourton, C. (2003). The fate of mercury species in a sub-Arctic snowpack during snowmelt. *Geophysical Research Letters*.

Dommergue, A., Larose, C., Fain, X., Clarisse, O., Foucher, D., Hintelmann, H., Schneider, D. and CP, F. (2010). Deposition of mercury species in the Ny-Alesund area (79oN) and their transfer during snowmelt. *Environmental Science and Technology* **44**: 901-907.

Douglas, T. and Sturm, M. (2004). Arctic Haze, mercury and the chemical composition of snow across north-western Alaska. *Atmospheric Environment* **38**(6): 805-820.

Douglas, T., Sturm, M., Simpson, W., Brooks, S., Lindberg, S. and DK, P. (2005). Elevated mercury measured in snow and frost flowers near Arctic sea ice leads. *Geophysical Research Letters* **32**.

Douglas, T., Sturm, M., Simpson, W., JD, B., Alvarez-Aviles, L., Keeler, G., Pervoich, D., Biswas, A. and Johnson, K. (2008). Influence of snow and ice crystal formation and accumulation on mercury deposition to the Arctic. *Environmental Science and Technology* **42**: 1542-1551.

Durnford, D. and Dastoor, A. (2011). The behaviour of mercury in the cryosphere: A review of what we know from observations. *Journal of Geophysical Research* **116**.

Eicken, H. (2003). Growth, Microstructure and properties of sea ice. *Sea Ice: An Introduction to its Physics, Chemistry, Biology and Geology*. D. N. Thomas, Dieckmann, G.S. Oxford, Blackwell**:** 22-81.

Fain, X., Ferrari, C., Dommergue, A., Albert, M., Battle, M., Arnaud, L., Barnola, J., Cairns, W., Barbante, C. and Boutron, C. (2008). Mercury in the snow and fern at Summit Station, central Greenland, and implications for the study of past atmospheric mercury levels. *Atmospheric Chemistry and Physics* **8**: 3441-3457.

Fain, X., Grangeon, S., Bahlmann, E., Fritsche, J., Obrist, D., Dommergue, A., Ferrari, C., Cairns, Q., Ebinghaus, R., Barbante, C., Cescon, P. and Boutron, C. (2007). Diurnal production of gaseous mercury in the alpine snowpack before snowmelt. *Journal of Geophysical Research* **112**.

Ferrari, C., Dommergue, A., Boutron, C., Jitaru, P. and Adams, F. (2004). Profiles of mercury in the snow pack at Station Nord, Greenland shortly after polar sunrise. *Geophysical Research Letters* **31**: 1-4.

Ferrari, C., Gauchard, P., Aspmo, K., Dommergue, A., Magand, O., Bahlmann, E., Nagorski, S., Temme, C., Ebinghaus, R., Steffen, A., Banic, C., Berg, T., Planchon, F., Barbante, C., Cescon, P. and Boutron, C. (2005). Snow-to-air exchange of mercury in an Arctic seasonal snow pack in NY-Alesund, Svalbard. *Atmospheric Environment* **39**: 7633 - 7645.

Ferrari, C., Padova, C., Fain, X., Gauchard, P., Dommergue, A., Aspmo, K., Berg, T., Cairns, W., Barbante, C., Cescon, P., Kaleschke, L., Richter, A., Wittrock, F. and Boutron, C. (2008). Atmospheric mercury depletion event study in Ny-Alesund (Svalbard) in spring 2005. Deposition and transformation of Hg in surface snow during springtime. *Science of the Total Environment* **397**: 167-177.

Fitzgerald, W. (1999). Clean hands, dirty hands: Clair Patterson and the aquatic biogeochemistry of mercury. *Clean hands, Clair Patterson's crusade against environmental lead contamination*. C. I. Davidson. New York, Nova Science**:** 119 - 137.

Flato, G. and Boer, G. (2001). Warming asymmetry in climate change simulations. *Geophysical Research Letters* **28**: 195-198.

Gaden, A., Ferguson, S., Harwood, L., Melling, H. and GA, S. (2009). Mercury trends in ringed seals (Phoco hispida) from the Western Canadian Arctic since 1973: Associations with length of ice-free season. *Environmental Science and Technology* **43**(10): 3646-3651.

Garfeldt, K. and Jonsson, M. (2003). Is bimolecular reduction of Hg(II) complexes possible in aqueous systems of environmental importance. *Journal of Physical Chemistry A* **107**: 4478-4482.

Graydon, J., Emmerton, C., Lesack, L. and Kelly, E. (2009). Mercury in the Mackenzie River delta and estuary: Concentrations and fluxes during open-water conditions
*Science of the Total Environment* **407**: 2980-2988.

Hallwag, T., Gilmour, C. and RP, M. (2009). Methylmercury production in sediments of Chesapeake Bay and the mid-Atlantic continental margin. *Marine Chemistry* **114**: 86-101.

Hirdman, D., Aspmo, K., Burkhart, J., Eckhart, S., Sodemann, H. and Stohl, A. (2009). Transport of mercury in the Arctic atmosphere: evidence for a spring-time net sink and summer-time source. *Geophysical Research Letters* **36**.

Holland, M., Biz, C. and Tremblay, B. (2006). Future abrupt reduction in the summer Arctic sea ice. *Geophysical Research Letters* **33**.

Hylander, L. and Goodsite, M. (2006). Environmental costs of mercury pollution. *Science of the Total Environment* **368**: 352 - 370.

Johnson, K., Blum, J., Keeler, G. and Douglas, T. (2008). Investigation of the deposition and emissino of mercury in arctic snow during an atmospheric mercury depletion event. *Journal of Geophysical Research* **113**.

Jones, A., Anderson, P., Wolff, E., Turner, J., Rankin, A. and Colwell, S. (2006). A role for newly forming sea ice in springtime polar tropospheric ozone loss? Observational evidence from Halley station, Antarctica. *Journal of Geophysical Research - Atmospheres* **111**.

Kaleschke, L., Richter, A., Burrows, J., Afe, O., Heygster, G., Notholt, J., Rankin, A., Roscoe, H., Hollwedel, J., Wagner, T. and Jacobi, H. (2004). Frost flowers on sea ice as a source of sea salt and their influence on tropospheric halogen chemistry. *Geophysical Research Letters* **31**.

Kirk, J., St Louis, V., Hintelmann, H., Lehnherr, I., Else, B. and Possant, L. (2008). Methylated mercury species in marine waters of the Canadian high and sub Arctic. *Environmental Science and Technology* **42**(22): 8367-8373.

Kirk, J., St Louis, V. and Sharp, M. (2006). Rapid reduction and reemission of mercury deposited into snowpacks during atmospheric mercury depletion events at Churchill, Manitoba, Canada. *Environmental Science and Technology* **40**: 7590-7596.

Kirk, J. and St. Louis, V. (2009). Multiyear total and methyl mercury exports from two major sub-Arctic rivers draining into Hudson's Bay, Canada. *Environmental Science and Technology* **43**: 2254-2261.

Kuhn, M. (2001). The nutrient cycle through snow and ice, a review. *Aquatic Science* **63**: 150-167.

Lahoutifard, N., Poissant, L. and Scott, S. (2006). Scavenging of gaseous mercury by acidic snow at Kuujjuarapik, Northern Quebec. *Science of the Total Environment* **355**: 118-126.

Lahoutifard, N., Sparling, M. and Lean, D. (2005). Total and methyl mercury patterns in Arctic snow during springtime at Resolute, Nunavut, Canada. *Atmospheric Environment* **39**(7597 - 7606).

Lalonde, J., Amyot, M., J, O., Morel, F., Auclair, J. and Ariya, P. (2004). Photoinduced Oxidation of $Hg^0$(aq) in the Waters from the St. Lawrence Estuary *Environmental Science and Technology* **38**: 508-514.

Lalonde, J., Amyot, M., Kraepiel, A. and Morel, F. (2001). Photooxidation of Hg(0) in Artificial and Natural Waters. *Environmental Science and Technology* **35**: 1367 - 1372.

Lalonde, J., M, A., Doyon, M. and Auclair, J. (2003). Photo-induced Hg(II) reduction in snow from the remote and temperate Experimental Lakes Area (Ontario, Canada). *Jounral of Geophysical Research - Atmosphere* **108**(D6).

Lalonde, J., Poulain, A. and Amyot, M. (2002). The role of mercury redox reactions in snow on snow-to-air mercury transfer. *Environmental Science and Technology* **36**: 174-178.

Lamborg, C., Fitzgerald, W., O'Donnell, J. and Torgenrson, T. (2002). A non-stead-state compartmental model of global-scale mercury biogeochemistry with inter-hemispheric gradients. *Geochimica et Cosmochimica Acta* **66**: 1105-1118.

Larose, C., Dommergue, A., De Angelis, M., Cossa, D., Averty, B., Marusczak, N., Soumis, N., Schneider, D. and Ferrari, C. (2010). Springtime changes in snow chemistry lead to new insights into mercury methylation in the Arctic. *Geochimica et Cosmochimica Acta* **74**: 6263-6275.

Larose, C., Dommergue, A., Marusczak, N., Coves, J., Ferrari, C. and S, D. (2011). Bioavailable mercury cycling in polar snowpacks. *Environmental Science and Technology* **45**: 2150-2156.

Legagneux, L., Cabanes, A. and Domine, F. (2002). Measurement of the specific surface area of 176 snow samples using methane adsorption at 77K. *Journal of Geophysical Research* **107**.

Lehnherr, I., St. Louis, V., Hintelmann, H. and Kirk, J. (2011). Methylation of inorganic mercury in polar marine waters. *Nature geosciences*.

Leitch, D., Carrie, J., Lean, D., Macdonald, R., Stern, G. and Wang, F. (2007). The delivery of mercury to the Beaufort Sea of the Arctic Ocean by the Mackenzie River. *Science of the Total Environment* **373**: 1245 - 1256.

Lin, C., Pongprueksa, S., Lindberg, E., Pehkonen, S., Byun, D. and Jang, C. (2006). Scientific uncertainties in atmospheric mercury models I: Model science evaluation *Atmosphere Environment* **33**: 2067-2079.

Lindberg, S., Brooks, S., Lin, C.-J., Scott, K., Landis, M., Stevens, R., Goodsite, M. and Richter, A. (2002). Dynamic oxidation of gaseous mercury in the arctic troposphere at polar sunrise. *Environmental Science and Technology* **36**: 1245 - 1256.

Lockhart, W., Stern, G., Wagemann, R., Hunt, R., DeLaronde, J., Dunn, B., Stewart, R., Hyatt, C., Harwood, L. and Mount, K. (2005). Concentrations of mercury in tissues of beluga whales (Delphinapterus leucas) from several communities in the Canadian Arctic from 1981 to 2002. *Science of the Total Environment* **351 - 351**: 178 - 179.

Loseto, L., Lean, D. and Siciliano, S. (2004). Snowmelt sources of methylmercury to high Arctic ecosystems. *Environmental Science and Technology* **38**: 3004 - 3010.

Loseto, L., Stern, G., Deibel, D., Connelly, T., Prokopowicz, A., Lean, D., Fortier, L. and Ferguson, S. (2008). Linking mercury exposure to habitat and feeding behaviours in Beaufort Sea beluga whales. *Journal of Marine Systems* **74**: 1012-1024.

Lu, J., Schroeder, W., Barrie, L., Steffen, A. and Welch, H. (2001). Magnification of atmospheric mercury deposition to polar regions in springtime: the link to tropospheric ozone depletion chemistry. *Geophysical Research Letters* **28**: 3219-3222.

Macdonald, R., Harner, T. and Fyfe, J. (2005). Recent climate change in the Arctic and its impact on contaminant pathways and interpretation of temporal trend data. *Science of the Total Environment* **342**(1-3): 5 - 86.

Mann, J., Long, S., Shuman, A. and Kelly, W. (2005). Determination of mercury content in a shallow firn core from Greenland by isotope dilution inductively coupled plasma mass spectrometry. *Water Air Soil Pollution* **163**: 19-32.

Mason, R. and Fitzgerald, W. (1990). Alkylmercury species in the equatorial Pacific. *Nature* **290**: 457-459.

Mason, R. and Fitzgerald, W. (1996). Sources, sinks and biogeochemical cycling of mercury in the ocean. *Global and regional mercury cycles: sources, fluxes and mass balances*. W. Baeyens. Netherlands, Kluwer Academic Publishers**:** 249-272.

Mason, R., Fitzgerald, W. and FMM, M. (1994). The biogeochemical cycling of elemental mercury: anthropogenic influences. *Geochimica et Cosmochimica Acta* **58**: 3191-3198.

Mason, R., Morel, F. and Hemond, H. (1995). The role of microorganisms in elemental mercury formation in natural waters. *Water Airl Soil Pollution* **80**: 775-787.

Maykut, G. A. (1978). Energy exchange over young sea ice in the central Arctic. *Journal of Geophysical Research* **83**: 3646 - 3658.

Møller, A., Barkay, T., Abu Al-Soud, W., Sørensen, S., Skov, H. and Kroer, N. (2010). Diversity and characterization of mercury-resistant bacteria in snow, freshwater, and sea-ice brine from the High Arctic. *FEMS Microbiology Ecology* **75**(3): 390-401.

Muir, D., Braune, B., DeMarch, B., Norstrom, R., Wagemann, R. and Lockhart, L. (1999). Spatial and temporal trends and effects of contaminants in the Canadian Arctic marine ecosystem: a review. *Science of the Total Environment* **230**: 83-144.

Notz, D., et.al. (2003). Impact of underwater-ice evolution on Arctic summer sea ice. *Journal of Geophysical Research* **108**(C7).

Ogrinc, N., Monperrus, M., Kotnik, J., Fajon, V., Vidimova, K., Amouroux, D., Kocman, D., Tessier, E., Zizek, S. and Horvat, M. (2007). Distribution of mercury and methylmercury in deep-sea surficial sediments of the Mediterranean Sea. *Marine Chemistry* **107**: 31-48.

Outridge, P. M., Macdonald, R. W., Wang, F., Stern, G. A. and Dastoor, A. P. (2008). A mass balance inventory of mercury in the Arctic Ocean. *Environ. Chem.* **5**: 89-111.

Pacyna, E., Pacyna, J., Steenhuisen, F. and Wilson, S. (2006). Global anthropogenic mercury emission inventory for 2000. *Atmospheric Environment* **40**: 4048-4063.

Parkinson, C. and Cavalieri, D. (2008). Arctic sea ice variability and trends, 1979 - 2006. *Jounral of Geophysical Research* **113**(CO7003).

Parkinson, C., Cavalieri, D., Gloersen, P., Zwally, H. and Comiso, J. (1999). Arctic sea ice extents, areas and trends, 1978-1996. *Journal of Geophysical Research* **104**(20): 837-856.

Petrich, C. and Eicken, H. (2010). Growth, Structure and Properties of Sea Ice. *Sea Ice, 2nd Ed.* D. Thomas and G. Dieckmann. Chichester, Blackwell Publishing**:** 23 - 78.

Poulain, A., Garcia, E., Amyot, M., Campbell, P. and Ariya, P. (2007). Mercury distribution, partitioning, and speciation in coastal vs. inland High Arctic snow. *Geochimica et Cosmochimica Acta* **71**: 3419 - 3431.

Poulain, A., Garcia, E., Amyot, M., Campbell, P., Raofie, F. and Ariya, P. (2007). Biological and Chemical Transformations of Mercury in Fresh and Salt Waters of the High Arctic during Spring and Summer. *Environmental Science and Technology* **41**: 1883-1888.

Poulain, A., Lalonde, J., Amyot, M., Shead, J., Raofie, F. and Ariya, P. (2004). Redox transformations of mercury in an Arctic snowpack at springtime. *Atmosphere Environment* **38**: 6763-6774.

Poulain, A., Ni Chadhain, S., Ariya, P., Amyot, M., Garcia, E., PCG, C., Zylstra, G. and Barkay, T. (2007). Potential for mercury reduction by microbes in the High Arctic. *Applied and Environmental Microbiology* **73**(7): 2230-2238.

Rankin, A. and Wolff, E. (2002). Frost Flowers: Implications for tropsospheric chemistry and ice core interpretation. *Environmental Science and Technology* **44**: 644-649.

Rigor, I. (2005). International Arctic Buoy Programme: Monitoring the Arctic Ocean since 1979. Sea Ice Mass Budget of the Arctic (SIMBA), Workshop report. Seatlle, WA, USA, Applied Physics Laboratory, University of Washington

Schroeder, W., Anlauf, K., Barrie, L., Lu, J., Steffen, A., Schneeberger, D. and Berg, T. (1998). Arctic springtime depletion of mercury. *Nature* **394**: 331 - 332.

Sherman, L., Blum, J., Johnson, K., Keeler, G., Barres, J. and Douglas, T. (2010). Mass-independent fractionation of mercury isotopes in Arctic snow driven by sunlight. *Nature Geoscience* **3**.

Sicilano, S., O'Driscoll, N. and Lean, D. (2002). Microbial reduction and oxidation of mercury in freshwater lakes. *Environmental Science and Technology* **36**: 3064-3068.

Simpson, W., Alvarez-Aviles, L., Douglas, T., Sturm, M. and Domine, F. (2005). Halogens in the coastal snow pack near Barrow, Alaska: Evidence for active bromine air-snow chemistry during springtime. *Geophysical Research Letters* **32**.

Simpson, W., Carlson, D., Honninger, G., Douglas, T., Strum, M., Perovich, D. and Platt, U. (2007). First-year sea-ice contact predicts bromine monoxide (BrO) levels at Barrow, Alaska better than potential frost flower contact. *Atmospheric Chemistry and Physics* **7**: 621-627.

Skov, H., Christensen, J., Goodsite, M., Heidam, N., Jensen, B., Wahlin, P. and Geernaert, G. (2004). Fate of elemental mercury in the Arctic during atmospheric mercury depletion episodes and the load of atmospheric mercury to the Arctic. *Environmental Science and Technology* **38**: 2373 - 2382.

Slemr, F., Schuster, G. and W, S. (1985). Distribution, speciation and budget of atmospheric mercury. *Journal of Atmospheric Chemistry* **3**: 407-434.

St. Louis, V., Hintelmann, H., Graydon, J., Kirk, J., Barker, J., Dimock, B., Sharp, M. and Lehnherr, I. (2007). Methylated mercury species in Canadian high Arctic marine surface waters and snowpacks *Environmental Science and Technology* **41**: 6433-6441.

St. Louis, V., Sharp, M., Steffen, A., May, A., Barker, J., Kirk, J., Kelly, D., Arnott, S., Keatley, B. and Smol, J. (2005). Some sources and sinks of monomethyl and inorganic mercury on Ellesmere Island in the Canadian High Arctic. *Environmental Science and Technology* **39**: 2686 - 2701.

Steffen, A., Douglas, T., Amyot, M., Ariya, P., Aspmo, K., Berg, T., Bottenheim, J., Brooks, S., Cobbett, F., Dastoor, A., Dommergue, A., Ebinghaus, R., Ferrari, C., Gardfeldt, K., Goodsite, M., Lean, D., Poulain, A., Scherz, C., Skov, H., Sommar, J. and Temme, C. (2007). A synthesis of atmospheric mercury depletion event chemistry linking atmosphere, snow and water. *Atmospheric Chemistry and Physics Discussions* **7**: 10837-10931.

Steffen, A., Schroeder, W., Bottenheim, J., Narayan, J. and Fuentes, J. (2002). Atmospheric mercury concentrations: measurements and profiles near snow and ice surfaces in the Canadian Arctic during Alert 2000. *Atmospheric Environment* **36**: 2653 - 2661.

Steffen, A., Schroeder, W., Macdonald, R., Poissant, L. and Konoplev, A. (2005). Mercury in the Arctic atmosphere: An analysis of eight years of measurements of GEM at Alert (Canada) and a comparison with observations of Amderma (Russia) and Kuujjuarapik (Canada). *Science of the Total Environment* **342**: 185-198.

Untersteiner, N. (1968). Natural desalination and equilibrium salinity profile of perennial sea ice. *Journal of Geophysical Research* **73**: 1251 - 1257.

USEPA (2002). Method 1631, Revision E: Measurement of mercury in water by CVAFS.

Van Loon, L., Mader, E. and Scott, S. (2000). Reduction of the aqueous mercuric ion by sulfite; UV spectrum of HgSO3 and its intramolecular redox reaction. *Journal of Physical Chemistry A* **104**: 1621-1626.

Van Oostdam, J., Gilman, A., Dewailly, E., Usher, P., Wheatley, B., Kuhmlein, H., Neve, S., Walker, J., Tracy, B., Feeley, M., Jerome, V. and Kwanvick, B. (2005). Human health implications of environmental contaminants in Arctic Canada: A review. *Environmental Science and Technology* **351-352**: 165-246.

Wang, F., Macdonald, R., Stern, G. and Outridge, P. (2010). When noise becomes the signal: Chemical contamination of aquatic ecosystems under a changing climate. *Marine Pollution Bulliten* **60**: 1633-1635.

Weeks, W. (1988). Profile properties of undeformed first-year sea ice. *CRREL Monogr.* **88**(13).

Weeks, W. and Ackley, S. (1982). The growth, structure and properties of sea ice. *CRREL Monogr.* **82**(1).

Wennberg, P. (1999). Bromine explosion. *Nature* **397**: 299-301.

Zhang, H. and Lindberg, S. (2001). Sunlight and iron(III)-induced photochemical production of dissolved gaseous mercury in freshwater. *Environmental Science and Technology* **35**: 928-935.

Zhao, T., Gong, S., Bottenheim, J., McConnell, J., Sander, R., Kaleschke, L., Richter, A., Kerkweg, A., Toyota, K. and Barrier, L. (2008). A three-dimensional model study on the production of BrO and Arctic boundary layer ozone depletion. *Journal of Geophysical Research* **113**.

# Chapter 2: Mercury Distribution and Transport across the Ocean-Sea Ice-Atmosphere Interface in the Western Arctic Ocean

The following chapter is a manuscript published in the journal of Environmental Science and Technology. The full citation is:

Chaulk A., Stern G.A., Armstrong D., Barber D., and Wang F. 2011. Mercury distribution and transport across the ocean-sea ice-atmosphere interface in the Arctic Ocean. Environ. Sci. Technol. 45, 1866-1872.

I was involved in field sampling, collecting a large portion of the data presented in this manuscript. As first author, I was responsible for completing a first draft of the manuscript, which including compiling data, generating tables, graphs and figures, and providing insight to interpretation of the data. With the guidance and input of the co-authors I completed several revised versions of the manuscript.

## Abstract

The Arctic sea ice environment has been undergoing dramatic changes in the past decades; to which extent this will affect the deposition, fate and effects of chemical contaminants remains virtually unknown. Here we report the first study on the distribution and transport of mercury (Hg) across the ocean-sea ice-atmosphere interface in the Southern Beaufort Sea of the Arctic Ocean. Despite being sampled at different sites under various atmospheric and snow cover conditions, Hg concentrations in first-year ice cores were generally low and varied within a remarkably narrow range (0.5 – 4 ng $L^{-1}$), with the highest concentration always in the surface granular ice layer which is characterized by enriched particle and brine pocket concentration. Atmospheric Hg depletion events appeared not to be an important factor in determining Hg concentrations in sea ice except for frost flowers and in the melt season when snowpack Hg leaches into the sea ice. The multi-year ice core showed a unique cyclic feature in the Hg profile with multiple peaks potentially corresponding to each ice growing/melting season. The highest Hg concentrations (up to 70 ng $L^{-1}$) were found in sea ice brine, and decrease as the melt season progresses. As brine is the primary habitat for microbial communities responsible for sustaining the food web in the Arctic Ocean, the high and seasonally changing Hg concentrations in brine and its potential transformation may have a major impact on Hg uptake in Arctic marine ecosystems under a changing climate.

## 2.1 Introduction

Mercury (Hg) is a global contaminant, and its persistently high concentrations in Arctic marine mammals (Lockhart *et al.* 2005; AMAP 2009; Dietz *et al.* 2009) have raised concerns over the health of these animals and the Northern People who consume these animals' tissues as part of their traditional diet (AMAP 2009). As a result, major research initiatives have been undertaken to understand the sources and pathways for Hg bioaccumulation in the Arctic marine ecosystems (Macdonald *et al.* 2005; Outridge *et al.* 2008). Evidence is now mounting that the highly variable Hg concentrations in Arctic marine mammals in recent decades are no longer a simple function of external, anthropogenic Hg emissions; instead, they are increasingly driven by changes in post-depositional processes that control the transport, transformation and biological uptake of stored Hg in the Arctic Ocean (Outridge *et al.* 2008; Wang *et al.* 2010). While such post-depositional processes are arguably of equal importance in determining Hg bioaccumulation in any ecosystems, what sets the Arctic Ocean apart is the vast sea-ice environment that has been undergoing dramatic changes due to climate warming (Macdonald *et al.* 2005; Barber *et al.* 2009; Kwok and Rothrock 2009). As a dynamic interface between the atmosphere and the ocean, the sea-ice environment in the Arctic has been postulated to play a major role in the occurrence of the atmospheric Hg depletion events (MDEs) (Schroeder *et al.* 1998), in controlling the magnitude and timing of atmospheric Hg flux to the aquatic system (Lalonde *et al.* 2002; Poulain *et al.* 2007), and potentially in affecting the biological Hg uptake with the changing epontic community. There are also suggestions that methylation of Hg may take place in the snowpack (Constant *et al.* 2007; Larose *et al.* 2010), producing monomethylmercury

($CH_3Hg^+$ and its complexes; MeHg hereafter) which is primarily responsible for the biomagnification and neurotoxicity of Hg. However, beyond a few studies on Hg in the overlying snow (Douglas *et al.* 2005; Poulain *et al.* 2007) and frost flowers (Douglas *et al.* 2005; Douglas *et al.* 2008), the dynamics of Hg in the Arctic sea-ice environment and across the ocean-sea ice-atmosphere (OSA) interface remains essentially unknown (Macdonald *et al.* 2005; Poissant *et al.* 2008).

Sea ice is a heterogeneous, semi-solid matrix composed of ice, brine, gases, particles, and biota (e.g., bacteria, viruses, algae). After the initial freezing of seawater, the microstructure and overall property of sea ice is modified by the interaction of physical, biological, and chemical processes; the details of sea ice dynamics are described elsewhere (Petrich and Eicken 2010; Thomas *et al.* 2010; Weeks 2010). Of particular importance related to Hg transport and transformation is the presence and dynamics of brine pockets and drainage tubes which are a unique feature of sea-ice formed when the sea water freezes and sea ice consolidates pushing out the enclosed salts. Brine pockets and drainage channels make sea ice permeable to the transport of gases and solutes, with the vertical fluid permeability being dependent upon the sea ice microstructure and brine volume fraction, which are, in turn, dependent upon temperature and salinity of the ice (Petrich and Eicken 2010). The distribution and transport of gases, inorganic macro-nutrients, and dissolved organic matter in sea ice have received increasing attention in recent years (Thomas *et al.* 2010), but the role of sea ice in polar and global biogeochemical processes has only started to be appreciated. As part of the International Polar Year (IPY) Circumpolar Flaw Lead (CFL) System Study (Barber *et al.* 2010), we report here the first comprehensive study on the distribution and transport

of Hg in various types of the sea ice environments in the southern Beaufort Sea and the processes governing the Hg dynamics across the OSA interface.

## 2.2 Materials and Procedures

### *2.2.1 Study Area*

The overall CFL study was carried out in the southern Beaufort Sea (Figure 2-1) from December 2007 to July 2008 onboard the CCGS Amundsen. The icebreaker remained mobile during the entire sampling period, allowing various ice types at multiple locations to be sampled (Barber *et al.* 2010). The results from 12 stations sampled from the period March 1 to May 25, 2008 are presented in this paper. These samples covered a range of ice types (newly formed ice, first-year ice (drift or landfast), and multi-year ice), thickness (0.5-380 cm), stages of ice formation (initial freeze-up, growth, and melt onset), extent of snow covers (0-40 cm), and atmospheric temperatures (-29.7 to 3.9 $^{o}$C) (see Table S1 in the Appendix).

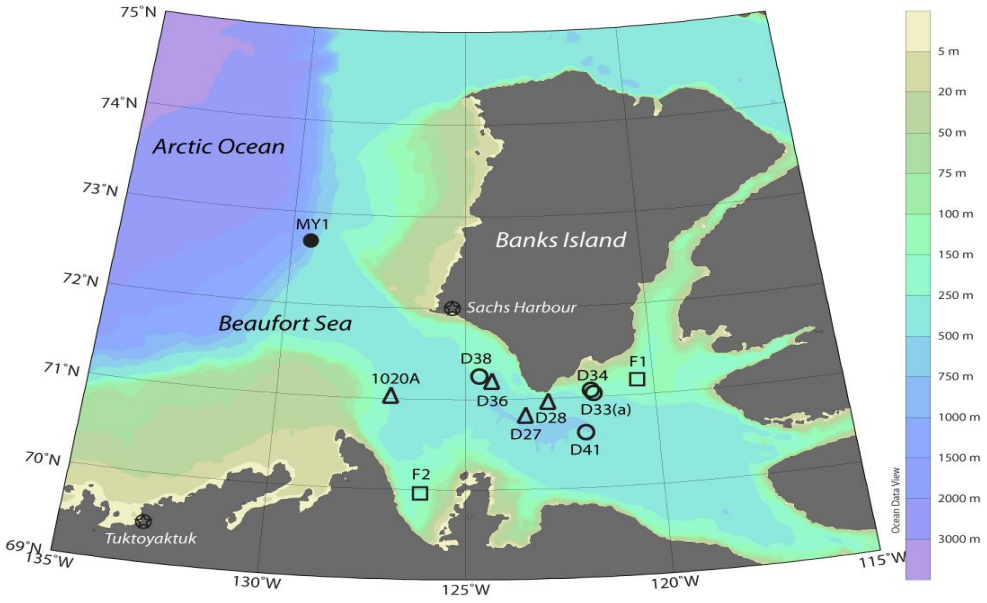


**Figure 2-1: Map of the study area showing the sampling stations. Open triangle: new ice; open circle: first-year drift ice; open square: land-fast ice; filled circle: multi-year ice. The base map was created by Ocean Data View (version 4.0) showing the bathymetry**

*2.2.2 Sampling*

All the sampling and sample preparation for Hg analysis were done following the clean-hands-dirty-hands sampling protocol (Fitzgerald 1999) to avoid cross contamination. Sample preparation and analysis were done at the Portable In-situ Laboratory for Mercury Speciation (PILMS), a Class 100 cleanroom laboratory onboard the icebreaker. All the sampling tools and Teflon sample bottles were pre-cleaned at PILMS and tested for acceptable Hg background (< 0.1 ng $L^{-1}$). The new 50-mL polypropylene Falcon sample tubes (BD) were found to contain extremely low Hg and thus no pre-cleaning was necessary as long as they were not re-used. However, each batch of the tubes was randomly tested for Hg before use. All the sampling tools and bottles were then doubly bagged in clean Zip-lock bags before being brought to the field. Field and procedural blanks were also performed along with each sampling or sample preparation. Ultrapure, Milli-Q element water (Millipore) produced from PILMS was

used as the laboratory water. Real-time in situ Hg speciation in the lower troposphere was continuously measured for the entire sampling duration (Latonas 2010). Seawater at various depths at most of the stations was also sampled for total Hg. The sampling was done via either the ship-borne rosette bottles or Teflon-coated Niskin bottles.

Newly formed thin ice was sampled on four occasions. The samples were collected in triplicate from a cage suspended directly over the ice using a ship-operated crane into 2-L Teflon bottles. After melted in PILMS, the samples were spiked with 250 µL ultrapure HCl (JT Baker) and 250 µL BrCl (prepared from KBr and $KBrO_3$ in ultrapure HCl) before being analyzed for Hg.

Sea ice cores were taken from 5 first-year, 1 multi-year and 2 land-fast ice stations. At each station, ice cores were retrieved using a Kovacs core barrel (I.D. = 9 cm). One core per station was designated for Hg, with the exception of Station D33 where two duplicate cores were taken for Hg. Replicate cores were also taken for measurements of temperature and ice texture, among many others. The Hg cores were stored in plastic bags in a chest freezer (-18$^{o}$C) onboard the icebreaker and then processed within 36 hr inside a cold lab (-20 $^{o}$C). Each core was cut into approximately 8-15 cm sections depending on the ice texture. Each section was halved to produce replicates, and the outer 0.5-1 cm was scraped off using a pre-cleaned ceramic blade knife (Kyocera, USA). The remaining samples were doubly bagged in clean zip-lock bags, melted in PILMS, decanted into new 50-mL polypropylene Falcon tubes, and spiked with ultrapure HCl and BrCl before being analyzed for Hg. Aliquots of the melted samples were also collected for the measurement of salinity. At two of the ice coring stations (D33 and F2), the overlying snowpack was also sampled; the depths ranged from

35 cm (D33) to 70 cm (F2). Samples for Hg analysis were collected, in duplicate, every 2-5 cm along a vertical profile into new 50 mL polypropylene Falcon tubes. Samples were brought back to PILMS, spiked with 125 μL of ultrapure HCl and melted before analysis.

Brine samples were collected from the vicinity of three of the ice core stations by the sump-hole method (Pucko *et al.* 2010) on a 12-hr cycle. In brief, 5 brine holes, less than 50 cm apart from each other, were drilled using the same core barrel used for ice core retrieval. The sump-holes were dug to a depth of 20, 40, 60, 80, and 100$\pm$1cm (never penetrating to the underling seawater), respectively, capped with a Styrofoam plug encased in a clean zip-lock bag to avoid cross contamination and refreezing, and left to allow the adjacent brine to seep in. After approximately 12 hr, seeped brine was collected using a pre-cleaned silicon baster. Samples were collected in duplicate from each hole into 50-mL new polypropylene Falcon tubes and doubly bagged in zip-lock bags. After the sampling, each hole was capped, and sampled for brine again approximately 24, 36 and 48 hr after it was initially dug. Upon returning to PILMS, the brine samples were diluted using the ultrapure water and analyzed for salinity and Hg.

*2.2.3 Analysis*

The analysis for Hg was done at PILMS by cold vapour atomic fluorescence spectroscopy on a Tekran 2600 Hg analyzer following the U.S. EPA Method 1631 (USEPA 2002). All the samples were analyzed within 24-36 hr after sampling. Certified reference material BCR-579 coastal seawater ([Hg] = 1.85 $\pm$ 0.5 ng $kg^{-1}$) was used as a quality control and the recovery varied from 91 – 110 %. The method detection limit was

0.01 ng $L^{-1}$, and the Hg in the field blanks were < 0.09 ng $L^{-1}$; field blank corrections were not applied to the data. Since no filtration was performed on the samples, the Hg data reported here are total Hg and are expressed based on per liter of melted water (snow or ice) or brine.

Temperature profiles of ice cores were established by in situ measurement performed on an additional ice core collected from each station. A model 4000 thermometer (Traceable Control Company) was inserted into freshly drilled holes (~ 5 mm deep) on the ice core at a resolution of 5 – 10 cm. The conductivity of the melted ice and brine samples was measured in the airlock of PILMS using a sensION5 conductivity meter (Hach). Salinity of the brine samples and bulk ice core samples was calculated from temperature and conductivity and reported unitless according to the practical salinity scale, and the brine volume fraction, $V_b$, in the sea ice samples was calculated from temperature and salinity (Cox and Weeks 1983).

Sea ice texture was determined following the method described by Sinha (Sinha 1977). In brief, the sea ice core was partitioned into 10-cm sections, with each section being cut into a rectangle and frozen onto a glass plate. The ice was then shaved down to a thickness of ~1 mm. Photographs of the thin ice section were taken under both non-polarized and polarized light to highlight ice crystal shape, size, and orientation. Sea ice texture was classified as granular (G), transitional granular (TG), columnar (C), and transitional columnar (TC).

## 2.3 Results

### *2.3.1 Sea Ice*

The concentration of Hg in newly formed thin ice samples ranged from 0.22 to 0.53 ng $L^{-1}$, which was about two fold the Hg concentration in the underlying surface seawater at the corresponding site (0.11-0.28 ng $L^{-1}$) (Table S2). MDEs (characterized by the 3-hr average [GEM] dropping below 1ng $m^{-3}$; (Latonas 2010)) occurred at the time of sampling at 3 of the stations (D27, D28, and 1020A; Figure S1). The Hg concentrations in the new ice (0.45-0.53 ng $L^{-1}$) and the surface seawater (0.24-0.28 ng $L^{-1}$) from these three stations were higher than those at Station D36 (0.22 ng $L^{-1}$ for new ice and 0.11 ng $L^{-1}$ for surface seawater) where no MDE was occurring at the time of sampling. The sample size is, however, not large enough to conclude whether the slightly higher Hg in the new ice and surface seawater was due to the enhanced Hg deposition as a result of MDEs.

Profiles of Hg, salinity and temperature in a first-year drift ice core (D33) and a landfast ice core (F2) and in their respective overlying snowpack are shown in Figure 2-2. Complete profiles for all the sea ice cores can be found in Figures S2 and S3. In all the first-year ice cores, the Hg concentration was the highest near the surface, decreasing sharply downwards to concentrations just above the underlying sea water (typically around 0.2 ng $L^{-1}$). Along with surface peaks of Hg, salinity in the surface of all ice cores was also elevated. With the exception of Station F2, the salinity profiles showed the characteristic C-shape, and the temperature profiles showed thermal stratification, increasing from the surface downward to the sea ice-water interface. The landfast ice

station F2 was sampled later in the season, with a near-isothermal temperature greater than -5°C and salinity of around 5, suggesting that the ice was in the early stage of melt.

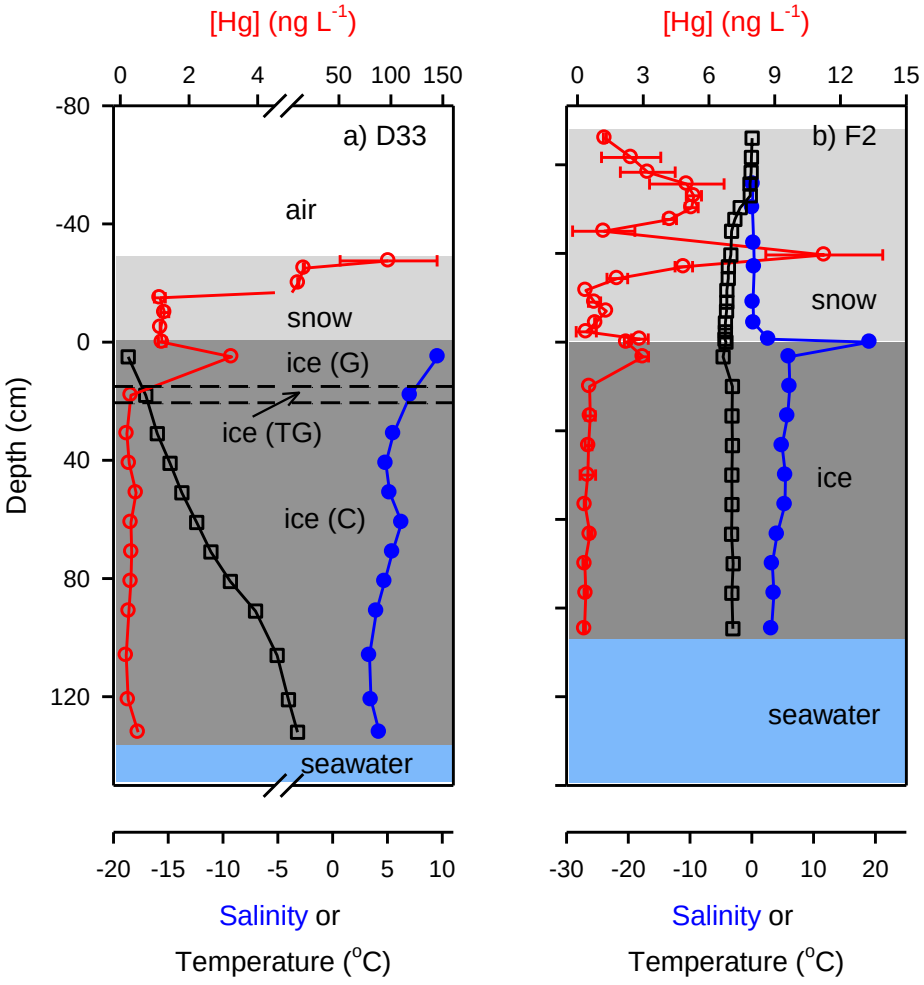


**Figure 2-2: Profiles of Hg (open circles), salinity (filled circles) and temperature (open squares) in the snow-covered ice cores from a drift ice station (D33, sampled on March 25, 2008) and a landfast ice station (F2, sampled on May 14, 2008). The air, snow, sea water boundaries are shown.**

The Hg concentration in the 380-cm multi-year sea ice core MY1 was elevated at the surface (> 4 ng $L^{-1}$) and then decreased sharply downwards to levels similar to that of the underlying sea water (Figure 2-3). A unique feature of this multi-year ice core is, however, that Hg concentrations showed a cyclic feature with several peaks spiking up to ~ 1.5 ng $L^{-1}$. Salinity of the multi-year ice was always lower than the critical value of 5.

Some but not all of the Hg and salinity peaks seem to be co-occurring, but there is no statistically significant correlation between Hg and salinity throughout the core ($p = 0.57$). The temperature profile was C-shaped ranging from -5.5 to -1 $^{o}$C.

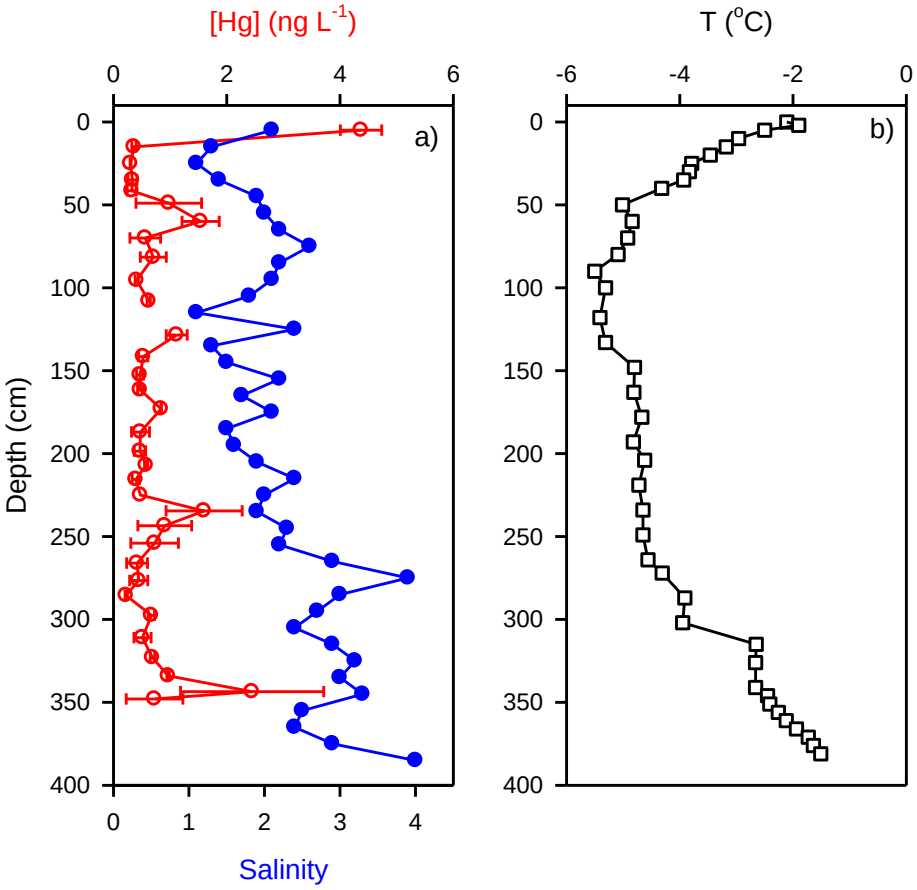


**Figure 2-3: Profiles of Hg (open circles), salinity (filled circles), and temperature (open squares) in a snow-covered multi-year ice core (MY1; May 25, 2010). The overlying snowpack was not analyzed for Hg.**

*2.3.2 Brine*

The Hg concentrations in the brine were markedly higher than those in the corresponding bulk ice cores (Figures 2-2, S2 and S3), although both showed a surface enrichment. The total Hg concentration in brine ranged from 2.6 to 71.2 ng $L^{-1}$, decreasing from the shallower sump-holes near the surface to deeper holes, and was

always much higher than that in the underlying seawater. Brine collected at various times after the sump-holes were drilled showed similar Hg distribution profiles, though the concentrations varied to a great extent (Figure S4). It should be noted that the depth data shown in Figure S4 refer to the depths to which the sump-holes were drilled. Because brine channels are interconnected and extend throughout the ice, mixture of brine pockets is not uncommon, resulting in uncertainty in the actual depth where the brine was associated. This is further complicated by the fact that the horizontal permeability of sea ice is poorly understood. For this reason, the depth data in Figure S4 can only be regarded as "nominal" depth of the brine samples.

## 2.4 Discussion

Mercury in sea ice ultimately originates from the underlying seawater and/or overlying atmosphere, potentially via three major processes: 1) freeze rejection of Hg from seawater; 2) scavenging of atmospheric Hg by the "bare" (i.e., not covered by snow) sea ice surfaces; and, 3) leaching of Hg from the overlying snow cover (where applicable). Once incorporated in the sea ice matrix, further internal transport and transformation may occur due to the permeability of sea ice, dynamics of brine movement, changing redox conditions, and presence of sea ice biota (Thomas *et al.* 2010). The relative importance of each of these processes is discussed below.

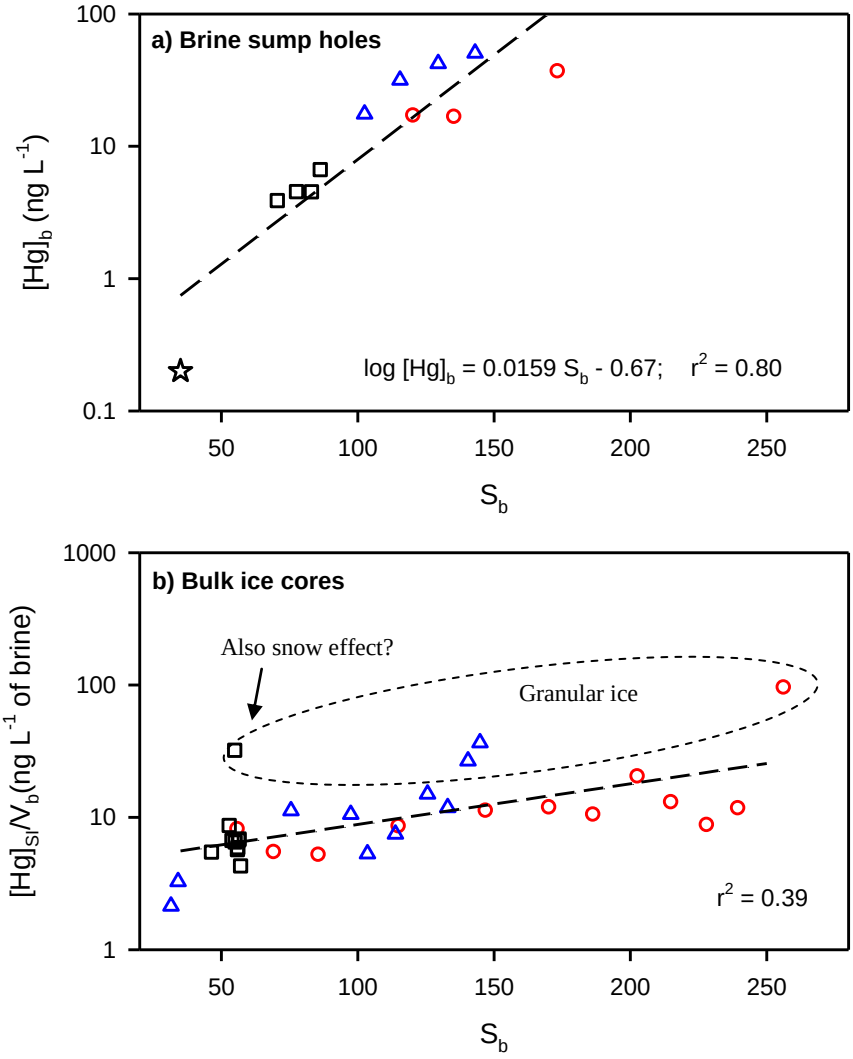


**Figure 2-4: Mercury concentrations in brine (a) or bulk sea ice (b) normalized to the brine volume fraction Vb) as a function of salinity.**

*2.4.1 Freeze rejection of Hg from seawater to sea ice*

During the sea ice formation process, major and minor dissolved species are known to be expelled from the ice crystal matrix, resulting in their accumulation and enrichment in brine pockets (Thomas *et al.* 2010; Weeks 2010). To test the relative contribution of freeze rejection in controlling the distribution of Hg in sea ice, we examined the relationship between salinity, $V_b$, and Hg concentration at three stations

(D33, D41 and F2) where both ice cores and brine drainage were sampled. Station D33 was sample in March during the ice growth season, whereas Stations F2 and D41 were sampled later in the season and the high $V_b$ values (> 5%) suggest that macroscopic fluid transport was occurring within the sea ice at these two stations during the time of sampling. Despite this difference, a strong logarithm relationship was found between the Hg concentration and salinity (Figure 2-4a), suggesting that Hg concentrations in the brine which seeps into the sump-holes can be explained reasonably well with salinity:

$$\log [Hg]_b = 0.0159\ S_b - 0.67 \qquad (r^2 = 0.80,\ n = 11,\ p < 0.001) \tag{1}$$

where $[Hg]_b$ and $S_b$ denote the Hg concentration and salinity of brine, respectively.

At a first approximation, the Hg concentration in bulk sea ice, $[Hg]_{si}$, can be described as:

$$[Hg]_{si} = [Hg]_{pi}(1-V_b) + [Hg]_b V_b \tag{2}$$

where $[Hg]_{pi}$ denotes Hg concentration in the pure ice phase, respectively. Assuming $[Hg]_{pi} << [Hg]_b$, Eq (2) can be simplified to:

$$[Hg]_{si}/V_b = [Hg]_b \tag{3}$$

If freeze rejection is the dominant process for Hg concentration in the bulk sea ice, then a linear log $[Hg]_{si}/V_b$ relationship would be expected with $S_b$. As shown in Figure 2-4b, although there is a general increasing trend in log ($[Hg]_{si}/V_b$) with increasing $S_b$, $S_b$ only explains about 39% of the variance in log $[Hg]_{si}/V_b$, suggesting that the Hg concentration in the bulk sea ice core cannot be explained by freeze rejection only. Therefore, either $[Hg]_{pi}$ is not negligible when compared with $[Hg]_b$ due to, for example, the presence of Hg-containing particulates, or there are other pathways of Hg to the sea ice other than freeze rejection. This is particularly the case for the surface ice

layer where the Hg concentration was much more elevated than the salinity curve would have predicted.

*2.4.2 Influence of granular ice on Hg distribution in sea ice*

The observations that the surface enrichment occurred to all the ice cores and that the surface sea ice Hg concentration varied within a rather narrow range (0.5–4.0 ng $L^{-1}$), regardless of season or brine Hg concentrations, suggest that this surface enrichment is a ubiquitous phenomenon related to the growth of sea ice. In the initial stages of sea ice growth, frazil ice crystals form in the near-surface layer of the water column before rising to the surface (Weeks 2010). In nature, such nucleation of frazil sea ice crystals occurs almost always heterogeneously with the aid of existing particles (Weeks 2010). Although sea ice particles were not collected and analyzed in this study, Hg is known to have a high affinity to aquatic particles. Furthermore, the surface frazil layer of sea ice is known to have the highest number densities of brine pockets when compared with the transitional and columnar sea ice (Weeks 2010) (see also Figure S5). The enrichment of particles and brine pockets in frazil ice is thus most likely responsible for the enrichment of Hg in the surface layer of the ice core. This is confirmed by the sea ice texture analysis. As shown in Figures S2, S5 and S6, except for Core D33a, granular ice (where frazil ice is located) was present in the top 4-26 cm of the ice core in all the cores that were analyzed (Cores F2 and MY1 were not examined for texture), the same depths where Hg enrichment was generally observed. Indeed, the three surface points in sea ice Cores D33 and D41 that positively deviate the salinity relationship in Figure 2-4b are all corresponding to granular ice.

*2.4.3 Sea ice scavenging of atmospheric Hg*

After the frazil ice crystals rise to the surface of the ocean, the new ice is exposed to the atmosphere. The observation that the Hg concentration in new ice, even when it was formed during active MDEs, was in the same order of magnitude to that of the underlying seawater (Table S2) suggests that the surface of new ice is not an effective scavenger of Hg(0) or Hg(II) from the troposphere. This is in sharp contrast from Arctic frost flowers which have been shown to contain extremely high Hg concentrations, particularly when in the vicinity of open leads during the MDEs (Douglas *et al.* 2005). This difference is, however, not unexpected, as ice crystals of frost flowers grow kinetically from the vapour phase and thus are more affected by Hg concentrations in the atmosphere (Douglas *et al.* 2008), whereas the frazil ice crystals grow from the underlying seawater.

*2.4.4 Snow cover as a source of Hg enrichment in surface sea ice*

Different from sea ice, snow has been shown to be an effective scavenger of atmospheric Hg; Hg concentrations in Arctic snow typically range from the low ng $L^{-1}$ to tens of ng $L^{-1}$, and can reach as high as several hundreds of ng $L^{-1}$ during AMDEs (Douglas *et al.* 2008). Although Hg(II) deposited in surface snow is known to undergo photoreduction and reemit back to the atmosphere as Hg(0) (Lalonde *et al.* 2002), accumulation of Hg in snowpack occurs when the previously exposed snow is covered by new snowfall. As a result, the snow – sea ice interface has been shown to be a site for Hg accumulation (Poulain *et al.* 2007), and the Hg accumulated at the interface could be leached to the underlying sea ice by upwards migration of brine (Hudier and Shirasawa

1995), or by melting of snow later in the season.

The impact of Hg in snow cover on Hg in surface sea ice was studied at two first-year sea ice stations D33 and F2 where Hg profiles in both the snow cover and underlying sea ice core were measured (Figure 2-2). D33 was sampled in the midst of an MDE (Table S2) which gave rise to the very high and variable Hg concentration (~100 ng $L^{-1}$) in the surface snow (Figure 2-2a). F2 was sampled after the MDE season and thus the surface snow Hg concentration was much lower (~1 ng $L^{-1}$). However, the sub-surface peaks in the snow cover at F2 may have recorded the signature of earlier MDE events, though the peak Hg concentration was much lower than the surface peak of D33 likely due to the loss via photoreduction.

As shown in Figure 2-2b, the concentration of Hg in the topmost layer of sea ice at Station F2 agreed very well with those in the deepest layer of snow that was immediately above it, suggesting a possible pathway of Hg transport from the overlying snow to surface sea ice. However, no such transport is evident at Station D33 (Figure 2-2a). Despite very high Hg concentration in the surface snow at this site, the Hg concentration remained very low (1 ng $L^{-1}$) at the deeper layer of the snowpack. The observation that a much higher Hg concentration (~ 4 ng $L^{-1}$) was found in the topmost sea ice suggests that snowpack did not affect the Hg concentration in the sea ice at this site. The different results observed at these two stations may be due to the difference in the sampling season. Station F2 was sampled at a time when partial melting had occurred, which would have facilitated the leaching of Hg from snowpack to the underlying sea ice. Such leaching could not have occurred to any significant extent at D33 which was sampled in the ice growth season.

*2.4.5 Perennial variations in Hg concentrations in multi-year sea ice*

Whereas first-year sea ice cores generally showed one surface Hg peak, at least 5 Hg peaks can be identified in the 350-cm multi-year sea ice core MY1, at approximately 0 cm, 60 cm, 120 cm, 230 cm, and 350 cm (Figure 2-3). If the surface enrichment in first-year sea ice is due to the frazil ice (granular ice) and/or snow melt, each of these peaks in the multi-year ice core may have corresponded to the growth of a distinct snow-ice layer during a period of surface melt and refreeze. We thus estimate that the multi-year ice at Station MY1 has been growing for at least 5 years, with the top 60 cm representing the most recent year (2008 in this case). The peaks at lower depths had lower Hg concentrations, likely due to loss of Hg via brine drainage (see below) and melting over the years. Unfortunately no other data were available for this core to verify its age independently; $\delta^{18}O$ was only measured in three discrete sections of the core, the resolution of which was insufficient to date the core.

*2.4.6 Hg transport via brine*

Different from the sea ice Hg profiles, Hg profiles in brine showed significant seasonal variations. The brine stations sampled in April (D33 and D41), when the atmospheric temperature was low, showed much higher Hg concentrations (up to 70 ng $L^{-1}$) than in the brine sampled at station F2 (up to 6 ng $L^{-1}$) in mid-May when the atmospheric temperature was close to $0^{o}C$. It has been generally thought that, in first-year sea ice, when $V_b$ is greater than 5% (approximately corresponding to a salinity of <5 and temperature of < $-5^{o}C$; "Rule of 5s") brine pockets interconnect and fluid transport occurs at the macroscopic level and is the predominate mechanism of fluid transport

through brine channels within the ice (Petrich and Eicken 2010; Weeks 2010). Therefore, as the ice warms, solid ice begins to melt adding fresh water to the brine pockets causing a dilution of ions and other chemicals within (Weeks 2010). Brine pockets then begin to interconnect to form brine channels. As the melt season progresses, sea ice is rapidly desalinated as the melt water begins to flush brine out of the ice into the underlying seawater (Weeks 2010). This is clearly shown in the Hg and salinity profiles of sea ice cores at Station F2 and MY1, and in the brine at station F2 (Figures 2-2,2-3,S4).

*2.4.7 Transformation of Hg in sea ice*

In addition to physical transport, chemical transformation among various Hg species could also occur within sea ice, particularly in highly saline and redox-sensitive brine. In natural waters it has been shown that high concentrations of $Cl^-$ can enhance the photo-oxidation of dissolved elemental Hg ($Hg^0_{aq}$) to Hg(II) in the presence of a suitable oxidant (e.g., biogenic organic compounds) (Lalonde *et al.* 2004; Poulain *et al.* 2007), though the mechanism remains to be elucidated (Qureshi *et al.* 2010). The porous nature of sea ice suggests that the $Hg^0_{aq}$ diffused into brine could be subject to oxidation due to the availability of UV radiation and high $Cl^-$ concentrations as indicated by the high salinity (Fig. S4). However, such $Cl^-$-enhanced oxidation of $Hg^0_{aq}$ is unlikely a significant source of the observed high Hg(II) concentration in brine, as concurrent measurements showed that the concentration of dissolved gaseous Hg (the majority of which is $Hg^0_{aq}$) in the sea-ice covered seawater in the study area was typically around 0.1 ng $L^{-1}$ , and rarely exceeded 0.3 ng $L^{-1}$ (Latonas 2010). On the contrary, photoreduction of Hg(II) in surface brine is probably of more significance, which could result in

localized enrichment of GEM. Furthermore, the recent discovery that anaerobic conditions can develop in sea ice (Rysgaard and Glud 2004) suggests that the production of MeHg, with sulfate reducing bacteria being the major Hg(II) methylator (Fitzgerald *et al.* 2007), could potentially occur in sea ice. Seasonal measurement of MeHg in sea ice brine is thus warranted.

Since sea ice brine is the primary habitat for microbial communities responsible for sustaining the food web in the Arctic Ocean (Thomas and Dieckmann 2002), the high and seasonally changing Hg concentrations and speciation of Hg in sea ice brine could potentially have a major impact on Hg uptake by the Arctic marine ecosystem. As perennial sea ice is melting at an alarming rate (Barber *et al.* 2009; Kwok and Rothrock 2009), the Arctic Ocean will shift to a primarily first-year ice regime. The seasonal increase in first-year sea ice will likely provide more Hg-rich environments (i.e., brine) for primary producers, potentially increasing food web exposure to this contaminant.

Acknowledgments. This research was part of the Circumpolar Flaw Lead System Study and ArcticNet. Funding was provided by the International Polar Year Program, the Natural Science and Engineering Research Council of Canada, the Canadian Foundation for Innovation, the Canada Research Chair program, and the Northern Scientific Training Program of Indian and Northern Affairs Canada. We thank M. Pucko, J. Latonas, A. Burt, A. Rossnagel and many other scientists onboard the CCGS Amundsen for their assistance in field sampling, and the crew for facilitating all the sampling endeavors.

Supporting Information - Two tables and 6 figures (in Appendix).

## 2.5 References


AMAP (2009). AMAP Assessment 2009: Human Health in the Arctic. Arctic Monitoring and Assessment Program. Oslo, Norway.

Barber, D., Asplin, M., Gratton, Y., Lukovich, J., RJ, G., Raddatz, R. and Leitch, D. (2010). The International Polar Year (IPY) Circumpolar Flaw Lead (CFL) System Study: Overview and the Physical System. *Atmosphere-Ocean*.

Barber, D., Galley, R., Asplin, M., De Abreu, R., Warner, K., Pucko, M., Gupta, M., Prinsenberg, S. and Julien, S. (2009). Perennial pack ice in the southern Beaufort Sea was not as it appeared in the summer of 2009. *Geophysical Research Letters* **36**(L24501).

Constant, P., Poissant, L., Villemur, R., Yumvihoze, E. and Lean, D. (2007). Fate of inorganic mercury and methyl mercury within the snow cover in the low Arctic tundra on the shore of Hudson Bay (Quebec, Canada). *Journal of Geophysical Research* **112**.

Cox, G. and Weeks, W. (1983). Equations for Determining the Gas and Brine Volumes in Sea Ice Samples.

Dietz, R., Outridge, P. and Hobson, K. (2009). Anthropogenic contributions to mercury levels in present-day Arctic animals - A review. *Science of the Total Environment* **407**: 6120-6130.

Douglas, T., Sturm, M., Simpson, W., Brooks, S., Lindberg, S. and DK, P. (2005). Elevated mercury measured in snow and frost flowers near Arctic sea ice leads. *Geophysical Research Letters* **32**.

Douglas, T., Sturm, M., Simpson, W., JD, B., Alvarez-Aviles, L., Keeler, G., Pervoich, D., Biswas, A. and Johnson, K. (2008). Influence of snow and ice crystal formation and accumulation on mercury deposition to the Arctic. *Environmental Science and Technology* **42**: 1542-1551.

Fitzgerald, W. (1999). Clean hands, dirty hands: Clair patterson and the aquatic biogeochemistry of mercury. *Clean hands, Clair Patterson's crusade against environmental lead contamination*. C. I. Davidson. New York, Nova Science**:** 119 - 137.

Fitzgerald, W., Lamborg, C. and Hammerschmidt, C. (2007). Marine biogeochemical cycling of mercury. *Chemical Review* **107**: 641-662.

Hudier, E. and Shirasawa, K. (1995). Upward Flushing of Seawater through First Year Ice. *Atmosphere-Ocean* **33**(3): 569-580.

Kwok, R. and Rothrock, D. (2009). Decline in Arctic sea ice thickness from submarine ICESat records: 1958-2008. *Geophysical Research Letters* **36**.

Lalonde, J., Amyot, M., J, O., Morel, F., Auclair, J. and Ariya, P. (2004). Photoinduced Oxidation of $Hg^0$(aq) in the Waters from the St. Lawrence Estuary *Environmental Science and Technology* **38**: 508-514.

Lalonde, J., Poulain, A. and Amyot, M. (2002). The role of mercury redox reactions in snow on snow-to-air mercury transfer. *Environmental Science and Technology* **36**: 174-178.

Larose, C., Dommergue, A., De Angelis, M., Cossa, D., Averty, B., Marusczak, N., Soumis, N., Schneider, D. and Ferrari, C. (2010). Springtime changes in snow chemistry lead to new insights into mercury methylation in the Arctic. *Geochimica et Cosmochimica Acta* **74**: 6263-6275.

Latonas, J. (2010). Measurements of Atmospheric Mercury, Dissolved Gaseous Mercury, and Evasional Fluxes in the Amundsen Gulf: The Role of the Sea-Ice Environment. Department of Environment and Geography. Winnipeg, University of Manitoba. **Master of Science**.

Lockhart, W., Stern, G., Wagemann, R., Hunt, R., DeLaronde, J., Dunn, B., Stewart, R., Hyatt, C., Harwood, L. and Mount, K. (2005). Concentrations of mercury in tissues of beluga whales (Delphinapterus leucas) from several communities in the Canadian Arctic from 1981 to 2002. *Science of the Total Environment* **351 - 351**: 178 - 179.

Macdonald, R., Harner, T. and Fyfe, J. (2005). Recent climate change in the Arctic and its impact on contaminant pathways and interpretation of temporal trend data. *Science of the Total Environment* **342**(1-3): 5 - 86.

Outridge, P., Macdonald, R., Wang, F., Stern, G. and Dastoor, A. (2008). A mass balance inventory of mercury in the Arctic Ocean. *Environmental Chemistry* **5**: 89-111.

Petrich, C. and Eicken, H. (2010). Growth, Structure and Properties of Sea Ice. *Sea Ice, 2nd Ed.* D. Thomas and G. Dieckmann. Chichester, Blackwell Publishing**:** 23 - 78.

Poissant, L., Zhang, H., Canario, J. and Constant, P. (2008). Critical review of mercury fates and contamination in the arctic tundra ecosystem. *Science of the Total Environment* **400**: 173-211.

Poulain, A., Garcia, E., Amyot, M., Campbell, P. and Ariya, P. (2007). Mercury distribution, partitioning, and speciation in coastal vs. inland High Arctic snow. *Geochimica et Cosmochimica Acta* **71**: 3419 - 3431.

Poulain, A., Garcia, E., Amyot, M., Campbell, P., Raofie, F. and Ariya, P. (2007). Biological and Chemical Transformations of Mercury in Fresh and Salt Waters of the High Arctic during Spring and Summer. *Environmental Science and Technology* **41**: 1883-1888.

Pucko, M., Stern, G., Macdonald, R. and Barber, D. (2010). α- and γ-hexachlorocyclohexane (HCH) measurements in the brine fraction of sea ice in the Canadian High Arctic using a sump-hole technique. *Environmental Science and Technology* **44**(24): 9258-9264.

Qureshi, A., O'Driscoll, N., Macleod, M., Neuhold, Y. and Hunggerbuhler, K. (2010). Photoreactions of Mercury in Surface Ocean Water: Gross Reaction Kinetics and Possible. *Environmental Science and Technology* **44**: 644-649.

Rysgaard, S. and Glud, R. (2004). Anaerobic $N_2$ production in Arctic sea ice. *Linology and Oceanography* **49**: 86-94.

Schroeder, W., Anlauf, K., Barrie, L., Lu, J., Steffen, A., Schneeberger, D. and Berg, T. (1998). Arctic springtime depletion of mercury. *Nature* **394**: 331 - 332.

Sinha, N. (1977). Technique for studying structure of sea ice. *Journal of Glaciology*(18): 315 - 323.

Thomas, D., Papadimitriou, S. and Michel, C. (2010). Biogeochemistry of Sea Ice. *Sea Ice, 2nd Ed.* . D. Thomas and G. Dieckmann. Chickester, UK, Wiley-Blackwell**:** 425-467.

Thomas, D. N. and Dieckmann, G. (2002). Antarctic sea ice: A habitat for extremophiles *Science* **295**: 641-644.

USEPA (2002). Method 1631, Revision E: Measurement of mercury in water by CVAFS.

Wang, F., Macdonald, R., Stern, G. and Outridge, P. (2010). When noise becomes the signal: Chemical contamination of aquatic ecosystems under a changing climate. *Marine Pollution Bulletin* **60**: 1633-1635.

Weeks, W. (2010). *On Sea Ice*. Fairbanks, AK, USA, University of Alaska Press.

# Chapter 3: Mercury Behavior in the Snow Pack: from Spring-Time Deposition to Melt


## Abstract

Significantly high concentrations of neurotoxic methylmercury (MeHg) in Arctic marine mammals have driven wide spread investigation of the processes involved in mercury cycling and bioaccumulation in the Arctic. Here we report a comprehensive time series of total mercury (THg) measurements in surface snow, snow pits, and melt ponds in the Beaufort Sea of the Arctic Ocean during and after the 2008 atmospheric mercury depletion events (AMDE) season (February – June). The THg concentration in surface snow varied greatly, ranging from 1.0 – 290 ng $L^{-1}$, with the highest values observed during active AMDEs. Analysis of surface snow and vertical profiles of snow pits revealed a net accumulation of THg in the snow pack due to the short time intervals between successive AMDE events, as well as the continuous burial by new or windblown snowfall. Contrary to coastal sites, in the Beaufort Sea there is insufficient time between subsequent AMDEs to allow for re-volatilization of deposited Hg. Rates of deposition of atmospheric Hg ranged from 200 – 784 ng $m^{-2}$ into the top 1cm of snow. At one station it is estimated at less than 50% of the deposited Hg is re-emitted to the atmosphere. The THg concentration in melt ponds in later spring was 20- to 40- fold higher than that measured in the underlying seawater. It is suggested that in the Beaufort Sea, where AMDEs occur frequently due to dynamic nature of the sea ice environment, a larger than previously reported portion of atmospherically deposited Hg can be retained in the snow

pack and enter the underlying marine system upon melt later in the season.

## 3.1 Introduction

Despite there being no anthropogenic sources of Hg, the Arctic has become exposed to anthropogenic Hg primarily via long-range atmospheric transport (Cheng and Schroeder 2000). Methyl mercury (MeHg), the biomagnifying and neurotoxic form of Hg, has been found to be present at significantly high concentrations in a range of Arctic marine mammals, raising serious concern over the health of these animals and the Northerners who consume animal tissues as part of their traditional diet (Macdonald *et al.* 2005; Van Oostdam *et al.* 2005; Hylander and Goodsite 2006).

The processes involved in Hg cycling and biomagnification in the Arctic marine environment are widely investigated. Atmospheric mercury depletion events (AMDEs) were first characterized at Alert, Canada in 1995 (Schroeder *et al.* 1998) and involve the oxidation of gaseous elemental mercury (GEM, $Hg^0$) in the lower troposphere to the divalent reactive gaseous mercury (RGM, Hg(II)) and particulate mercury (PHg). They occur seasonally during polar sunrise (occurring anytime from late January to early June in the Arctic) in high-latitude regions concurrently with the depletion of atmospheric ozone (Schroeder *et al.* 1998). In brief, the process begins with photochemically formed halogen radicals which react with ozone and generating halide oxide radicals, producing more halogen radicals. These highly reactive halogen radicals, especially Br, are thought to be primarily responsible for the oxidation of GEM to produce RGM (Schroeder *et al.* 1998). It is postulated that AMDEs are an important pathway by which atmospheric Hg could enter into the Arctic marine aquatic ecosystem (Schroeder *et al.* 1998; Lu *et al.*

2001; Lindberg *et al.* 2002; Steffen *et al.* 2005).

The occurrence and intensity of AMDEs is linked with reactive halogens derived from sea salt aerosols (Lindberg *et al.* 2002; Skov *et al.* 2004). The RGM generated *via* this series of reactions exhibits a much shorter atmospheric lifetime than GEM as it is rapidly scavenged from the atmosphere by aerosols and snowfall (Lindberg *et al.* 2002; Skov *et al.* 2004). Concentrations of Hg in surface snow only a few hours post-AMDE have been reported to be 200- to 800-times higher than background Hg levels (Lu *et al.* 2001; Steffen 2008; Dommergue 2010). It has been estimated, using kinetic models, that the gross input of Hg *via* AMDEs to the Arctic is 100-120 tons $year^{-1}$ (Ariya *et al.* 2004; Skov *et al.* 2004). However, these model predictions may be erroneous as they fail to take into account the spatial and temporal variability in Hg concentrations in snow (Douglas *et al.* 2005; Douglas *et al.* 2008), and do not adequately estimate post depositional Hg loss from the snow pack. A growing body of evidence suggests that the majority of RGM deposited during an AMDE is photo-reduced and re-emitted to the atmosphere (Steffen *et al.* 2002; Dommergue *et al.* 2003; Lalonde *et al.* 2003; Poulain *et al.* 2004; Lahoutifard *et al.* 2005; Dommergue 2010). The remaining RGM could potentially be transferred to the aquatic system during the spring melt (Domine *et al.* 2002; Lindberg *et al.* 2002; Steffen *et al.* 2002; Dommergue *et al.* 2003; Ferrari *et al.* 2005; Chaulk *et al.* 2011). The timing of this melt and subsequent delivery of Hg to the aquatic system can be important as it coincides with a period of increasing biological activity (Loseto *et al.* 2004).

In the Arctic, the snow pack can dramatically affect atmosphere-surface interactions and associated feedbacks to the climate system. For example, given its high albedo, snow can reflect as much as 90% of incoming radiation thus acting as an insulator

and affecting the growth of sea ice (Maykut 1986; Hinkler *et al.* 2008). It also has a strong impact on tropospheric chemistry, mediating gaseous and particulate exchange of chemicals between the atmosphere, as well as hosting a series of chemical reactions (Domine *et al.* 2002). The distribution of these chemicals within the snow pack is also mediated by snow metamorphism and seasonal progression (Kuhn 2001; Domine *et al.* 2002).

As incoming solar radiation increases and temperatures warm up the Arctic cryosphere begins to melt. Melt ponds on sea ice are formed when the oceanic heat flux into the ice-water interface exceeds the conductive heat flux out of the interface (Petrich and Eicken 2010). Melt ponds form at the ice-water interface (under-ice) as well as the ice-atmosphere interface and are considerably less saline than the underlying seawater or ice that separates them (Petrich and Eicken 2010). This is attributed to the fact that melt ponds are formed primarily of the melted snow. It has been estimated that approximately 25% of the melt water remains in the pond while 50% percolates down through the ice, flushing out salt in the process. The remaining 25% runs off into the ocean (Petrich and Eicken 2010).

Here, we present a series of total Hg measurements in surface snow, snow pits, and melt ponds sampled over a five month period (February to June 2008) in the Beaufort Sea of the Western Arctic Ocean. The transfer, storage, and subsequent release of Hg from the snow pack are discussed. The potential for atmospherically derived mercury to enter the water column is discussed as well as the implications on the marine biological system under a changing climate.

## 3.2 Methods & Materials

### *3.2.1 Sampling Location*

Sampling was carried out in the Western Arctic Ocean and Beaufort Sea from 4 February 2008 to 12 June 2008, as part of an 18-month scientific expedition (Circumpolar Flaw Lead System Study) of the Canadian Research Icebreaker CCGS Amundsen (Barber *et al.* 2010). The ship remained mobile during the entire sampling period, allowing various drifting and land fast ice locations to be sampled throughout the winter season and spring melt (Figure 3-1). All sampling was conducted upwind of the ice-breaker and away from other on ice activities in an effort to minimize contamination from the exhaust produced by the ship, generators and snowmobiles.

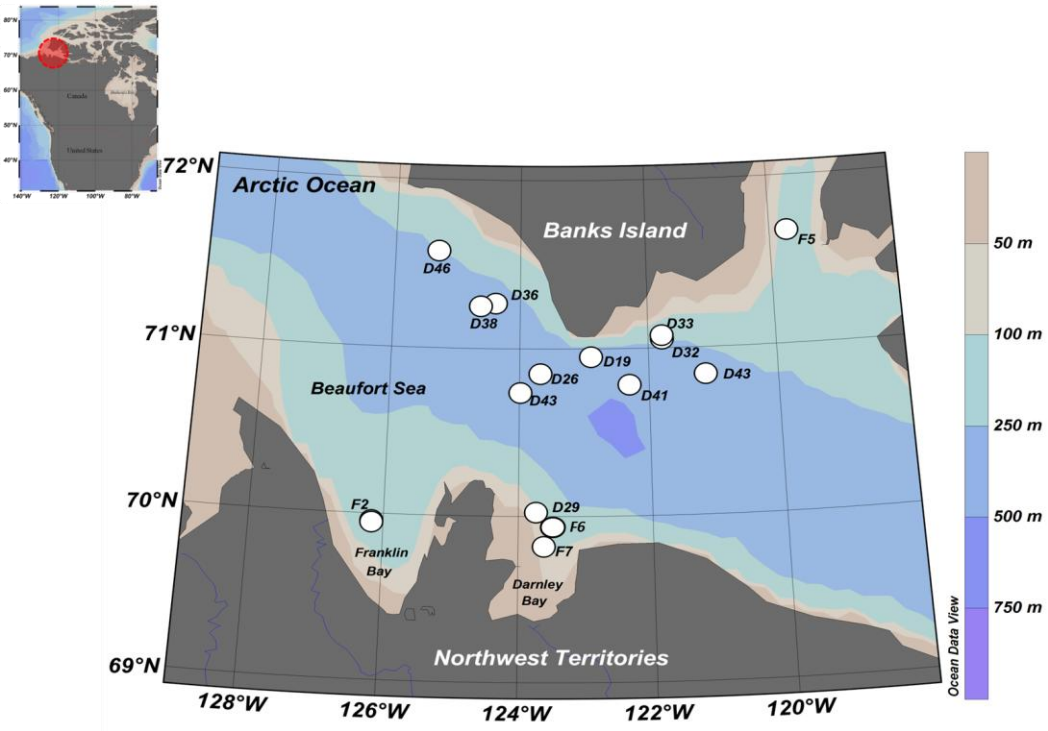


**Figure 3-1: Map of the study location (shown in the red circle of inset map). Stations beginning with F represent fast ice stations and D represent drift ice stations. Fir drift ice stations, the location on the map represents the position of the ice floe on day 1 at the station. While remaining with the same floe of ice the station was subject to drift.**

*3.2.2. Sample collections*

All the sample preparation, pretreatment and analysis were carried out at the Portable In-situ Laboratory for Mercury Speciation (PILMS), a Class 100 clean room laboratory onboard the icebreaker (Chaulk *et al.* 2011). Milli-Q Element water produced from PILMS was used as the ultra-pure water for all purposes. All lab ware and sampling equipment was cleaned (by soaking in a 10% HCl acid bath and then rinsing with Milli-Q water) and tested (by soaking in Hg free water, then analyzing the water) for Hg contamination prior to use. A subset of the sample vials 50 mL Falcon tubes (VWR) were also pre-tested for Hg contamination. Levels were consistently low and ranged from a peak area count <30 or [Hg] < 0.1 ng $L^{-1}$. All field samples were collected using the clean hands/dirty hands sampling protocol to avoid contamination (Fitzgerald 1999) and the filled Falcon tubes double bagged in clean zip-locks. All samples collected for Hg analysis were brought back to PILMS, spiked to 0.5% acid with ultrapure HCl (JT Baker), melted and stored at 4$^{o}$C until analysis.

Surface snow (< the topmost 50 mm of snow) was collected twice daily (morning and afternoon, conditions permitting) and in triplicate from 4 February to 30 June 2008 (Figure 3-1). Samples were collected by skimming the Falcon tube along the surface of the snow. One site at each station was designated for surface snow collected and all surface snow samples from that station were collected in the same spot. Two field blanks were collected during each sampling event.

Snow pits were sampled at different times and locations: February 4 (Station D19), March 26 (Station D33), April 20 (Station D43) and May 13 (Station F2) 2008 (Figure 3-1). The snow pit depths ranged from 9 cm (April 30) to 70 cm (May 13). Samples for total mercury analysis were collected, in duplicate at a vertical resolution of

2-5 cm. Snow temperature was measured at the time of sampling by inserting a model 4000 thermometer (Traceable Control Company) into the snow pack at the desired depth. At two stations (April 20 and May 13), samples of snow at depths were also collected for salinity measurement using a 2cm x 2cm density snow cuter. Samples for salinity analysis were collected and left to melt in whirlpool bags. Once melted, the conductivity of snow samples was measured using a sensION5 conductivity meter (Hach) which calculated salinity (based on measured conductivity and temperature).

Melt ponds (< 10 cm deep) were sampled daily for water, in triplicate, from 30 May to 9 June 2008 at two landfast ice stations (Station F6 & F7) in Darnley Bay (Figures 3-1 & 3-2). At each station, samples were collected from melt ponds with and without a thin layer of surface ice. Upon visual inspection, care was taken to make sure that the two pond types were isolated from each other. A sample of the over lying ice cover was collected only from station F7. Sampling of overlying snow cover had limited success as most of the snow had already melted.

**Figure 3-2: Melt pond sampling using the baster at a melt pond in Darnley Bay. Photo: J. Latonas**

Real time measurement of mercury species in the atmosphere (GEM, RGM & PHg) was carried out using a Tekran model 1130/1135 Hg speciation system. The pyrolyzer unit was mounted on the port side of the Amundsen, just off the bow. Quantification of all mercury species was done using a Tekran 2537 unit. AMDEs were numbered in chronological order, with AMDE 1 being the first event that occurred in the study area. Details of atmospheric mercury measurements are provided elsewhere (Latonas 2010).

*3.2.3 Sample Treatment & Analysis*

Snow samples collected during active AMDEs were diluted (once melted) volumetrically five times with ultra-pure water prior to any further sample treatment and

analysis. Total mercury analysis was carried out on a Tekran 2600 mercury analyzer at PILMS following USEPA Method 1630 (USEPA 2002). In brief, acidic samples were spiked with excess amount of BrCl (prepared freshly from KBr and $KBrO_3$) in ultrapure concentrated HCl) to oxidize all mercury species to Hg(II) and left to react for a minimum of 12 hours. Just prior to analysis samples are spiked with 50 μL hydroxyolamine hydrochloride to neutralize the remaining BrCl. The sample was then introduced to the sample inlet and reacted with a 10% $SnCl_2$ solution reducing Hg(II) to $Hg^0$ which was then determined by atomic fluorescence spectroscopy. All samples were analyzed within 24 - 36 hr after sampling. Accuracy, precision, and instrumental quality was monitored by the use of analytical blanks, an operating standard ($[Hg]_T \sim 5ng\ L^{-1}$), and certified reference material BCR-579 coastal seawater ($[Hg]_T = 1.85 \pm 0.5\ ng\ kg^{-1}$). The recovery of the BCR-579 was always found to be within 90% of the certified value. Method detection limits, defined as 3 times the standard deviation of a series of 5 blanks, were in the order of 0.01 ng $L^{-1}$ and field blanks as low as 0.01-0.09 ng $L^{-1}$ were achieved.

## 3.3 Results

### *3.3.1 Surface Snow Samples – Time Series*

As shown in Table 3-1 and Figure 3-3, mean total mercury concentrations (THg) in surface snow samples collected over the entire field season varied greatly, ranging from 1.0 to 290 ng $L^{-1}$. During this same time period ground-level tropospheric GEM concentrations and atmospheric temperatures ranged from 0 – 4 ng $m^{-3}$ and -29 to +4.8°C, respectively. Between Feb 4 – Mar 15, AMDEs were infrequent and tropospheric RGM low compared to atmospheric measurements from later in the year. Snow samples

collected during this period were intermittent but always under non-AMDE conditions; correspondingly, the surface snow THg was very low (1.68 – 8.01 ng $L^{-1}$). From Mar 16 – May 11, AMDEs increased in frequency and THg surface snow concentrations became highly variable, ranging from 5.29 to 214 ng $L^{-1}$. A potential out-gassing event, characterized by a large spike in GEM (potentially being released from snow and surface water), occurred May 11, while in Franklin Bay (Station F2) during which a very low THg was recorded in surface snow (1.88 ng $L^{-1}$). On May 27, 2008 the Amundsen returned north to a station East of Banks Island (Station F5). It was here that one final AMDE was recorded, which was accompanied by a sharp spike in surface snow THg (104.6 ng $L^{-1}$). From this point in time onward, all surface snow samples collected had relatively low concentration of THg.

**Table 3-1: Total mercury measurements in surface snow in the Beaufort Sea collected during this study**

| Station | Sample ID | Latitude | Longitude | UTC (dd/mm/yyyy h:mm) | Ambient T ($^{o}$C) | Surface Snow Total Mercury (ng $L^{-1}$) | | | |
|---|---|---|---|---|---|---|---|---|---|
| | | | | | | n | Mean (SD) | Min | Max |
| D19 | 1 | 70.94917 | 122.89278 | 04/02/2008 7:35 | -24.6 | 2 | 1.68 (0.04) | | |
| D26 | 2 | 70.84917 | -123.67556 | 28/02/2008 0:00 | - | 2 | 3.15 (0.62) | 2.71 | 3.59 |
| D26 | 3 | 70.84917 | -123.67556 | 29/02/2008 8:40 | -29.0 | 2 | 3.77 (0.87) | 3.16 | 4.39 |
| D26 | 4 | 70.80806 | -123.02361 | 02/03/2008 6:10 | -26.2 | 4 | 6.78 (0.64) | 6.22 | 7.47 |
| D26 | 5 | 70.97611 | -123.18806 | 04/03/2008 0:00 | - | 3 | 1.68 (0.04) | 1.64 | 1.72 |
| D26 | 6 | 70.0225 | -123.4925 | 07/03/2008 2:40 | -26.1 | 2 | 8.01 (0.94) | 7.34 | 8.67 |
| D29 | 7 | 70.02306 | -123.7344 | 08/03/2008 4:00 | -21.3 | 3 | 5.26 (0.24) | 5.01 | 5.48 |
| D29 | 8 | 70.90139 | -123.46833 | 17/03/2008 4:05 | -27.0 | 3 | 215 (73.4) | 143 | 290 |
| D29 | 9 | 70.90139 | -123.46833 | 18/03/2008 12:30 | -25.4 | 2 | 128 (39.0) | 75.6 | 148 |
| D29 | 10 | 70.90139 | -123.46833 | 19/03/2008 3:30 | -24.6 | 2 | 144 (29.7) | 123 | 165 |
| D32 | 11 | 71.0525 | -121.78389 | 22/03/2008 4:00 | - | 2 | 89.1 (1.17) | 88.3 | 89.9 |
| D33 | 12 | 71.07361 | -121.78389 | 23/03/2008 4:00 | -26.6 | 6 | 63.9 (12.2) | 51.3 | 78.8 |
| D33 | 13 | 71.07361 | -121.78389 | 25/03/2008 11:00 | -30.4 | 3 | 63.9 (19.1) | 46.0 | 83.9 |
| D33 | 14 | 71.0525 | -121.78389 | 26/03/2008 8:00 | -25.2 | 4 | 135 (17.3) | 131 | 154 |
| D33 | 15 | 71.0525 | -121.78389 | 28/03/2008 4:00 | -23.7 | 3 | 20.9 (4.4) | 16.0 | 24.3 |
| D33 | 16 | 71.0525 | -121.78389 | 30/03/2008 4:00 | -21.4 | 5 | 35.0 (6.90) | 31.6 | 45.6 |
| D33 | 17 | 71.0525 | -121.78389 | 31/03/2008 9:45 | -23.4 | 5 | 88.9 (18.9) | 75.6 | 115 |
| D33 | 18 | 71.0525 | -121.78389 | 01/04/2008 4:00 | -27.6 | 4 | 113 (29.0) | 76.2 | 141 |
| D33 | 19 | 71.0525 | -121.78389 | 03/04/2008 10:30 | -18.8 | 3 | 127 (37.2) | 101 | 169 |
| D33 | 20 | 71.0525 | -121.78389 | 04/04/2008 3:00 | -24.2 | 3 | 137 (11.9) | 123 | 146 |
| D36 | 21 | 71.26778 | -124.38333 | 07/04/2008 5:00 | -11.7 | 3 | 51.9 (17.1) | 36.0 | 69.9 |
| D36 | 22 | 71.26833 | -124.50000 | 08/04/2008 3:30 | -14.2 | 3 | 5.29 (0.38) | 4.85 | 5.54 |
| D36 | 23 | 71.30056 | -124.56833 | 09/04/2008 4:00 | -13.5 | 2 | 19.3 (1.02) | 18.6 | 20.0 |
| D38 | 24 | 71.25083 | -124.61667 | 11/04/2008 15:00 | -16.2 | 3 | 16.4 (2.95) | 13.3 | 19.2 |
| D38 | 25 | 71.23472 | -124.6025 | 12/04/2008 7:00 | -14.3 | 3 | 18.6 (1.41) | 17.9 | 20.2 |
| D38 | 26 | 71.26861 | -124.80028 | 13/04/2008 3:00 | -12.1 | 2 | 43.2 (0.33) | 43.0 | 42.4 |
| D41 | 27 | 70.78361 | -122.30056 | 16/04/2008 4:00 | -15.3 | 3 | 79.0 (15.7) | 68.3 | 96.9 |
| D41 | 28 | 70.76806 | -122.1675 | 16/04/2008 14:00 | -14.4 | 3 | 64.2 (5.99) | 57.3 | 68.4 |
| D41 | 29 | 70.73361 | -122.13556 | 17/04/2008 3:30 | -14.6 | 3 | 115 (18.4) | 94.1 | 129 |
| D41 | 30 | 70.68361 | -122.10167 | 17/04/2008 10:00 | -13.8 | 3 | 128 (23.2) | 112 | 145 |
| D41 | 31 | 70.6175 | -121.91778 | 18/04/2008 3:00 | -15.7 | 3 | 134 (11.5) | 123 | 146 |
| D41 | 32 | 70.58583 | -121.91778 | 19/04/2008 3:30 | -15.0 | 3 | 97.6 (2.10) | 96.0 | 100 |
| D43 | 33 | 70.83944 | -121.11917 | 28/04/2008 4:30 | -13.7 | 3 | 40.2 (5.27) | 35.2 | 45.7 |
| D43 | 34 | 70.72139 | -123.31944 | 28/04/2008 16:00 | -10.0 | 3 | 62.9 (12.3) | 54.8 | 77.0 |
| D43 | 35 | 70.78583 | -123.82722 | 29/04/2008 2:00 | -11.0 | 3 | 31.6 (4.10) | 26.9 | 34.0 |
| D43 | 36 | 70.78583 | -123.82722 | 29/04/2008 10:00 | -10.1 | 3 | 47.4 (6.12) | 42.0 | 54.0 |
| D43 | 37 | 70.73694 | -123.98417 | 30/04/2008 10:00 | -5.1 | 2 | 79.4 (7.88) | 73.9 | 85.0 |
| D43 | 38 | 70.83278 | -124.25861 | 01/05/2008 4:00 | -9.0 | 3 | 116 (67.9) | 38.0 | 162 |

**Table 3-1: Continued**

| Station | Sample ID | Latitude | Longitude | UTC (dd/mm/yyyy h:mm) | Ambient T ($^{o}$C) | Surface Snow Total Mercury (ng $L^{-1}$) | | | |
|---|---|---|---|---|---|---|---|---|---|
| | | | | | | n | Mean (SD) | Min | Max |
| D43 | 39 | 70.99583 | -124.99417 | 02/05/2008 4:00 | -6.6 | 3 | 124 (35.5) | 83.2 | 149 |
| D43 | 40 | 71.04194 | -126.02139 | 04/05/2008 9:00 | -6.8 | 4 | 84.1 (20.7) | 66.1 | 109 |
| F2 | 41 | 69.95556 | -126.17556 | 12/05/2008 15:00 | -1.6 | 2 | 1.85 (0.88) | 1.22 | 2.47 |
| F2 | 42 | 69.95556 | -126.17556 | 13/05/2008 4:00 | -0.6 | 4 | 1.55 (0.47) | 1.20 | 2.24 |
| F2 | 43 | 69.95556 | -126.17556 | 13/05/2008 12:00 | 4.8 | 4 | 1.85 (1.05) | 1.20 | 3.41 |
| F2 | 44 | 69.95556 | -126.17556 | 14/05/2008 4:00 | 1.2 | 2 | 2.00 (0.67) | 1.53 | 2.48 |
| F2 | 45 | 69.95556 | -126.17556 | 14/05/2008 12:00 | 2.6 | 2 | 1.73 (0.07) | 1.67 | 1.78 |
| F2 | 46 | 69.95556 | -126.17556 | 17/05/2008 8:30 | -1.7 | 4 | 1.25 (0.46) | 0.98 | 1.94 |
| F5 | 47 | 71.67222 | -119.71528 | 28/05/2008 3:00 | -2.1 | 3 | 105 (4.73) | 100 | 110 |
| D46 | 48 | 71.57528 | -125.30417 | 30/05/2008 4:00 | 1.5 | 3 | 2.53 (0.1) | 2.47 | 2.65 |
| F7 | 49 | 69.81833 | -123.61889 | 07/06/2008 17:00 | - | 3 | 4.63 (1.72) | 3.04 | 6.45 |
| F7 | 50 | 69.81833 | -123.61889 | 08/06/2008 17:30 | - | 2 | 10.2 (0.16) | 10.13 | 10.4 |
| F7 | 51 | 70.65139 | -122.98583 | 09/06/2008 14:00 | - | 2 | 4.62 (1.02) | 3.90 | 5.35 |
| F7 | 52 | 69.81778 | -123.61917 | 11/06/2008 10:00 | - | 2 | 5.87 (0.23) | 5.71 | 6.03 |
| F7 | 53 | 69.81778 | -123.61917 | 12/06/2008 13:30 | - | 2 | 7.74 (0.72) | 7.23 | 8.25 |

The highest THg concentration in surface snow recorded during this study (290 ng $L^{-1}$) occurred during the AMDE on March 17 (AMDE 6, Figure 3-3b). During this time the Amundsen was beset in the ice at a drift station (Station D29, with >90% ice coverage) near the southern tip of Banks Island. As expected, THg surface snow concentrations increased during AMDEs and decreased shortly after due to photoreduction of $Hg^{2+}$ (Figure 3-3b, c). A large spike in atmospheric GEM occurred on May 11, 2008 in Franklin Bay. THg concentration in snow dropped to <4ng $L^{-1}$ and GEM reached 3.96 ng $m^{-3}$.

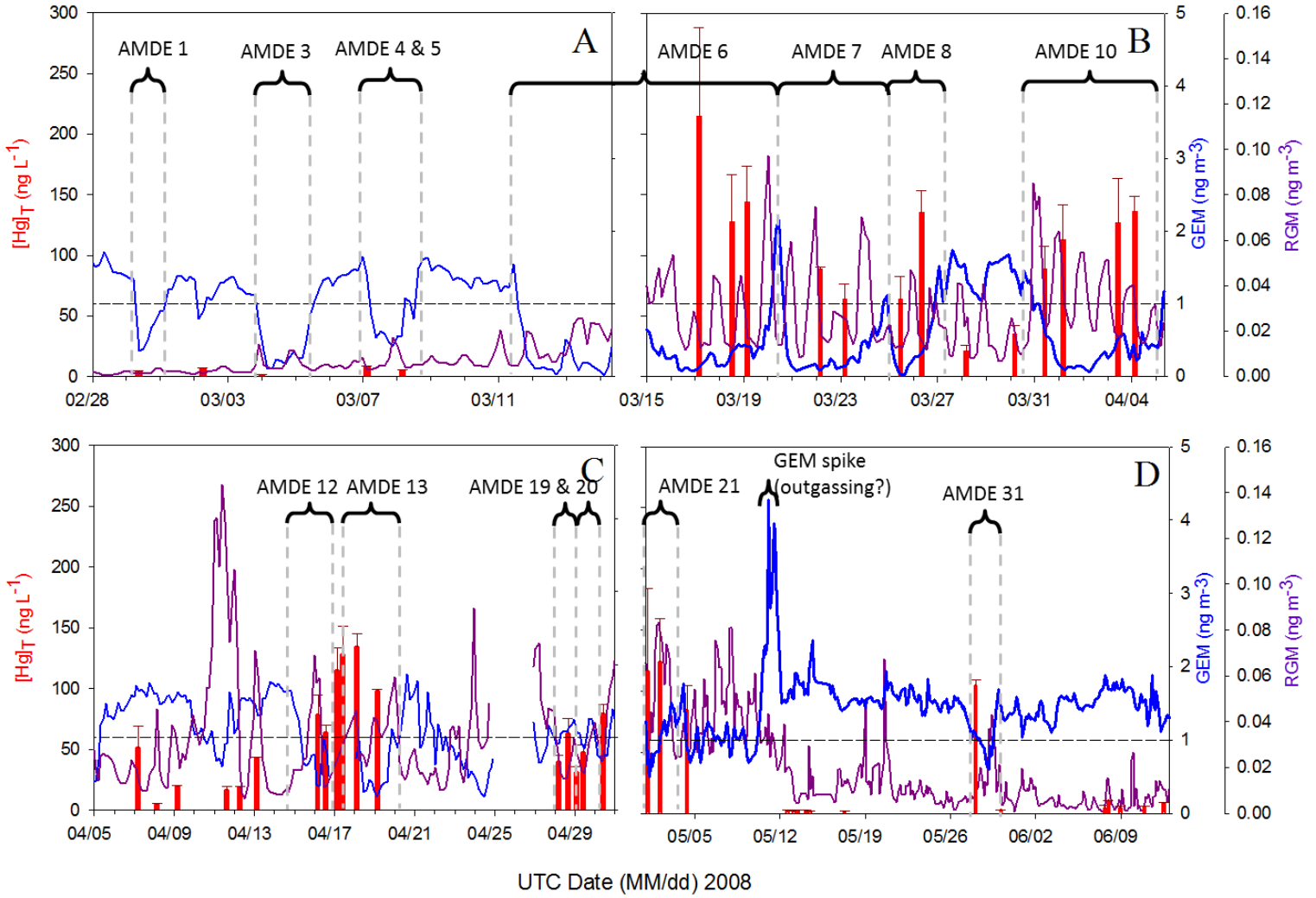


**Figure 3-3: $[Hg]_T$ in surface snow and accompanying [GEM] & [RGM] measured in the lower troposphere.; a) February 28 – March 14 b) March 15 – April 5 c) April 5 – April 30 d) May 1 – June 12, 2008. The dashed line represents the operational definition of an AMDE: when atmospheric [GEM] falls below 1 ng $m^{-3}$ for a period over 3 hours it is considered a depletion event (Schroeder *et al.* 1998) Major AMDEs and those discussed in more detail throughout the manuscript are identified**

A concurrent study has shown that in the Beaufort Sea, AMDEs occur at a much higher frequency than previously reported from coastal areas (Latonas 2010). This high frequency of AMDEs is evident when examining Hg in surface snow; depletion events occur in such rapid succession that the surface Hg from the previous AMDE has yet to photo-reduce and re-emit Hg. In coastal regions, surface snow concentrations often return to pre-AMDE levels 2 -3 days following the event (Steffen *et al.* 2002; Dommergue *et al.* 2003; Lalonde *et al.* 2003; Poulain *et al.* 2004; Lahoutifard *et al.* 2005; Dommergue 2010). Between each event the THg concentrations always dropped to <10 ng $L^{-1}$ (Dommergue 2010). In the region of the Beaufort Sea covered in this study, a return to background THg surface snow levels is not always observed. During the AMDE season, THg in surface snow in the Beaufort most closely matched the levels reported during AMDEs at Ny-Alesund and Alert (see Table 3-2, adapted from Durndord and Dastoor (2011)).

**Table 3-2: Concentrations of THg in surface snow from various Arctic regions over periods between January and June. Adapted from Dunford and Dastoor, 2011.**

| Location | Time Period | Conditions | Total Mercury (ng $L^{-1}$) | | | | Reference |
|---|---|---|---|---|---|---|---|
| | | | n | Mean (SD) | Min | Max | |
| Barrow | Jan - May | - | 4 | - | 1 | 94 | (Lindberg *et al.* 2002) |
| Barrow | 23 Mar to 1 Apr | offshore: AMDEs | - | 64.7 (41.4) | 35 | 198 | (Douglas *et al.* 2008) |
| Barrow | 23 Mar to 1 Apr | offshore: non-AMDEs | - | 40.7 (17.5) | 17 | 74 | (Douglas *et al.* 2008) |
| Barrow | 23 Mar to 1 Apr | onshore: wind slab | 79 | 38.7 (38.5) | 3.7 | 203 | (Douglas *et al.* 2008) |
| Barrow | 23 Mar to 1 Apr | onshore: fresh snow | 35 | - | 3 | 350 | (Douglas *et al.* 2008) |
| Barrow | 30 Apr to 15 May | refreezing lead | - | 58 | 38 | 108 | (Brooks *et al.* 2008) |
| Arctic Ocean | Nov - Jun | Ship-based | - | 58 | 38 | 108 | (Lu *et al.* 2001) |
| Resolute | Mar - May | - | - | - | 30 | 156 | (Lu *et al.* 2001) |
| Resolute Bay | 7 May to 12 Jun | - | 26 | 7 | <1.8 | 35 | (Lahoutifard *et al.* 2005) |
| Ny-Alesund | 29 Feb to 15 Jun | pre-AMDE period | 14 | 10 (11) | - | - | (Steen *et al.* 2009) |
| Ny-Alesund | 29 Feb to 15 Jun | AMDE period | 12 | 142 (61) | - | - | (Steen *et al.* 2009) |
| Ny-Alesund | 10 Apr to 10 May | AMDE period | 14 | 11.0 (7.8) | - | - | (Ferrari *et al.* 2005) |
| Ny-Alesund | 10 Apr to 10 May | non-AMDE period | 10 | 10.4 (4.8) | - | - | (Ferrari *et al.* 2005) |
| Ny-Alesund | 16 Apr to 8 Jun | all days | 26 | 14.2 | 0.9 | 90 | (Larose *et al.* 2010) |
| Beaufort Sea | 28 Feb to 8 Mar | Pre-AMDE | 16 | 4.30 (2.50) | 1.64 | 8.67 | This study[1] |
| Beaufort Sea | 17 Mar to 4 May | AMDE | 109 | 82.5 (48.0) | 4.85 | 289 | This study[2] |
| Franklin Bay | 12 – 17 May | Post-AMDE | 18 | 1.71 (0.30) | <DL | 2.47 | This study[3] |

[1]data tabulated from stations D19, D26
[2]data tabulated from stations D29, D32, D33, D36, D38, D41, and D43
[3]data tabulated from stations F2, F7, D46

Two drift ice stations (D33 and D43) were chosen for closer investigation (Figure 3-4; Table 3-3). At each station three AMDEs occurred.

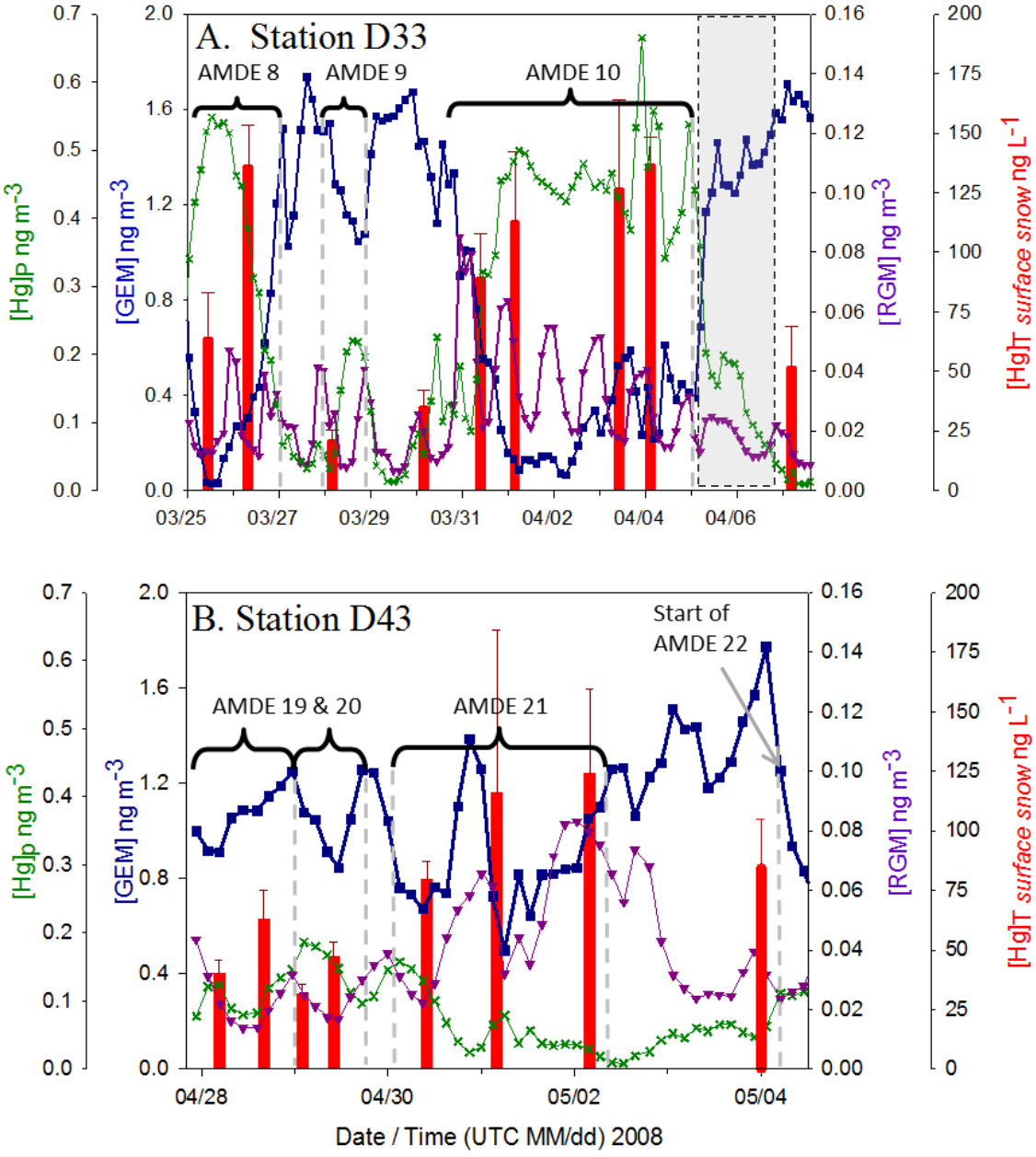


**Figure 3-4: Atmospheric mercury species and surface snow [THg] at two drift ice stations. a) Station D33; b) Station D43. The grey shaded area represents a time when the Amundsen was in transit to a new station. Atmospheric Hg monitoring continued during transit**

At both stations presented in Figure 3-4 an increase in THg in surface snow is observed coinciding with the decrease of atmospheric GEM at the onset of the depletion event. However, instances where atmospheric GEM began to rise (signifying the end of a

depletion event) and THg concentrations in surface snow continued to rise are observed (Eg. The final surface snow measurement collected during AMDE 21).

**Table 3-3: Ancillary data for AMDEs presented in Figure 3-4 & Figure 3-5**

| Station | Event | Start (UTC date:time) | End (UTC date:time) | Duration (hh:mm) | $T_{average}$ ($^{o}$C) | Ice Cover (/10) |
|---|---|---|---|---|---|---|
| D33 | AMDE8 | 24/03/2008 21:45 | 27/03/2008 1:35 | 51:50 | -26.6 | 10 |
| D33 | AMDE9 | 24/03/2008 2:15 | 28/03/2008 23:30 | 21:15 | -25.9 | 10 |
| D33 | AMDE10 | 30/03/2008 19:35 | 05/04/2008 7:35 | 131:59 | -23.1 | 10 |
| D43 | AMDE19 | 28/04/2008 22:40 | 29/04/2008 15:40 | 17:0 | -10.4 | 9 |
| D43 | AMDE20 | 29/04/2008 20:20 | 30/04/2008 19:20 | 23:00 | -7.00 | 9 |
| D43 | AMDE 21 | 30/04/2008 23:20 | 02/05/2008 8:05 | 32:45 | -7.43 | 9 |
| F2 | GEM Spike | 11/05/2008 1:40 | 11/5/2008 20:20 | 18:40 | +1.26 | 5 |

At station D33, three AMDEs occurred (Figure 3-4a, Table 3-3). AMDEs 8 and 9 were relatively shorter in duration, lasting 52 hours and 21 hours respectively. AMDE 10 occurred over a 131-hour period. During this event, GEM concentrations dropped to as low as 0.066 ng $m^{-3}$ while snow Hg concentrations peaked at 127 ng $L^{-1}$.

At station D43, three full AMDEs occurred; a fourth began as the Amundsen was re-locating to a new station. AMDEs 19 and 20 occurred within hours of each other together lasting 17.6 hours. During this period, THg in surface snow concentrations increased from 63 to 124 ng $L^{-1}$. AMDE 21 lasted 33 hours. It can be seen in Figure 3-4b that during the tail end AMDE 21as atmospheric GEM concentrations are rising, THg in surface snow continues to rise, peaking at 134 ng $L^{-1}$, while atmospheric GEM concentrations are actually returning to pre-AMDE levels.

On May 11, 2008 the ice-breaker moved south into a fast ice station in Franklin Bay, characterized by a sparse ice cover. A large spike in tropospheric GEM was observed which, is believed to be the result of an out gassing of reduced Hg from snow and surface water to the atmosphere (Table 3-3, Figure 3-5). The average temperature

over the five day period was +1.26$^{o}$C.

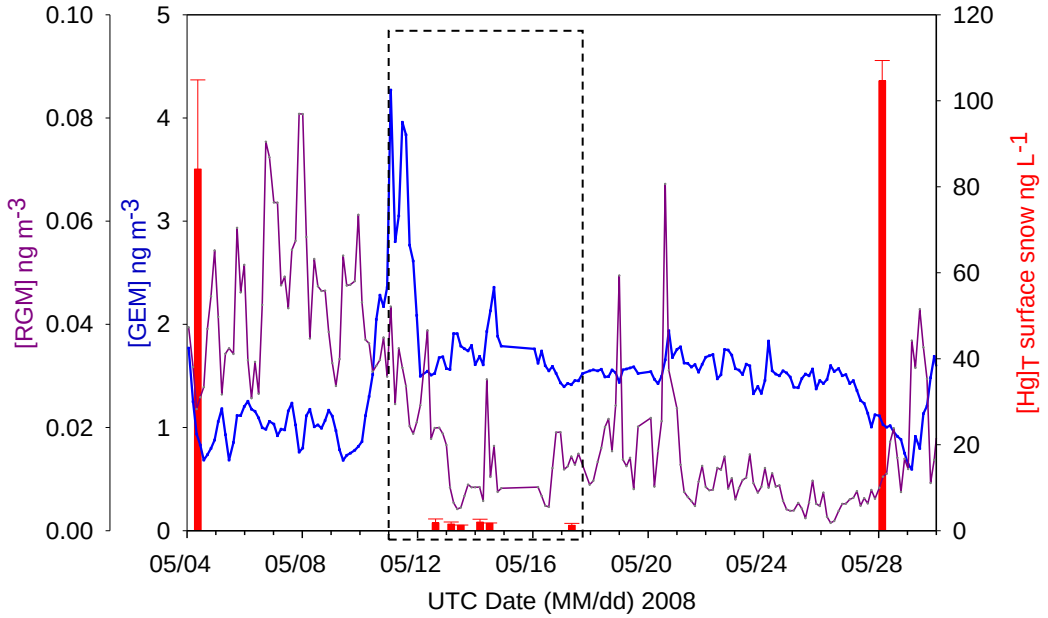


**Figure 3-5: GEM, RGM and surface snow THg concentrations measured over the period from May 4th through to May 30th. The dashed box indicated the time when the icebreaker was stationary in Franklin Bay and over which time the suspected out-gassing event was observed**

*3.3.2 Snow Pit Profiles*

Atmospheric and ice conditions during sampling of the 4 vertical snow pits are outlined in Tables 3-4. The corresponding THg, temperature and salinity profiles are shown in Figure 3- 6. As has been reported previously (Lalonde *et al.* 2002; Steffen *et al.* 2002; Ferrari *et al.* 2004; Poulain *et al.* 2004; Ferrari *et al.* 2008; Johnson *et al.* 2008), the snow pits sampled during active AMDEs (D33 and D43) show surface Hg enrichment, as expected (Steffen *et al.* 2002; Steffen *et al.* 2007; Ferrari *et al.* 2008; Johnson *et al.* 2008)

**Table 3-4: Atmospheric and ice conditions during snow pit sample collections.**

| Station | UTC Date; Time | Atmospheric T ($^{o}$C) | Ice Type | Ice Depth (cm) | Ice Coverage (/10) |
|---|---|---|---|---|---|
| D19 | 04-Feb-08; 16h00 | -30.5 | drift | 92 | 10 |
| D33* | 26-Mar-08; 16h00 | -25.2 | drift | 138 | 10 |
| D43* | 30-Apr-08; 16h00 | -8.7 | drift | 132 | 9 |
| F2 | 13-May-08; 16h00 | -0.6 | landfast | 114 | 10 |

*AMDE during collections

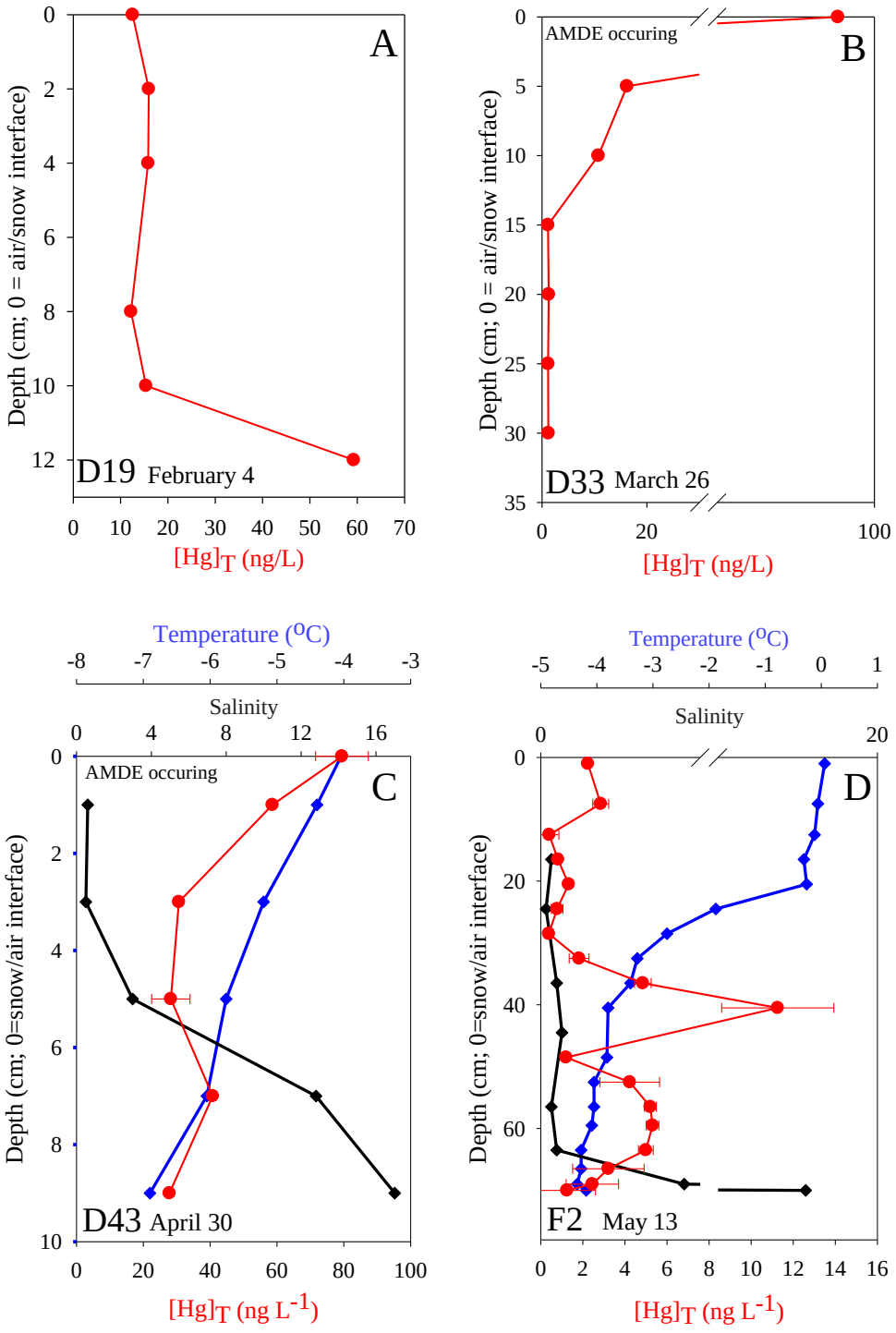


**Figure 3-6: THg profiles for four snow pits collected from the Beaufort Sea. Temperature and salinity profiles were collected only at station D43 and F2.**

The snow pack at station D19 (Figure 3-6a) showed consistently low THg concentrations from the surface down and a dramatic increase at the ice – snow interface. The samples were collected on February 4, 7 days prior to the first recorded AMDE. It is, therefore, unlikely that this increase in THg concentration is the result of atmospherically deposited Hg buried by a heavy snowfall. It is more probable that it is the result of upward migration of Hg rich brine (Hudier and Shirasawa 1995; Chaulk *et al.* 2011).

Snow pit D33, sampled during an active AMDE shows elevated THg in the surface snow as expected (Lindberg *et al.* 2002). After a depth of 15cm Hg in the snow pack remains low, similar to non-AMDE concentrations.

In late April, prior to sampling the snow pack at station D43, AMDEs occurred frequently and varied between 17 – 23 hours in duration. An AMDE also occurred during the collection period on April 30. High winds and significant snowfall began approximately 12 hr prior to sampling. The elevated THg concentrations measured throughout the snow pack at this sampling location (Figure 3-6c) likely, therefore, a result of the previous AMDE Hg being buried by windblown snow, and fresh snow fall scavenging Hg from the atmosphere. The elevated salinity at the ice-snow interface is likely caused by upward migration of brine from the sea-ice or a result of frost flowers that formed on the ice while it was thin being buried by snowfall.

Snow pit F2 was sampled at the onset of melt, the average temperature in the snow pack was -2.82$^{o}$C. As temperatures approach zero, soluble contaminants are mobilized and begin to percolate down the snow pack (Kuhn 2001). This may explain why, in the top layers of the snow pack where temperatures are near 0$^{o}$C, the THg

concentrations are low but lead up to a THg peak concentration at 40cm depth. A second smaller peak is seen between 55 – 60 cm depth. The salinity peak at the snow – sea ice interface may indicate that solutes have already percolated through the snow pack and are settling at the interface.

*3.3.3 Melt Ponds*

Four melt ponds were sampled at two stations during the spring melt when atmospheric temperatures were at or near 0°C (Table 3-5). Atmospheric mercury chemistry, depletion events (frequency and intensity), and background snow THg concentrations are assumed to be similar to those monitored in the Beaufort (mentioned previously in this chapter). The salinity of melt ponds in Darnley Bay at the stations sampled during this study ranged from 0 and increased to values <5 psu as the ice breakup began (Mundy 2008).

**Table 3-5: THg in melt pond water, snow and surface ice at two fast ice stations in Darnley Bay.**

| Station | Pond | Date | Atmosphere T (°C) | Water in melt pond THg (ng $L^{-1}$) | | | |
|---|---|---|---|---|---|---|---|
| | | | | n | Mean (SD) | Minimum | Maximum |
| F6 | 1** | 05/30/2008 | 0.0 | 4 | 7.34 (0.18) | 7.09 | 7.48 |
| F6 | 2 | 05/30/2008 | 0.0 | 4 | 8.72 (0.66) | 7.93 | 9.02 |
| F6 | 3* | 02/06/2008 | -0.6 | 3 | 5.57 (0.32) | 5.20 | 5.78 |
| F6 | 4 | 02/06/2008 | -0.6 | 3 | 7.46 (0.31) | 7.25 | 7.82 |
| F6 | 5 | 03/06/2008 | -1.4 | 4 | 8.62 (0.19) | 8.43 | 8.83 |
| Station Average | | | | 18 | 7.48 (1.23) | 5.20 | 9.02 |
| F7 | 6** | 08/06/2008 | 0.0 | 4 | 3.39 (0.84) | 2.64 | 4.26 |
| F7 | 7 | 08/06/2008 | 0.0 | 2 | 14.9 (3.15) | 12.7 | 17. 1 |
| F7 | 8** | 09/06/2008 | 1.2 | 2 | 2.13 (0.36) | 2.13 | 2.64 |
| F7 | 9 | 09/06/2008 | 1.0 | 4 | 3.40 (0.52) | 3.04 | 4.17 |
| Station Average | | | | 12 | 6.07 (5.60) | 2.13 | 17.09 |
| F7 | under-ice ocean water | 10/06/2008 | | 2 | 0.19 (0.007) | 0.18 | 0.19 |

** THg in surface snow collected during these sampling events ranged from 3 – 10 ng $L^{-1}$

* Thin ice cover that had formed over the melt pond contained THg 6.32 $\pm$ 0.3 ng $L^{-1}$

Most important to note is that the concentration of THg in the melt ponds sampled is 20 – 40 times higher than the concentration of THg measured in the water column 1m under the ice.

Variability between different melt ponds sampled at the same time can be seen. On June 2 (station F6), two discrete open melt ponds were sampled and average THg in each pond was 7.5 and 5.6 ng $L^{-1}$ respectively, a statistically significant difference (t-test, p=0.0018). A larger difference is seen on June 8 (station F7), again between two ponds sampled at the same time. The average THg in each pond was 15 and 2 ng $L^{-1}$ respectively; this represents a statistically significant difference (t-test, p=0.0016) in the THg concentrations in melt ponds waters collected at the same station. This is likely representative of the spatial variability and local nature of AMDEs and subsequent deposition of Hg species onto the snow pack (Douglas *et al.* 2005; Douglas *et al.* 2008).

The average THg in melt pond water collected from station F7, later into the melt season, showed no statistically significant difference from the average THg in melt pond water collected at station F6 (t-test, p=0.3073). The Hg in melt ponds is only slightly higher than pre-AMDE surface snow measurements taken during this study, and on par with pre-AMDE surface snow measurements from previous studies (Durnford, 2011 and references within). Although the THg in melt ponds is similar to THg in surface snow pre-AMDE, it is an order of magnitude higher then THg in under-ice water (~ 0.2 ng $L^{-1}$) also measured during this study. Deposited Hg that has accumulated in snow will likely end up in melt ponds during snowmelt (Dommergue *et al.* 2003).

## 3.4 Discussion

Atmospherically deposited Hg is subject to a variety of processes in the snow pack. Proposed pathways are depicted in Figure 3-7.

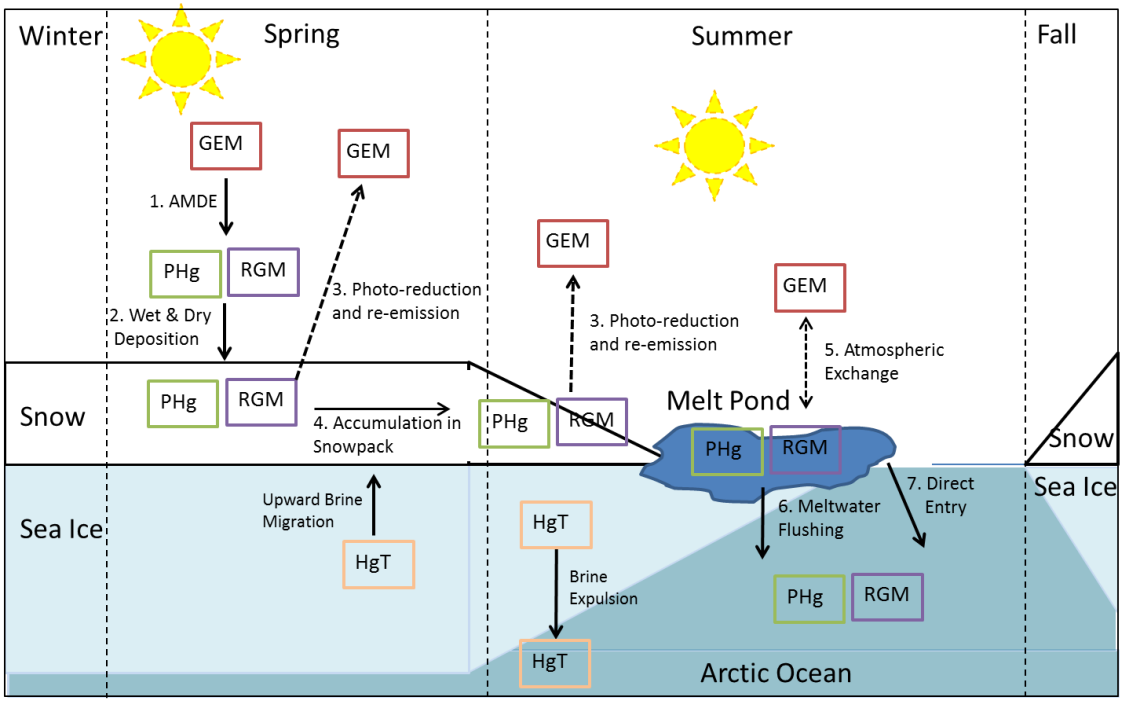


**Figure 3-7: Scheme showing pathways by which atmospheric mercury can enter into the Arctic marine ecosystem**

### *3.4.1 Mercury Deposition to Surface Snow*

The dynamic lead system in the Beaufort Sea results in a constant supply of young ice as leads re-freeze. The highly saline brine on the surface of newly formed ice is a source of reactive bromine, known to play a key role in the atmospheric GEM to RGM conversion (Lu *et al.* 2001; Lindberg *et al.* 2002). Latonas (2010) reported frequent and highly variable durations of AMDEs in the Beaufort region compared to other sites and attributed this to the dynamic environment created by the flaw leads. While direct deposition of AMDE-Hg on sea ice seems to be negligible (Chaulk *et al.* 2011), it is

known that snowfall during AMDEs can effectively scavenge AMDE-Hg (Douglas and Sturm 2004; Douglas *et al.* 2008; Johnson *et al.* 2008). Results from this study suggest that the higher frequency of AMDEs in the Beaufort region lead to greater accumulation of Hg in the snow pack relative to coastal sites such as Alert and Barrow (Durnford and Dastoor 2011). The majority of Hg deposited onto snow packs is in its oxidized form and must be reduced to GEM prior to being re-emitted to the atmosphere. The expansive areas of open water in Beaufort Sea, relative to coastal area, results in higher snow halide ions concentrations (Lindberg *et al.* 2002; Douglas *et al.* 2005) which, in turn, has been shown to increase the stability of deposited mercury (Lalonde *et al.* 2002; Poulain *et al.* 2007; St. Louis *et al.* 2007).

Latonas (2010) reported that PHg, which is known to be minimally reduced and emitted from snow surfaces (Dommergue *et al.* 2003), was the predominate oxidized Hg species in the early AMDE season (Latonas 2010). By mid-April the dominant atmospheric species shifted from PHg to RGM. It was also during this early spring period that the highest recorded concentration of THg in surface snow was measured. As noted previously, AMDE 10 is characterized by high atmospheric PHg and continually rising THg surface snow (Figure 3-4a). PHg retained in the snow pack may then be available to the marine system during the spring melt.

### *3.4.2 Fate of Hg in the Snow During the AMDE Season*

Of the four snow pits sampled during this study only two have elevated Hg at the snow / ice interface. The snow profiles reported by Poulain (2007) were sampled in June 2003 whereas the ones reported here span the late winter – spring season. Seasonal and

temporal variation may account for differences in the snow Hg profiles. Recent research has shown that Hg concentrations in the underlying snow pack show minimal variations between active and post- AMDE seasons (Johnson *et al.* 2008). Mercury deposited to the surface snow via AMDEs is subject to a variety of fates. The most common one being photo reduction to Hg(0) which re-emits back into the atmosphere. Previous studies estimate that the majority of deposited Hg is re-emitted back to the atmosphere 1-3 days following a depletion event (Steffen *et al.* 2002; Ferrari *et al.* 2005; Constant *et al.* 2007; Steffen *et al.* 2007; Douglas *et al.* 2008; Ferrari *et al.* 2008; Johnson *et al.* 2008; Dommergue 2010). As mentioned above (Section 3.1), the high frequency of AMDEs in the Beaufort region leads to a seasonal accumulation of Hg in the surface snow. Although some GEM is re-emitted to the atmosphere the time between subsequent depletion events is not enough to allow for near complete re-emission of deposited Hg as previously reported. This is evident when comparing THg in melt ponds collected during this study to values reported for other regions in the Arctic. Melt ponds sampled in Darnley Bay (stations F6 and F7) contain almost double the THg reported from stations in the Northern Arctic Ocean near Station Nord (Aspmo *et al.* 2006). Mercury accumulated in the snow can then be buried (by subsequent snowfall or wind mixing) and shielded from further photo reduction and re-emission; this is evident at Station F2 (Figure 3-6).

### *3.4.3 Fate of Hg in the Snow Pack During Melt*

As temperatures rise throughout the spring and summer seasons the cryosphere undergoes physical and chemical changes. Increasing temperatures enhance the photo-

reduction of RGM to GEM and as a result, the snow and ice surfaces act as a source of GEM to the atmosphere (Lalonde *et al.* 2002). The warming temperature, increased incoming solar radiation, and low winds present in mid-May made Station F2 in Franklin Bay an ideal site for GEM emission. Both the highest concentration of atmospheric GEM and the lowest concentrations of THg in surface snow during this study were observed in mid-May this station (Figure 3-1) in Franklin Bay (Figure 3-5).

As atmospheric temperatures rise and incoming solar radiation increases, a short lived phenomenon known as an "ionic pulse" wherein ions are preferentially eluted from the snow pack occurs (Kuhn 2001). Mercury elution has been reported in the ionic pulse (Lindberg *et al.* 2002; Dommergue 2010). The speciation of Hg in the snow pack will likely affect the permeability of species within the snow pack; particle bound Hg may remain trapped in the snow pack initially during the ionic pulse (Durnford and Dastoor 2011). Particulate mercury, deposited onto the surface snow in early spring may be the cause of these sub-surface peaks in the snow pack sampled at station F2.

As melt progresses melt ponds form on the sea ice surface. Snow pack Hg (of atmospheric origin) that has not been reduced and re-emitted is now a part of the melt pond environment. While it is possible for RGM to be photo reduced and re-emitted back to the atmosphere as GEM, this process is known to occur much more slowly in aqueous solution (Ariya *et al.* 2009; Hynes *et al.* 2009). If any GEM is emitted from melt ponds it is likely a minimal amount. Water samples collected from melt ponds in this study contain between 20 and 40-fold more THg than the underlying ocean water. As melt progresses, surface melt ponds and under-ice melt ponds eventually meet directly

delivering the atmospherically deposited Hg to the water below. During the melt period, microbial interactions with Hg species are possible (Amato *et al.* 2007; Mundy *et al.* 2011). These interactions may leave the Hg bound to organic substances and biologically available to enter into the food chain. In multi-year ice-cores, periodic THg peaks were observed, and are thought to represent yearly melt pond formation and re-freezing (Chaulk *et al.* 2011).

*3.4.4. THg Flux Within the Cryosphere*

The amount of THg deposited onto the snow pack is estimated during AMDE 10 at Station D33. Using snow density values ranging from 0.398 – 0.456 g $cm^{-3}$ (Barber *et al.* 2008), and after subtracting the initial background Hg concentrations in surface snow immediately before the AMDE began we estimate that between 406 – 784 ng $m^{-2}$ of Hg was deposited in the top 1cm of surface snow during this depletion event. This value was calculated as follows:

$$J = [Hg]_{ss}[(\rho_{snow})/(\rho_{water})](0.01m)$$

where J is the deposition flux (in ng $m^{-2}$) of Hg to the top 1cm of surface snow, $[Hg]_{ss}$ is the concentration of Hg deposited to the snow surface (in ng $m^{-3}$), $\rho_{water}$ the density of water (in g $m^{-3}$), and $\rho_{snow}$ the density of the snow (in g $m^{-3}$). This range of flux (406 – 784 ng $m^{-2}$) is comparable to those calculated for coastal regions at Barrow, Alaska: 320 – 700 ng $m^{-2}$ (Johnson *et al.* 2008) and Ny-Alesund, Svalbard: 200 – 2160 ng $m^{-2}$ (Dommergue 2010). Atmospheric PHg was particularly high during this event, reaching a maximum of 0.665 ng $m^{-3}$. As the ship left station D33 immediately following the end of AMDE 10 we are unable to determine the fraction of the deposited THg that was re-

emitted to the atmosphere.

Assuming the same snow densities as at station D33, 300 – 540 ng $m^{-2}$ of Hg was estimated to have been deposited to the top 1cm of surface snow during AMDE 21 (Station D43). Prior to AMDE 21 there was approximately 1.4 x more Hg in the surface snow than at the onset of AMDE 10; in addition, AMDE 10 lasted considerably longer than AMDE 21. It thus makes sense that more THg would be deposited during AMDE 10 compared to AMDE 21. A snow sample collected after AMDE 21 and prior to the beginning of AMDE 22 had elevated THg (84.1 ng $L^{-1}$). This corresponds to re-volatilization of less than 50% of the Hg deposited during AMDE 21.

*3.4.5. The Impact of a Changing Climate*

The current scientific consensus is that the Arctic is shifting to a system which will be ice-free during the summer and dominated by first year sea ice in the colder months(Comiso 2002; Comiso *et al.* 2008). While more mechanistic and modeling studies are needed to project how this would affect the Hg cycling in the Arctic, it is possible that frequency and intensity of AMDEs could increase at least regionally (Outridge *et al.* 2008). This would increase snow pack Hg concentrations and, with the prevalence of first year ice melt ponds as the direct conduit, could provide an enhanced pathway for atmospheric Hg to enter the underlying marine system. To which extent this will alter the already high Hg loading in Arctic marine mammals remains to be further studied.

## 3.5 References


Amato, P., Magand, O., Sancelme, M., Delort, A.-M., Barbante, C., Boutron, C. and Ferrari, C. (2007). Bacterial characterization of the snow cover at Spitzberg, Svalbard. *FEMS microbiology Ecology* **59**(2): 2054-2063.

Ariya, P., Dastoor, A., Amyot, M., Schroeder, W., Barrie, L., Anlauf, K., Raofie, F., Ryzhkov, A., Davignon, D., Lalonde, J. and Steffen, A. (2004). The Arctic: a sink for mercury. *Tellus* **56B**(5): 397 - 403.

Ariya, P., Peterson, K., Snider, G. and Amyot, M. (2009). Mercury chemical transformations in the gas, aqueous and heterogeneous phases: state-of-the-art science and uncertainties *Mercury fate and transport in the global atmosphere* 459-501.

Aspmo, K., Temme, C., Berg, T., Ferrari, C., Gauchard, P., Fain, X. and Wibetoe, G. (2006). Mercury in the atmosphere, snow and melt water ponds in the North Atlantic Ocean during Arctic summer. *Environmental Science and Technology* **40**: 4083 - 2089.

Barber, D., Asplin, M., Gratton, Y., Lukovich, J., RJ, G., Raddatz, R. and Leitch, D. (2010). The International Polar Year (IPY) Circumpolar Flaw Lead (CFL) System Study: Overview and the Physical System. *Atmosphere-Ocean*.

Barber, D., Rossnagel, A. and Hochheim, K. (2008). Density measurements of snow during CFL Leg 8, University of Manitoba.

Brooks, S., Lindberg, S., Southworth, G. and Arimoto, R. (2008). Spring-time atmospheric mercury speciation in the McMurdo, Antarctic coastal region. *Atmospheric Environment* **42**: 2885-2893.

Chaulk, A., Stern, G., Armstrong, D., Barber, D. and Wang, F. (2011). Mercury Distribution and Transport Across the Ocean-Sea Ice-Atmosphere Interface in the Arctic Ocean *Environmental Science and Technology* **45**(5): 1866-1872.

Cheng, M. and Schroeder, W. (2000). Potential atmospheric transport pathways for mercury measured in the Canadian high Arctic. *Journal of Atmospheric Chemistry* **35**: 101-107.

Comiso, J. (2002). A rapidly declining perennial sea ice cover in the Arctic. *Geophysical Research Letters* **29**(20).

Comiso, J., Parkinson, C., Gersten, R. and Stock, L. (2008). Accelerated decline in the Arctic sea ice cover. *Geophysical Research Letters* **35**.

Constant, P., Poissant, L., Villemur, R., Yumvihoze, E. and Lean, D. (2007). Fate of inorganic mercury and methyl mercury within the snow cover in the low Arctic tundra on the shore of Hudson Bay (Quebec, Canada). *Journal of Geophysical Research* **112**.

Domine, F., Cabanes, A. and Legagneux, L. (2002). Structure, microphysics, and surface area of the Arctic snowpack near Alert during the ALERT 2000 campaign. *Atmospheric Environment* **36**: 2753 - 2765.

Dommergue, A., Ferrari, C., Gauchard, P. and Bourton, C. (2003). The fate of mercury species in a sub-Arctic snowpack during snowmelt. *Geophysical Research Letters*.

Dommergue, A., Larose, C., Fain, X., Clarisse O., Foucher D., Hintelmann H., Schneider D., Ferrari C.P. (2010). Deposition of mercury species in the Ny-Alesund area (79$^{o}$N) and their transfer during snowmelt. *Environmental Science and Technology* **44**: 901-907.

Douglas, T. and Sturm, M. (2004). Arctic Haze, mercury and the chemical composition of snow across northwestern Alaska. *Atmospheric Environment* **38**(6): 805-820.

Douglas, T., Sturm, M., Simpson, W., Brooks, S., Lindberg, S. and DK, P. (2005). Elevated mercury measured in snow and frost flowers near Arctic sea ice leads. *Geophysical Research Letters* **32**.

Douglas, T., Sturm, M., Simpson, W., JD, B., Alvarez-Aviles, L., Keeler, G., Pervoich, D., Biswas, A. and Johnson, K. (2008). Influence of snow and ice crystal formation and accumulation on mercury deposition to the Arctic. *Environmental Science and Technology* **42**: 1542-1551.

Durnford, D. and Dastoor, A. (2011). The behavior of mercury in the cryosphere: A review of what we know from observations. *Journal of Geophysical Research* **116**.

Ferrari, C., Dommergue, A., Boutron, C., Jitaru, P. and Adams, F. (2004). Profiles of mercury in the snow pack at Station Nord, Greenland shortly after polar sunrise. *Geophysical Research Letters* **31**: 1-4.

Ferrari, C., Gauchard, P., Aspmo, K., Dommergue, A., Magand, O., Bahlmann, E., Nagorski, S., Temme, C., Ebinghaus, R., Steffen, A., Banic, C., Berg, T., Planchon, F., Barbante, C., Cescon, P. and Boutron, C. (2005). Snow-to-air exchange of mercury in an Arctic seasonal snow pack in NY-Alesund, Svalbard. *Atmospheric Environment* **39**: 7633 - 7645.

Ferrari, C., Padova, C., Fain, X., Gauchard, P., Dommergue, A., Aspmo, K., Berg, T., Cairns, W., Barbante, C., Cescon, P., Kaleschke, L., Richter, A., Wittrock, F. and Boutron, C. (2008). Atmospheric mercury depletion event study in Ny-Alesund (Svalbard) in spring 2005. Deposition and transformation of Hg in surface snow during springtime. *Science of the Total Environment* **397**: 167-177.

Fitzgerald, W. (1999). Clean hands, dirty hands: Clair Patterson and the aquatic biogeochemistry of mercury. *Clean hands, Clair Patterson's crusade against environmental lead contamination*. C. I. Davidson. New York, Nova Science**:** 119 - 137.

Hinkler, J., Hansen, B., Tamstorf, M., Sigsgaard, C. and Peterson, D. (2008). Snow and snow-cover in Central Northeast Greenland. *Advanced Ecology Research* **40**: 175-195.

Hudier, E. and Shirasawa, K. (1995). Upward Flushing of Seawater through First Year Ice. *Atmosphere-Ocean* **33**(3): 569-580.

Hylander, L. and Goodsite, M. (2006). Environmental costs of mercury pollution. *Science of the Total Environment* **368**: 352 - 370.

Hynes, A., Donohoue, D., Goodsite, M. and Hedgecock, I. (2009). Our current understanding of major chemical and physical processes affecting mercury dynamics in the atmosphere and at the air-water/terrestrial interfaces. *Mercury fate and transport in the global atmosphere***:** 427-457.

Johnson, K., Blum, J., Keeler, G. and Douglas, T. (2008). Investigation of the deposition and emissino of mercury in arctic snow during an atmospheric mercury depletion event. *Journal of Geophysical Research* **113**.

Kuhn, M. (2001). The nutrient cycle through snow and ice, a review. *Aquatic Science* **63**: 150-167.

Lahoutifard, N., Sparling, M. and Lean, D. (2005). Total and methyl mercury patterns in Arctic snow during springtime at Resolute, Nunavut, Canada. *Atmospheric Environment* **39**(7597 - 7606).

Lalonde, J., M, A., Doyon, M. and Auclair, J. (2003). Photo-induced Hg(II) reduction in snow from the remote and temperate Experimental Lakes Area (Ontario, Canada). *Jounral of Geophysical Research - Atmosphere* **108**(D6).

Lalonde, J., Poulain, A. and Amyot, M. (2002). The role of mercury redox reactions in snow on snow-to-air mercury transfer. *Environmental Science and Technology* **36**: 174-178.

Larose, C., Dommergue, A., De Angelis, M., Cossa, D., Averty, B., Marusczak, N., Soumis, N., Schneider, D. and Ferrari, C. (2010). Springtime changes in snow chemistry lead to new insights into mercury methylation in the Arctic. *Geochimica et Cosmochimica Acta* **74**: 6263-6275.

Latonas, J. (2010). Measurements of Atmospheric Mercury, Dissolved Gaseous Mercury, and Evasional Fluxes in the Amundsen Gulf: The Role of the Sea-Ice Environment. Department of Environment and Geography. Winnipeg, University of Manitoba. **Master of Science**.

Lindberg, S., Brooks, S., Lin, C.-J., Scott, K., Landis, M., Stevens, R., Goodsite, M. and Richter, A. (2002). Dynamic oxidation of gaseous mercury in the arctic troposphere at polar sunrise. *Environmental Science and Technology* **36**: 1245 - 1256.

Loseto, L., Lean, D. and Siciliano, S. (2004). Snowmelt sources of methylmercury to high Arctic ecosystems. *Environmental Science and Technology* **38**: 3004 - 3010.

Lu, J., Schroeder, W., Barrie, L., Steffen, A. and Welch, H. (2001). Magnification of atmospheric mercury deposition to polar regions in springtime: the link to tropospheric ozone depletion chemistry. *Geophysical Research Letters* **28**: 3219-3222.

Macdonald, R., Harner, T. and Fyfe, J. (2005). Recent climate change in the Arctic and its impact on contaminant pathways and interpretation of temporal trend data. *Science of the Total Environment* **342**(1-3): 5 - 86.

Maykut, G. (1986). The surface Heat and Mass Balance. *The Geophysics of Sea Ice*. N. Untersteiner. New York, Plenium Press**:** 395-464.

Mundy, C. (2008). Salinity of Melt-Ponds during Leg 8 & 9 of the IPY-CFL Study, University of Manitoba

Mundy, C., Gosselin, M., Ehn, J. K., Belzile, C., Poulain, M., Alou, E., Roy, S., Hop, H., Lessard, S., Papakyriakou, T., Barber, D. G. and Stewart, J. (2011). Characteristics of two distinct high-light acclimated algal communities during advanced stages of sea ice melt. *Polar Biology*.

Outridge, P., Macdonald, R., Wang, F., Stern, G. and Dastoor, A. (2008). A mass balance inventory of mercury in the Arctic Ocean. *Environmental Chemistry* **5**: 89-111.

Petrich, C. and Eicken, H. (2010). Growth, Structure and Properties of Sea Ice. *Sea Ice*. D. Thomas and G. Dieckmann. Chichester, Blackwell Publishing**:** 23 - 78.

Poulain, A., Garcia, E., Amyot, M., Campbell, P. and Ariya, P. (2007). Mercury distribution, partitioning, and speciation in coastal vs. inland High Arctic snow. *Geochimica et Cosmochimica Acta* **71**: 3419 - 3431.

Poulain, A., Lalonde, J., Amyot, M., Shead, J., Raofie, F. and Ariya, P. (2004). Redox transformations of mercury in an Arctic snowpack at springtime. *Atmosphere Environment* **38**: 6763-6774.

Schroeder, W., Anlauf, K., Barrie, L., Lu, J., Steffen, A., Schneeberger, D. and Berg, T. (1998). Arctic springtime depletion of mercury. *Nature* **394**: 331 - 332.

Skov, H., Christensen, J., Goodsite, M., Heidam, N., Jensen, B., Wahlin, P. and Geernaert, G. (2004). Fate of elemental mercury in the Arctic during atmospheric mercury depletion episodes and the load of atmospheric mercury to the Arctic. *Environmental Science and Technology* **38**: 2373 - 2382.

St. Louis, V., Hintelmann, H., Graydon, J., Kirk, J., Barker, J., Dimock, B., Sharp, M. and Lehnherr, I. (2007). Methylated mercury species in Canadian high Arctic marine surface waters and snowpacks *Environmental Science and Technology* **41**: 6433-6441.

Steen, A., Berg, T., Dastoor, A., Durnford, D., Hole, L. and Phaffhuber, K. (2009). Dynamic exchange of gasesous elemental mercury during polar night and day. *Atmospheric Environment* **43**: 5604-5610.

Steffen, A., Douglas, T., Amyot, M., Ariya, P., Aspmo, K., Berg, T., Bottenheim, J., Brooks, S., Cobbett, F., Dastoor, A., Dommergue, A., Ebinghaus, R., Ferrari, C., Gardfeldt, K., Goodsite, M., Lean, D., Poulain, A., Scherz, C., Skov, H., Sommar, J. and Temme, C. (2007). A synthesis of atmopsheric mercury depletion event chemistry linking atmosphere, snow and water. *Atmospheric Chemistry and Physics Discussions* **7**: 10837-10931.

Steffen, A., Schroeder, W., Bottenheim, J., Narayan, J. and Fuentes, J. (2002). Atmospheric mercury concentrations: measurements and profiles near snow and ice surfaces in the Canadian Arctic during Alert 2000. *Atmospheric Environment* **36**: 2653 - 2661.

Steffen, A., Schroeder, W., Macdonald, R., Poissant, L. and Konoplev, A. (2005). Mercury in the Arctic atmosphere: An analysis of eight years of measurements of GEM at Alert (Canada) and a comparison with observations of Amderma (Russia) and Kuujjuarapik (Canada). *Science of the Total Environment* **342**: 185-198.

USEPA (2002). Method 1631, Revision E: Measurement of mercury in water by CVAFS.

Van Oostdam, J., Gilman, A., Dewailly, E., Usher, P., Wheatley, B., Kuhmlein, H., Neve, S., Walker, J., Tracy, B., Feeley, M., Jerome, V. and Kwanvick, B. (2005). Human health implications of environmental contaminants in Arctic Canada: A review. *Environmental Science and Technology* **351-352**: 165-246.

# Chapter 4: Conclusions and Future Directions

## 4.1 Research Conclusions

Since the characterization of AMDEs in the mid 1990s, major research initiatives attempting to understand mercury behaviour (cycling & transformation) in the atmosphere, water column, snow and biota in the Arctic Ocean have been in progress. Despite ongoing and extensive research, many knowledge gaps still exist, the largest being to what extent does atmospheric Hg infringe on the underlying marine system? In order to answer this, we must first understand if and how atmospherically deposited Hg is transported through the seasonal snow pack and sea ice that covers a large portion of the Arctic region during the time of year that AMDEs occur.

As stated in Chapter 1, the overall objective of this thesis was to shed light on the distribution and behavior of Hg in an often overlooked component of the Arctic environment: the cryosphere. This was broken down into 3 specific key questions:

1. How do AMDEs affect Hg concentrations in snow and sea ice?

2. How is Hg distributed in snow and sea ice?

3. What is the role of brine drainage and melt pond in Hg transport between the atmosphere and the ocean?

Over a 5 month period (February – June 2008) cryospheric samples were collected from the Beaufort Sea region and analyzed for total Hg. These included surface snow

samples (collected twice daily, conditions permitting), first-year ice (both landfast and drift ice) and accompanying brine (collected at a series of stations), new ice (opportunistically) and multi-year ice (a single ice core). Real time measurements of Hg species in the atmosphere was measured during the entire study period by a fellow graduate student Jeffrey Latonas from the same group (Latonas 2010).

The Hg concentration in the new, thin ice samples doubled that in the underlying seawater. New ice sampled collected during AMDEs was higher than those collected during non-AMDE conditions however the sample size is not large enough to conclude if this is the result of an AMDE. In any case, the Hg concentration in new ice was much lower than that reported in snow and frost flowers during AMDEs, suggesting direct deposition of atmospheric Hg not to be a significant factor determining Hg concentration in sea ice (with the exception of frost flowers on new ice). Mercury concentration profiles from 5 first year ice stations and 2 landfast ice stations showed remarkably similarity in vertical distribution. Despite being collected at different times, in different locations, under different atmospheric and snow cover conditions all 7 cores had low Hg (0.4 – 4ng $L^{-1}$) and showed enrichment in the surface frazil layer of ice. A multiyear core showed a unique cyclic profile with multiple peaks believed to correspond to yearly cycles of freeze/thaw and ice growth. Brine in first year ice was enriched with Hg and showed the same surface enrichment as sea ice itself. Concentrations of Hg in brine sampled during this study range from 2.6 to 71.2 ng $L^{-1}$, much larger than the underlying seawater (~0.2 ng $L^{-1}$). This enrichment of Hg in sea ice brine is thought to be a result of both freeze rejection of Hg from sea-water and the enrichment of Hg-binding particles in

during frazil ice formation. Unlike sea ice, brine showed seasonal differences in Hg concentrations. As temperatures approach $0^{o}$C solid ice begins to melt which causes a dilution of the brine channels (and chemicals therein). This dilution was noticeable when comparing the brine Hg in stations D33 and D41 (sampled during when atmospheric temperature was near $0^{o}$C) to station F2 (sampled when atmospheric temperature was near $0^{o}$C). As melt progresses, brine pockets interconnect to form channels, and sea ice is desalinated. Melt water flushes brine, and accompanying contaminants, out of the ice and into the underlying seawater. The accumulation of Hg in sea ice brine makes FYI a potential means for re-distribution of Hg in the Arctic Ocean. The role sea ice plays in the transport of other contaminants in the Arctic Ocean has been previous discussed in literature (Masque *et al.* 2003; Camara-Mor *et al.* 2011)

A 5-month surface snow sampling campaign showed the expected trend: an increase in surface snow Hg as atmospheric GEM decreased during AMDEs (Steffen *et al.* 2002; Ferrari *et al.* 2004; Poulain *et al.* 2004; Lahoutifard *et al.* 2005; Poulain *et al.* 2007; Steffen *et al.* 2007). One notable finding is that the increased frequency of AMDEs in the Beaufort region (Latonas 2010) appears to cause an accumulation of Hg in surface snow. There is not enough time between subsequent depletion events to allow for re-volatilization of the Hg, as reported in literature (Steffen *et al.* 2007). A portion of the atmospherically deposited Hg may remain in the snowpack, by being buried by subsequent snowfall or wind mixing. Hg remaining in the snowpack is present throughout the melt season (melt ponds) and as the ice breaks up, it is then able to enter the marine system and potentially the food chain. If the Arctic shifts to a predominantly

first year ice regime in coming years, as suggested by several studies (Comiso 2002; Comiso 2002; Comiso *et al.* 2008) the dynamics of Hg in the Arctic will be affected. Should AMDEs occur at a higher frequency, more accumulation of AMDE-deposited Hg would be expected in the snowpack. An Arctic dominated by first year ice will have more snowpack surface, which will form melt ponds later in the season, available for Hg to accumulate.

On May 11, 2008 a suspected out-gassing event in Franklin Bay was observed; THg in surface snow dropped to <1ng $L^{-1}$ and atmospheric GEM exceeded 4ng $m^{-3}$.

As identified in Chapter 1, the current dataset on Arctic Hg chemistry is lacking information about the distribution and behavior of Hg in sea ice and brine and across the OSA interface (Macdonald *et al.* 2005). The major scientific contribution of this thesis is thus the obtaining of the first dataset along with preliminary analysis of Hg dynamics in sea ice and brine. This study highlights the importance of sea-ice in Hg cycling in the Arctic and raises more questions that need to be answered under a changing sea ice environment. The following sections present a critical analysis of this study, as well as introducing topics for further research.

## 4.2 Limitations and Successes of this study

There were several limitations to this study. The first was the discrete point sampling strategy which was dictated by the nature of the ship-based research and the dynamics of the Arctic sea ice. While this did allow for an incredibly large spatial variability in samples, point sampling had the disadvantage of the seasonal history of a

station being unknown. In dynamic sea ice environments like the Beaufort Sea, atmospheric, cryospheric and marine biogeochemistry must be heterogeneous in time and in space, and AMDEs have been shown to be local events and can vary in a small spatial and temporal scale (Lindberg *et al.* 2002; Latonas 2010). This may become important when attempting to interpret point samples from Franklin and Darnley Bay that may be influenced by different water inputs and air masses. Therefore, cautions are needed when interpreting the frequency of AMDEs and accumulation of Hg onto snow surfaces in different regions of the Beaufort Sea.

This study is the first to generate profiles of total Hg in first year sea ice. Some degree of trial-and-error was necessary to establish a protocol for cleanly sampling and processing ice cores. The integrity of the ice core samples was easily compromised as cores are subject to contamination while being processed. The cores needed to be "cleaned" and have the surfaces of ice that came in contact with the core barrel and the samplers hands scraped off. Care must be taken to ensure that the piece of ice is only in contact with clean gloved hands and the clean blade of the ceramic knife. Once being scraped the piece of ice must be quickly sealed in a clean zip-lock bag to melt. Gloves must be changed and knifes wiped cleaned in between scraping each 10cm section of the ice core. The ice core samples are being processed and scraped in a freezer lab onboard the CCGS Amundsen that is not a clean lab. Therefore, once the samples are scraped clean they must be stored and sealed in Ziploc bags quickly, and moved into PILMS to melt.

Sea-ice is a porous mixture of pure ice, brine, and gas inclusions; because of this

sampling each individually poses a problem: how to separate each of the components? The sump hole method, drilling a hole in the ice (not all the way to the underlying ocean) and allowing the adjacent brine to seep in has been most commonly used (Gleitz *et al.* 1995; Papadimitriou *et al.* 2007). Frequently employed to investigate biological parameters of brine, this method caries a degree of uncertainty in the origin of the brine sample. Depending on the sea ice texture, temperature, and salinity brine migration to the sack hole can vary. It is important to keep in mind that sump hole sampling carries ambiguity in the origin of the brine. Brine channels are interconnected and extend throughout the ice, because of this, mixture of brine pockets is not uncommon. In the deeper sump holes, brine from the upper layers is also able to seep into the hole, providing a mixed sampled of brine from the entire depth of the ice. However, the work of Pucko *et al* (2010), shows that the sump hole method is reliable for measurement of HCHs in sea ice brine, and the seepage of brine from surface layers into deep sump holes does not contribute a substantial amount of brine to the sump hole (Pucko *et al.* 2010).

When attempting to sample brine during the winter season, colder temperatures proved a challenge for the sump hole method. The cold temperate severely slowed and in some cases hindered brine drainage into the sump holes (despite sump holes being capped to prevent exposure to low atmospheric temperatures). When attempting to sample, the brine would often freeze in the inlet of the baster and clog it. When brine sampling during the melt season, the sump hole method may lose its applicability. At the onset of melt, ice and brine channels are rapidly desalinated, the melting ice matrix will begin to dilute the brine left in the channels and eventually melt water will flush out the brine

channels (Untersteiner 1968). During the melt season, it may be advantageous to have a scuba diver collect brine seepages from under the ice to compare with measurements of samples collected in sump holes. The applicability of the sump hole method for Hg brine sampling is limited during the winter and melt seasons, this method is best applied during the late-winter to early melt season.

In the original planning stages of this research, measurement of cryospheric MeHg was to be included in the data set for this thesis. A MeHg analysis system was installed in PILMS however in late 2007 it was discovered that the system was not functioning properly. The system was not replaced until June 2008. Due to the lack of analytical capabilities at PILMS, measurement of MeHg in snow and ice samples was not completed.

The largest advantage to this study, especially considering the novel nature of the sampling, was on-site sample analysis at PILMS. Over 25 ice cores were collected and only 8 provided acceptable, reliable results. Reliability of results was monitored using field blanks while collecting and processing ice cores. As discussed above, processing ice cores without contaminating them proved to be a challenge. With samples be analyzed on site, the need for improved attention to detail and processing to be completed in a timely fashion was made clear. On-site analysis also showed that brine collected at two different depths does contain very different levels of Hg thus a more detailed, depth-oriented sampling protocol was established for brine. Additionally, having all samples processed on-board the CCGS Amundsen within 24-48 hours of collection eliminated any risk of samples being contaminated, lost, or altered while being stored and transported back to a

clean lab facility in the south.

In December 2007, the Milli-Q Element water purification system in PILMS was not functioning. As a result, samples collected during this period were all shipped back to Winnipeg for analysis at the Ultra Clean Trace Elements Laboratory (UCTEL) at the University of Manitoba. Nearly all samples analyzed were contaminated; this highlights the importance and benefits of on-site sample analysis.

This research opens the doors for further investigations into Hg dynamics in the cryosphere. Through the course of this work sampling and processing protocols were established for the measurement of Hg in sea ice and in brine that can now be implemented in future work. A standard protocol was used for collection of all types of samples (snow, ice, brine) and field blanks used to ensure the integrity of samples and prevent the introduction of any bias in having different scientists collect the samples.

## 4.3 Future Directions

As mentioned in Chapter 1, atmospherically deposited Hg is subject to two fates. It can either be released into the marine system and potentially enter the food-web or it can be photo-reduced back to the atmosphere as $Hg^0$. The release of atmospherically deposited Hg into the marine system is largely mediated by its transport and behavior within the cryosphere (snow, ice and brine). The role the cryosphere plays in Arctic Hg cycling, as well as how a changing climate will affect this role is a subject for further investigation. The central gap in Hg polar chemistry remains to be quantifying the actual amount of AMDE Hg that is able to enter the marine environment. By understanding the role the cryosphere plays in Hg cycling, we can begin to determine the amount of

atmospheric Hg entering the marine system.

This research has met its primary object of shedding light on an often overlooked component of the cryosphere, and in the process raised more questions. In all first-year ice cores, a similar distribution of Hg was observed, regardless of location or season. It has been postulated that this observed distribution is a result of sea-ice formation processes. In order to further investigate the processes governing the distribution of Hg in sea ice future studies should focus and collecting ice samples from the onset of growth (new ice) and throughout the sea ice growth phase. The sample size of new ice collected during this study was too small to determine if AMDEs have an effect on newly formed ice. Additional samples of newly formed ice (grease and nilas ice) are therefore required.

Sea ice brine is a naturally occurring, unique environment characterized by high ionic strength, high salinity, and low temperatures; the biological and chemical processes occurring in this environment are of great interest. The characteristic environment in brine creates a potential for Hg transformation and Hg accumulation into the lower food web (via bacteria and algae). Research should be continued to identify the speciation of Hg in sea ice brine as well as identifying the chemical transformations occurring (methylation, oxidation, reduction). As the Arctic Ocean shifts to a primarily first year sea ice regime, more Hg-rich environments (sea ice brine) are available for primary producers. It has been hypothesized that this may lead to increasing food web exposure of Hg (and other contaminants). In the central Arctic, ice algae are thought to contribute as much as 57% of the primary production (Gosselin *et al.* 1997). Anaerobic conditions, known to occur in sea ice brine (Rysgaard and Glud 2004), make this environment a

potential site for microbial methylation of Hg. Conversely, recent literature reports that bacteria containing the *merA* gene, responsible for the reduction of Hg(II) to Hg(0), are present in sea ice brine (Møller *et al.* 2010). There is great potential for chemical reactions involving Hg in sea ice brine. Research efforts into both biotic and abiotic transformations of Hg in this media are essential. Mercury rejection from sea-ice accompanies the brine rejection from sea ice known to occur in springtime. Determining the speciation and bio-availability of Hg entering the marine system at this time is of great importance.

Multi-year sea ice is distinguished from first year sea-ice by its unique properties. Multi-year ice contains less brine and more air inclusions then first year ice. Multi-year ice in the Arctic is also diminishing at an alarming rate (Comiso 2002; Comiso *et al.* 2008). As outlined in Chapter 2, the single multi-year core analyzed during this study yielded interesting results; Hg peaks are hypothesized to be a result of seasonal melt – freeze cycles. However, having only one ice-core to draw conclusions from is not ideal. The processes responsible for the distribution of Hg in multi-year sea ice and behavior of Hg in this media need to be further investigated. From understanding this we can begin to hypothesize how a diminishing stock of multi-year ice will affect Hg dynamics in the Arctic. If multi-year ice is indeed acting as a sink and collecting a record of previously deposited Hg, this Hg will then enter the marine system when mutli-year ice is lost. Collection of multiple multi-year ice cores would shed further light on the different transport and transformation processes of Hg between first- and multi-year ice cores. Using ice beacons the movement of multi-year ice through the Arctic can be monitored to

investigate the potential for ice-driven Hg re-distribution in the Arctic Ocean.

In the future, the scope of analysis performed on cryospheric samples should be broadened to include MeHg, other trace elements, chlorophyll a, organic carbon, and oxygen-18 isotopes. With this expanded dataset the bioavailability and behavior of Hg in the cryosphere can be further understood. Ideally THg, MeHg, salinity, temperature and microstructural analysis (on sea ice) should all be completed in the field. Aliquots for trace elements, chlorophyll a, organic carbon and oxygen 18 isotopes may be collected, preserved, and shipped back to be analyzed in the south. With additional data on the pH, concentrations of major ions and organics in sea ice brine, there is potential for using chemical equilibrium software to model and predict the speciation of Hg in this media. However this may prove to be a difficult task, as most chemical equilibrium software readily available (such as MineQL+ and WHAM) are limited by the extremely low temperature and high ionic strength environments in brine.

As discussed in Chapter 1, MeHg is the toxic bioaccumulative Hg species that has the potential to negatively impact the health of Arctic marine mammals and Northern inhabitants. This contamination and toxic nature of MeHg is a driving factor to understand Hg cycling in the Arctic Environment. An increasing temperature may also increase the rate that Hg methylation occurs in the Arctic (Steffen *et al.* 2007). As snow and sea ice both present potential areas for Hg methylated, the potential for this process to occur needs to be investigated.

It has recently been reported that methylation of inorganic Hg occurs in polar waters (Lehnherr *et al.* 2011). The potential for Hg to be methylated in the snowpack has

only recently begun to be investigated (Larose *et al.* 2010). In order to be methylated biotically, Hg must be bio-available to microorganisms. The potential for biotic Hg methylation in the snowpack exists as a fraction of the Hg in the snow is known to be bio-available (Scott 2001; Larose *et al.* 2010; Larose *et al.* 2011). However, Lahoutifard *et.al.* (2005) argue that it is unlikely that MeHg in the snow is a result of biotic processes. If atmospherically deposited Hg is able to enter the marine system via melt-ponds, as suggested in Chapter 3, methylation of atmospherically deposited Hg in the snowpack would be important as it will influence which species of Hg are entering the marine system, and potentially the food web. It is therefore important to research the potential methylation, either via biotic or abiotic pathways, of Hg in the snowpack.

Quantifying the amount of atmospherically deposited Hg that is able to enter the marine system is of increasing importance as warmer temperatures threaten to shorten the time between Hg deposition and mobilization during the spring (Steffen *et al.* 2007). In order to better understand pathways of atmospherically deposited Hg entering the marine system an on-going study at one site (e.g., a landfast ice station) would be beneficial. In future studies, Hg in surface snow, and in the snow pack, should be continuously monitored up until the onset of melt and melt pond formation. Along with measurements of Hg in melt ponds, samples from under-ice water should be collected to test the hypothesis that melt ponds are delivering atmospherically derived Hg to the marine system. Having a diver able to collect under-ice water in early spring, during brine expulsion, and continuing into the melt season, where melt ponds breakthrough the ice, would be provide much needed data. These data would be helpful in accounting for

atmospherically deposited Hg, as well as in testing the hypothesis that melt ponds are delivering atmospherically derived Hg into the marine environment.

The dynamics of Hg in the Arctic environment is a broad research topic and encompasses a wide range of disciplines. Studies aimed at understanding Arctic Hg cycling and predicting changes associated with climate change should take a multi-disciplinary and collaborative approach to research.

## 4.4 References


Camara-Mor, P., Masque, P., Garcia-Orellana, J., Cochran, J., Mas, J., Chamizo, E. and C, H. (2011). *Radionuclides as tools to study the role of the Arctic Sea Ice in the interception, transport and redistribution of particlate matter and chemical species.* 43th International Liège Colloquium on Ocean Dynamcis, Liège, Belgium.

Comiso, J. (2002). Correlation and trend studies of the sea ice cover and surface temperatures in the Arctic. *Annals of Glaciology* **34**: 420-428.

Comiso, J. (2002). A rapidly declining perrenial sea ice cover in the Arctic. *Geophysical Research Letters* **29**(20).

Comiso, J., Parkinson, C., Gersten, R. and Stock, L. (2008). Accelarated decline in the Arctic sea ice cover. *Geophysical Research Letters* **35**.

Ferrari, C., Dommergue, A., Boutron, C., Jitaru, P. and Adams, F. (2004). Profiles of mercury in the snow pack at Station Nord, Greenland shortly after polar sunrise. *Geophysical Research Letters* **31**: 1-4.

Gleitz, M., Rutgers v.d. Loeff, M., Dieckmann, T. and Millero, F. J. (1995). Comparison of summer and winter inorganic carbon, oxygen and nutrient concentrations in Antarctic sea ice brine. *Marine Chemistry* **51**: 81-91.

Gosselin, M., Levasseur, M., Wheeler, P., Horner, R. and Booth, B. (1997). New measurements of phytoplankton and ice algal production in the Arctic Ocean. *Deep-Sea Research II* **44**: 1623-1644.

Lahoutifard, N., Sparling, M. and Lean, D. (2005). Total and methyl mercury patterns in Arctic snow during springtime at Resolute, Nunavut, Canada. *Atmospheric Environment* **39**(7597 - 7606).

Larose, C., Dommergue, A., De Angelis, M., Cossa, D., Averty, B., Marusczak, N., Soumis, N., Schneider, D. and Ferrari, C. (2010). Springtime changes in snow chemistry lead to new insights into mercury methylation in the Arctic. *Geochimica et Cosmochimica Acta* **74**: 6263-6275.

Larose, C., Dommergue, A., Marusczak, N., Coves, J., Ferrari, C. and S, D. (2011). Bioavailable mercury cycling in polar snowpacks. *Environmental Science and Technology* **45**: 2150-2156.

Latonas, J. (2010). Measurements of Atmospheric Mercury, Dissolved Gaseous Mercury, and Evasional Fluxes in the Amundsen Gulf: The Role of the Sea-Ice Environment. Department of Environment and Geography. Winnipeg, University of Manitoba. **Master of Science**.

Lehnherr, I., St. Louis, V., Hintelmann, H. and Kirk, J. (2011). Methylation of inoranic mercury in polar marine waters. *Nature geoscience*.

Lindberg, S., Brooks, S., Lin, C.-J., Scott, K., Landis, M., Stevens, R., Goodsite, M. and Richter, A. (2002). Dynamic oxidation of gaseous mercury in the arctic troposphere at polar sunrise. *Environmental Science and Technology* **36**: 1245 - 1256.

Macdonald, R., Harner, T. and Fyfe, J. (2005). Recent climate change in the Arctic and its impact on contaminant pathways and interpretation of temporal trend data. *Science of the Total Environment* **342**(1-3): 5 - 86.

Masque, P., Cochran, J., Hebbeln, D., Hirschberg, D., Dethleff, D. and WInkler, A. (2003). The role of sea ice in the fate of contaminants in the Arctic Ocean: plutonium atom ratios in the Fram Straight. *Environmental Science and Technology* **37**: 4848-4854.

Møller, A., Barkay, T., Abu Al-Soud, W., Sørensen, S., Skov, H. and Kroer, N. (2010). Diversity and characterization of mercury-resistant bacteria in snow, freshwater, and sea-ice brine from the High Arctic. *FEMS Microbiology Ecology* **75**(3): 390-401.

Papadimitriou, D., Thomas, D., Kennedy, H., Haas, C., H, K., Krell, A. and Dieckmann, G. (2007). Biogeochemical composition of natural sea ice brines from the Weddell Sea during early austral summer. *Linology and Oceanography* **52**(5): 1809-1823.

Poulain, A., Garcia, E., Amyot, M., Campbell, P. and Ariya, P. (2007). Mercury distribution, partitioning, and speciation in coastal vs. inland High Arctic snow. *Geochimica et Cosmochimica Acta* **71**: 3419 - 3431.

Poulain, A., Lalonde, J., Amyot, M., Shead, J., Raofie, F. and Ariya, P. (2004). Redox transformations of mercury in an Arctic snowpack at springtime. *Atmosphere Environment* **38**: 6763-6774.

Pucko, M., Stern, G., Macdonald, R. and Barber, D. (2010). α- and γ-hexachlorocyclohexane (HCH) measurements in the brine fraction of sea ice in the Canadian High Arctic using a sump-hole technique. *Environmental Science and Technology* **44**(24): 9258-9264.

Rysgaard, S. and Glud, R. (2004). Anaerobic $N_2$ production in Arctic sea ice. *Linology and Oceanography* **49**: 86-94.

Scott, K. (2001). Bioavailable mercury in Arctic snow determined by a light-emitting mer-lux bioreporter. *Arctic* **54**(1): 92-101.

Steffen, A., Douglas, T., Amyot, M., Ariya, P., Aspmo, K., Berg, T., Bottenheim, J., Brooks, S., Cobbett, F., Dastoor, A., Dommergue, A., Ebinghaus, R., Ferrari, C., Gardfeldt, K., Goodsite, M., Lean, D., Poulain, A., Scherz, C., Skov, H., Sommar, J. and Temme, C. (2007). A synthesis of atmopsheric mercury depletion event chemistry linking atmosphere, snow and water. *Atmospheric Chemistry and Physics Discussions* **7**: 10837-10931.

Steffen, A., Schroeder, W., Bottenheim, J., Narayan, J. and Fuentes, J. (2002). Atmospheric mercury concentrations: measurements and profiles near snow and ice surfaces in the Canadian Arctic during Alert 2000. *Atmospheric Environment* **36**: 2653 - 2661.

Untersteiner, N. (1968). Natural desalination and equilibrium salinity profile of perennial sea ice. *Journal of Geophysical Research* **73**: 1251 - 1257.

# Appendix

**Table S1. Sampling dates and locations for the ice and brine samples. FY: first-year; MY: multi-year.**

| Station | Sample | UTC Date | Latitude | Longitude | Ice Thickness (cm) | Snow Cover (cm) | Atmospheric $T_{avg}$ ($^0$C) |
|---|---|---|---|---|---|---|---|
| D27 | New ice | 01-Mar-08 | 70.774 | -123.503 | > 5 | NS | -25.9 |
| D28 | New ice | 04-Mar-08 | 70.949 | -122.869 | > 5 | NS | -24.6 |
| D33 | FY drift ice | 25-Mar-08 | 71.064 | -121.787 | 138 | 35 - 40 | -23.7 |
| | Brine | 1-3-Apr-08 | 71.064 | -121.787 | 138 | 35 - 40 | -25.7 |
| D34 | FY drift ice | 25-Mar-08 | 71.077 | -121.812 | 45 | NS, old FF | -24.0 |
| F1 | Landfast ice | 28-Mar-08 | 71.176 | -120.394 | 189 | 20 | N/A |
| D33a | FY drift ice | 04-Apr-08 | 71.064 | -121.787 | 64 | NS, old FF | -24.2 |
| D36 | New ice | 07-Apr-08 | 71.242 | -124.257 | 0.5 | NS or FF | -14.6 |
| | FY drift ice | 08-Apr-08 | 71.176 | -124.304 | 164 | 2.5 | -12.27 |
| D38 | Brine | 13-Apr-08 | 71.255 | -124.617 | 124 | 5 | -12.3 |
| D41 | FY drift ice | 20-Apr-08 | 70.609 | -121.872 | 130 | 5 | -7.9 |
| | Brine | 16 - 18 Apr-08 | 70.609 | -121.872 | 130 | 5 | -14.7 |
| 1020A | New ice | 06-May-08 | 71.026 | -126.965 | 2.5 | NS or FF | -5.6 |
| F2 | Landfast ice | 14-May-08 | 69.946 | -126.172 | 114 | 10 | 3.9 |
| | Brine | 16 - 18 May-08 | 69.946 | -126.172 | 114 | 10 | -0.5 |
| MY1 | MY ice | 25-May-08 | 72.653 | 129.443 | 380 | 23 | -0.4 |

**Table S2. Concentration of mercury in the newly formed sea ice in the Beaufort Sea compared with that in the air and underlying surface seawater**

| Station ID | Sampling Time (UTC) | Ice thickness (mm) | [Hg] in the new ice (ng/L) | AMDE occurring? | GEM[a] ($ng/m^3$) | RGM[b] ($pg/m^3$) | $Hg_P$[c] ($pg/m^3$) | [Hg] in the surface seawater (ng/L) |
|---|---|---|---|---|---|---|---|---|
| D27 | 01-Mar-08 07:00 | > 50 | 0.45 | Yes | 1.19 | 2.53 | 23.8 | 0.28 |
| D28 | 04-Mar-08 08:30 | > 50 | 0.53 | Yes | 0.10 | 3.50 | 246 | n.d.[d] |
| D36 | 07-Apr-08 08:30 | 5 | 0.22 | No | 1.63 | 9.3 | 9.8 | 0.11 |
| 1020A | 06-May-08 08:40 | 25 | 0.49 | Yes | 1.16 | 32.7 | 23.8 | 0.24 |

[a]Average gaseous elemental mercury concentration in the air in the 3-hr period immediately preceding the time of sampling
[b]Average reactive gaseous mercury concentration in the air in the 3-hr period immediately preceding the time of sampling
[c]Average particulate mercury concentration in the air in the 3-hr period immediately preceding the time of sampling
[d]Not determined

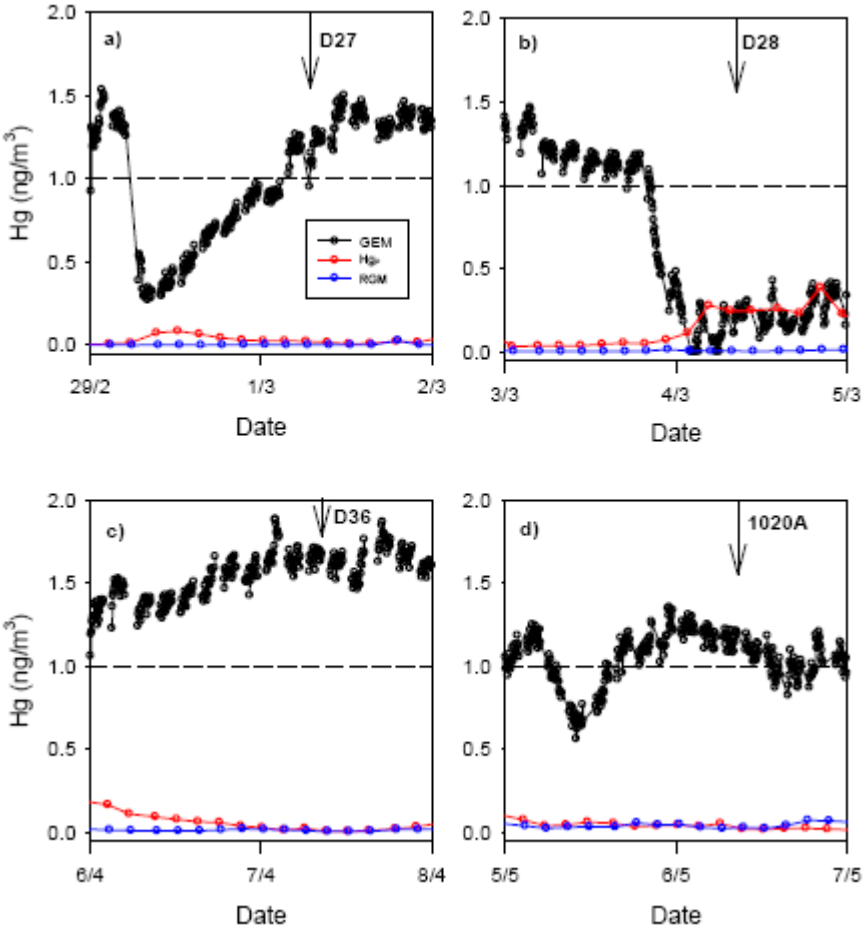


**Figure S1: Real-time atmospheric Hg speciation during the sampling of newly formed sea ice at stations D27, D28, D36 and 1020A. GEM: Gaseous elemental Hg; $Hg_p$: particulate Hg; RGM: reactive gaseous Hg. The dashed line shows the GEM threshold of 1.0 ng/m$^3$. The arrow shows when the newly formed ice was sampled at each station.**

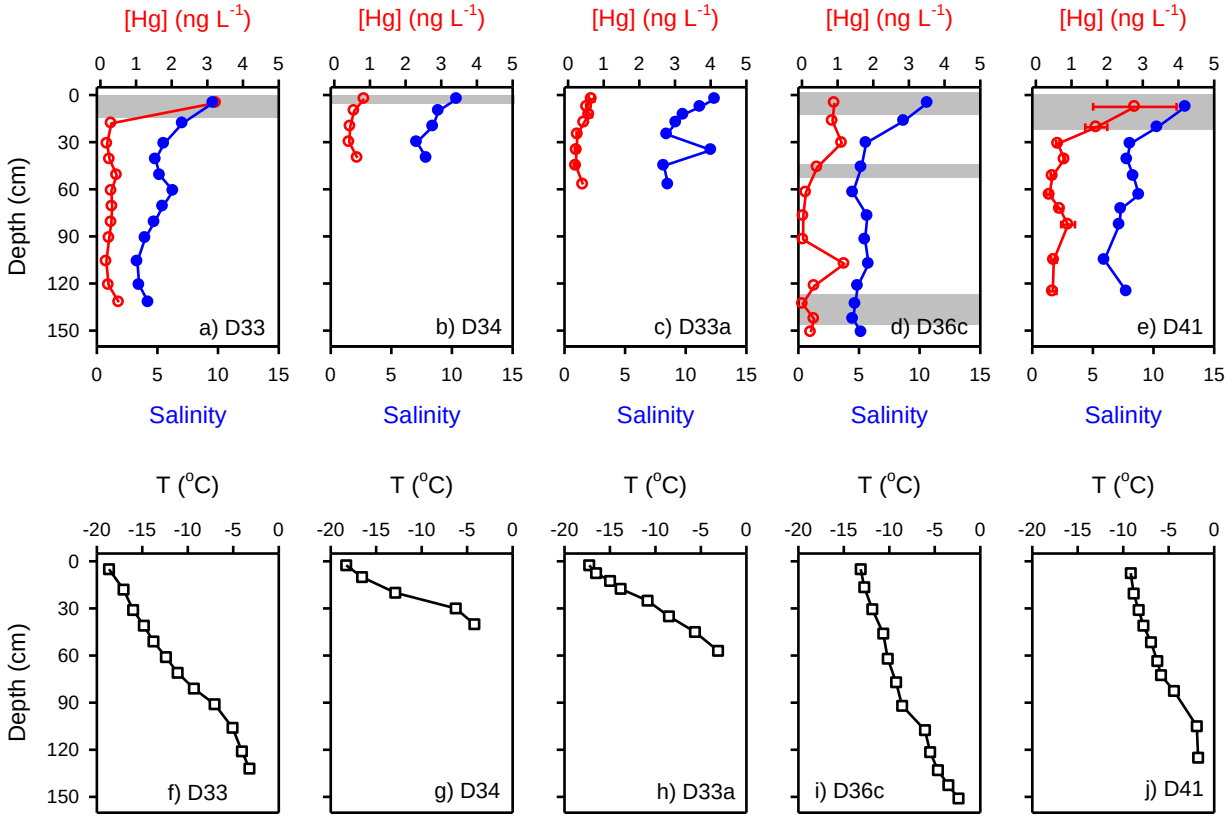


**Figure S2. Profiles of Hg (open circles), salinity (filled circles), and temperature (open squares) in the ice cores from the drift ice stations. The shaded gray bar shows the depth where granular ice was present. No granular ice was found in Core D33a.**

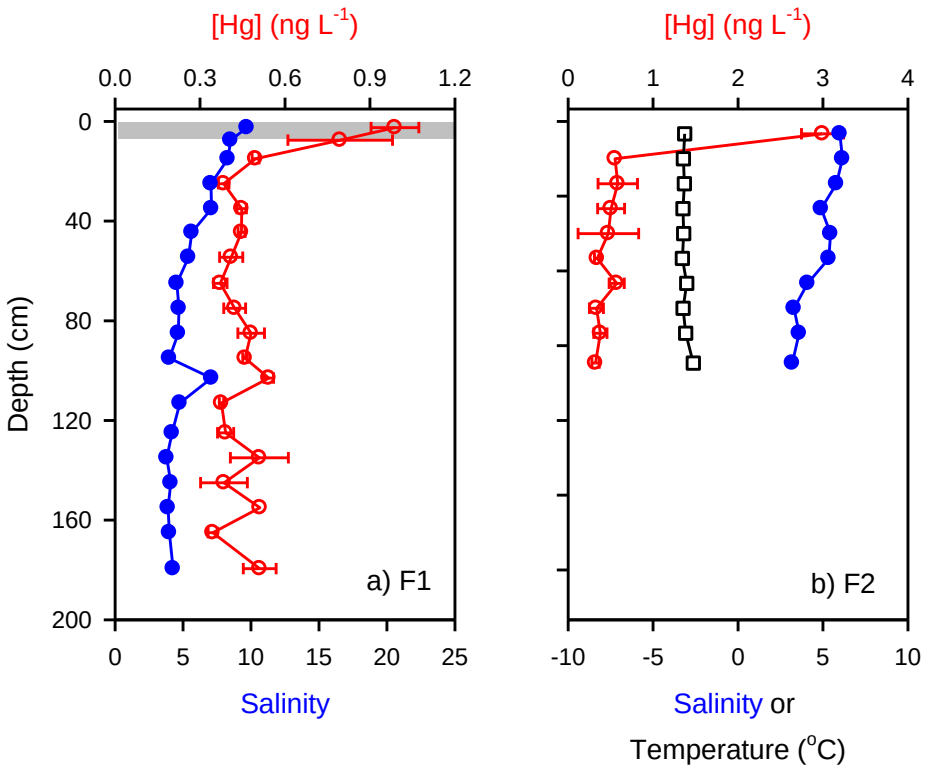


**Figure S3. Profiles of Hg (open circles), salinity (filled circles) and temperature (open squares) in the ice cores from the landfast ice stations. The shaded gray bar in a) shows the depth where granular ice was present. Sea ice texture in b) was not analyzed.**

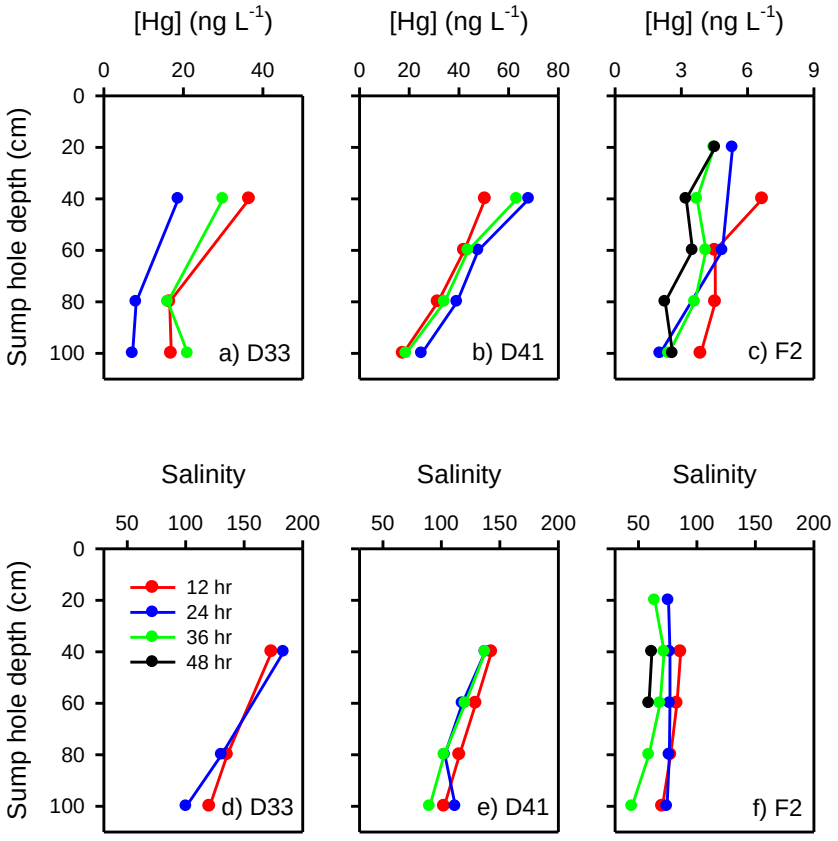


**Figure S4. Profiles of Hg and salinity in brine at various times after the sump holes were dug.**

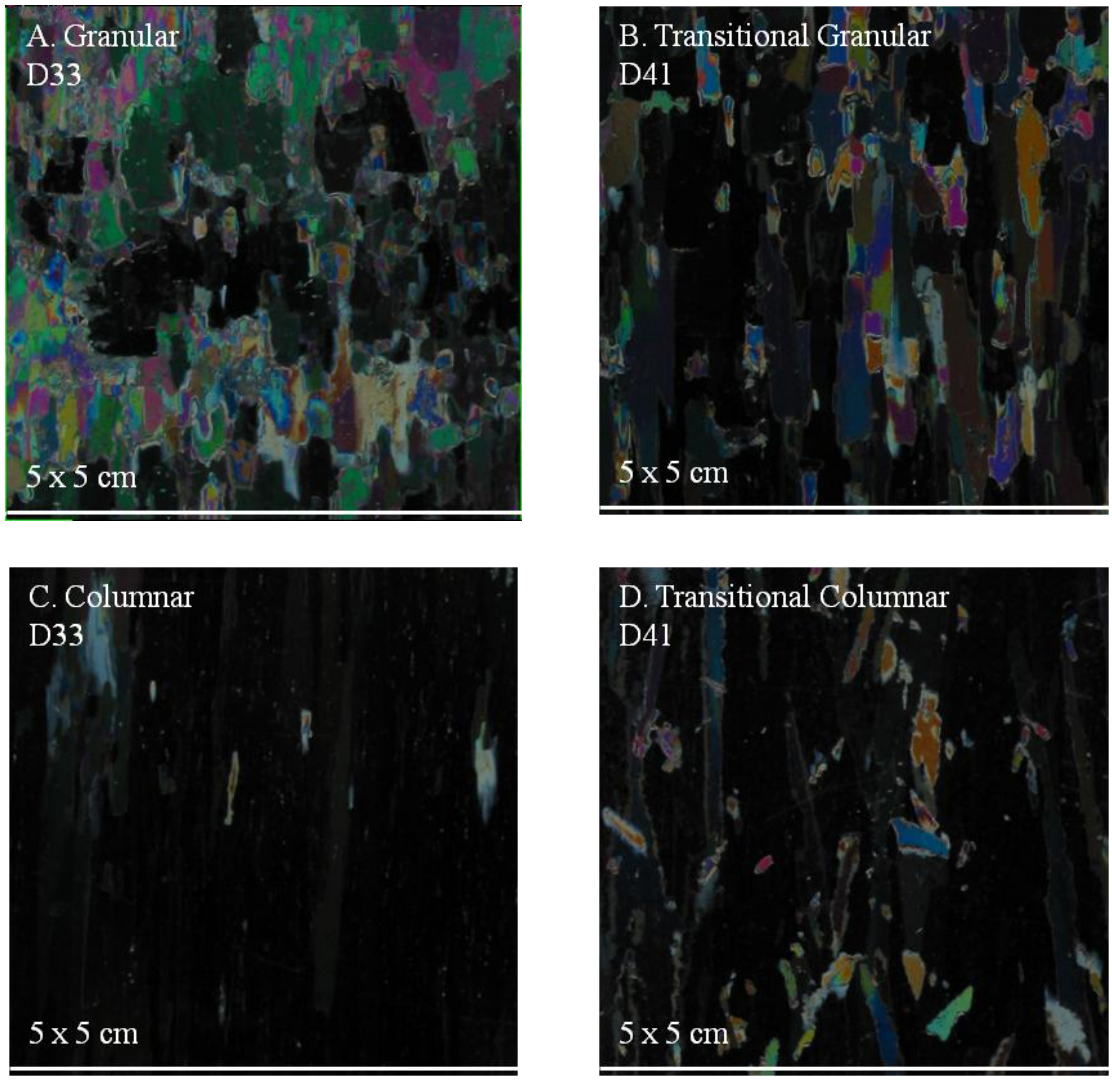


**Figure S5. 5 cm × 5 cm cross-polarized light photographs of ice thing sections showing different sea-ice textures**

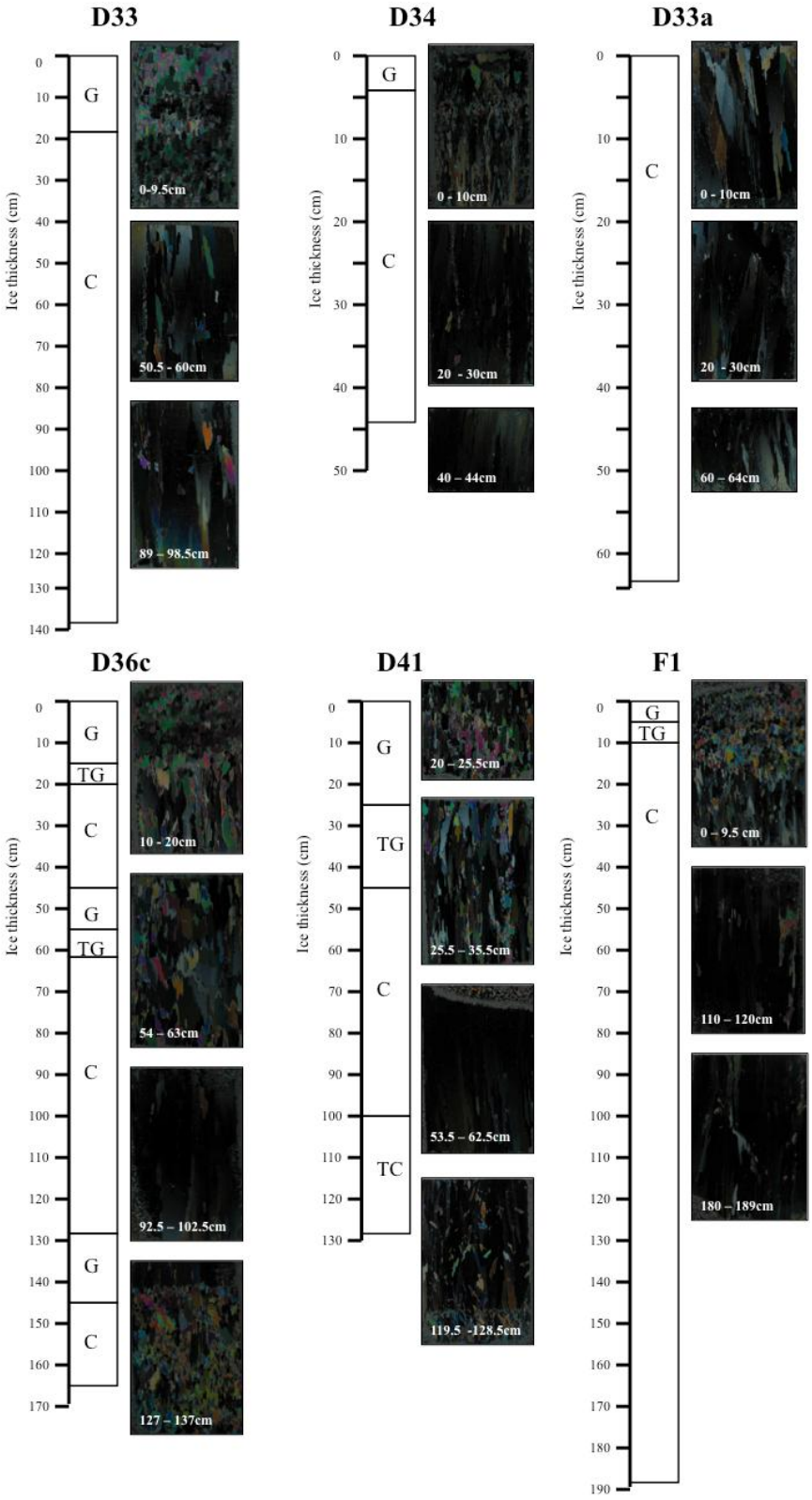


**Figure S6. Sea ice texture profiles of 6 ice cores with cross-polarized light photographs. G: granular; C: columnar; TG: transitional granular; TC: transitional columnar.**